# Preliminary stock assessment of Indian Ocean Bigeye tuna (*Thunnus obsesus*) using Stock Synthesis (2025)

Genevieve A.C. Phillips<sup>1</sup>, Gorka Merino<sup>2</sup>, Agurtzane Urtizberea Ijurco<sup>2</sup>, Giancarlo Correa Moron<sup>2</sup>, and Dan Fu<sup>1</sup>



- 1. Indian Ocean Tuna Commission Secretariat, FAO
- 2. AZTI, Spain, European Union.

# **CONTENTS**

Co	ontents		2
Li	st of Fi	gures	4
Li	st of Ta	bles	7
Ex	ecutive.	e summary	8
	Method Results Catch. Catch to Key se	rates	81111
A	cknowl	edgements	14
1.	Intro	oduction	15
2.	Bac	kground	17
	2.1.	Stock structure	17
	2.2.	Biology	
	2.3.	Indian Ocean bigeye tuna fishery overview	19
3.	Data	a inputs	20
	3.1.	General notes	20
	3.2.	Spatial stratification	
	3.3.	Temporal stratification	
	3.4.	Definition of model fleets	
	3.5.	Catch data	22
	3.6.	Abundance indices	27
	3.7.	Length frequency data	32
	3.8.	Tagging data	37
4.	Mod	del Description	42
	4.1.	Population dynamics	42
	4.2.	Dynamics of tagged fish	
	4.3.	Modelling methods, parameters, and likelihood	
5.	Ass	essment model runs	49
	5.1.	Base model	
	5.2.	Model sensitivity testing.	
	5.3.	Proposed ensemble models (Grid)	
6.		delling Results	
٠.	6.1.		
	6.2.	Continuity runs from 2022 model	
	6.3.	Model estimates	
	6.4.	Diagnostics	
7.		sitivity Runs	
′•		•	
	7.1.	Non-biological parameters	
	7.2. 7.3.	Biological parameters  Proposed final model options for grid / ensemble	
8	Stoc	ek Status	91

8	.1.	Current status and yields	91
9.	Disc	cussion	96
9.	.1.	Recommendations for future assessments	97
10.	Ref	erences	98
11.	APp	pendix A:	104
12.	App	pendix B: CPUE comparison	108
13	2.1.	Introduction	108
1.	2.2.	Data and methods	108
		Catch and effort data	
1.	2.4.	Methods	109
1.	3.1.	References	111

# LIST OF FIGURES

Figure i: Output from the KOBE plots from the ensemble of models in the grid9
Figure ii: Management outputs from the ensemble of models (grid) used in 2024. Bounds around the
main darker line represent the highest and lowest values from the grid of models. The grey band on the
catch graph represents estimated optimal catch at MSY (80 % confidence interval). The horizontal red
lines indicate limit or reference points for SSB/SSB <sub>MSY</sub> and F/F <sub>MSY</sub> . The red vertical line shows the
current year (2025)
Figure iii: Estimated raised catches for the Indian Ocean bigeye tuna fishery from 1975-2024
Figure 1: Spatial stratification of the Indian Ocean for the four-region assessment model
Figure 2: Fishery catches (x 1000 metric tonnes) aggregated by model region and coloured according
to fishing fleet in the model.
Figure 3: Fishery catches (metric tonnes) aggregated by year. Note the y-axes differ between plots. Red
lines are catches used in the 2022 assessment. The differences in catch are mainly due to the revision
of catch data by Indonesia, although some changes will be due to general improvements in the data
quality over time26
-Figure 4: Standardized CPUE series produced in 2019 (red), 2022 (blue), and 2025 (black).
Operational-level data were used in the 2019 and 2025 analyses, while aggregated data were used in
Figure 5: Comparison of 2022 (grey) and 2025 (purple) CPUE indices from the joint longline indices
from Taiwan (China), Korea, and Japan
Figure 6: Quarterly standardized CPUE index for the long and short time series superposed (Correa et
al., 2025)
Figure 7: The availability of length sampling data from each fishery by year. The grey circles denote
the presence of samples in a specific year (the size indicate number of quarters being sampled). The red
horizontal lines indicate the time period over which each fishery operated34
*
Figure 8: Length compositions of bigeye tuna samples aggregated by model fishery
Figure 9: Mean length (fork length, cm) of bigeye sampled from the principal fisheries by year quarter.
The grey line represents the fit of a loess smoother to the dataset
Figure 10: Location of releases (green) and density of recoveries for the bigeye tuna RTTO-IO tag
Program37
Figure 11: Number of tag releases by quarter and age class (year) included in the assessment data set.
All tag releases occurred in region 1S. Ages (year) were assigned based on the length of the fish, and
updated growth model from Eveson et al. (2025)
` '
Figure 12: Bigeye tag recoveries by year/quarter and fishery included in the assessment model. Purse
seine tag recoveries have not been corrected for reporting rate
Figure 13: Fixed growth functions for bigeye tuna from the 2022 and 2025 assessments (0_base_2022
and 4 update growth respectively) by Farley et al. 2021 and Eveson et al. 2025 (left), and length-based
maturity Ogive following Shono et al (2009) (RHS). For the growth functions, the shaded distributions
represent the assumed variability of mean size-at-age in the assessment models
Figure 14: The different instantaneous rates of natural mortality (M) used in the 2022 ("0 base 2022",
"6f_Mbase") and 2025 assessment models. The model "5_update_M" uses the Hamel & Cope model,
using 14.7 years as the Age <sub>max</sub> , while "6e_MHamel17" uses the Hamel & Cope model, using 17 years
as the Age <sub>max</sub> (for comparison). The models named "MLorHam6Q" are where M is internally estimated
within the model, using Age <sub>max</sub> at 14.7 years and 'adult' fish ages are from 4-10 years. Age in the graph
is in quarters as this is how it is structured in the model
Figure 15: Spawning biomass trajectories for IO bigeye tuna from the stepwise model updates. (from
the 2022 assessment reference model '0 base 2022').
Figure 16a: Fits to the joint regional frozen longline CPUE indices 1979-2024 in the base model
'6_update_bias'
Figure 16b: Fits to the joint regional frozen longline CPUE indices 1979-2024 in the base model
'7_update_cpue_LLq'60
Figure 17a: Standardised residuals from the fits to the CPUE indices from the base model
'6_update_bias'61

Figure 17b: Standardised residuals from the fits to the CPUE indices from the base model
'7_update_cpue_LLq'61
Figure 18a: Observed (grey bars) and predicted (red line) length compositions (in 4 cm intervals) for
each fishery of bigeye tuna aggregated over time for the base model '6_update_bias'62
Figure 18b: Observed (grey bars) and predicted (red line) length compositions (in 4 cm intervals) for
each fishery of bigeye tuna aggregated over time for the base model '7_update_cpue_LLq'63
Figure 29a: A comparison of the observed (grey points) and predicted (red points and line) average fish
length (FL, cm) of bigeye tuna by fishery for the main fisheries with length data for the base model
'6_update_bias'64
'6_update_bias'
length (FL, cm) of bigeye tuna by fishery for the main fisheries with length data for the base model
'7_update_cpue_LLq'65
Figure 20a: Estimated age-based (quarters) selectivity for model fleets within the base model
'6_update_bias'66
Figure 20b: Estimated age-based (quarters) selectivity for model fleets within the base model
'7_update_cpue_LLq'67
Figure 21a: Observed and predicted number of tags recovered by quarter for the PSLS fishery in region
1S (PSLS 1S). Only tags at liberty after the four quarter mixing period are included. Tag recoveries are
aggregated for each release group. Base model '6_update_bias'68
Figure 21b: Observed and predicted number of tags recovered by quarter for the PSLS fishery in region
1S (PSLS 1S). Only tags at liberty after the four quarter mixing period are included. Tag recoveries are
aggregated for each release group. Base model '7_update_cpue_LLq'
Figure 22a: Observed and predicted number of tags recovered by quarter for the PSLS fishery in region
1N (PSLS 1N). Only tags at liberty after the four quarter mixing period are included. Tag recoveries are
aggregated for each release group. Base model '6_update_bias'69
Figure 22b: Observed and predicted number of tags recovered by quarter for the PSLS fishery in region
1N (PSLS 1N). Only tags at liberty after the four quarter mixing period are included. Tag recoveries are
aggregated for each release group. Base model '7_update_cpue_LLq'69
Figure 23a: Observed and predicted number of tags recovered by year/quarter time-period (left), by age
(mid), and by time at liberty (in quarters, right) for main Purse seine and longline fisheries in region 1N
and 1S (PSLS 1S, 1N, PSFS 1S, 1N, and LL 1S, 1N) from '6_update_bias'. Only tags at liberty after
the four-quarter mixing period are included. Tag recoveries are aggregated for each of the regional
fisheries
Figure 23b: Observed and predicted number of tags recovered by year/quarter time-period (left), by age
(mid), and by time at liberty (in quarters, right) for main Purse seine and longline fisheries in region 1N
and 1S (PSLS 1S, 1N, PSFS 1S, 1N, and LL 1S, 1N) from '7_update_cpue_LLq. Only tags at liberty
after the four-quarter mixing period are included. Tag recoveries are aggregated for each of the regional
fisheries
Figure 24: Recruitment deviates from the SRR with 95% confidence interval from (LHS)
'6_update_bias' and (RHS) '7_update_cpue_LLq'74
Figure 25: Estimated age specific movement parameters for the base models: (LHS) '6_update_bias'
and (RHS) '7_update_cpue_LLq'74
Figure 26a: Tag reporting rates for each fishery from the base model '6_update_bias'. Purse seine
reporting rates were fixed at a value of 1.0. Reporting rates for the other fisheries were estimated. The
grey lines represent the 95% confidence interval for the estimated values
Figure 26b: Tag reporting rates for each fishery from the base model '7_update_cpue_LLq'. Purse seine
reporting rates were fixed at a value of 1.0. Reporting rates for the other fisheries were estimated. The
grey lines represent the 95% confidence interval for the estimated values
Figure 27a: Estimated spawning biomass trajectories for the individual model regions from the base
model '6_update_bias'
Figure 27b: Estimated spawning biomass trajectories for the individual model regions from the base
model '7_update_cpue_LLq'
Figure 28a: Trends in fishing mortality (yearly) by fleet for the base model '6_update_bias'
Figure 28b: Trends in fishing mortality (yearly) by fleet for the base model '7_update_cpue_LLq'78

Figure 29a: ASPM analysis for the base model 6 update bias: ASPMIXED (no recruitment
deviations), and ASPMrec (recruitment deviates from the reference model added back). Both runs
excluded the length composition data and fixed the selectivity parameters80
Figure 29b: ASPM analysis for the base model '7_update_cpue_LLq': ASPMfixed (no recruitment
deviations), and ASPMrec (recruitment deviates from the reference model added back). Both runs
excluded the length composition data and fixed the selectivity parameters80
Figure 30a: Retrospective analysis summary for the base model '6_update_bias'81
Figure 30b: Retrospective analysis summary for the base model '7_update_cpue_LLq'82
Figure 31a: The Hindcasting analysis summary for the base model '6_update_bias': each panel shows
the predicted quarterly83
Figure 31b: The Hindcasting analysis summary for the base model '6_update_bias': each panel shows
the predicted quarterly84
Figure 32: Spawning biomass trajectories from the proposed final model options in the grid92
Figure 33: KOBE PLOT FROM GRID RUNS94
Figure 34: Management outputs from the ensemble of models (grid) used in 2024. Bounds around the
main darker line represent the highest and lowest values from the grid of models. The grey band on the
catch graph represents estimated optimal catch at MSY (80 % confidence interval). The horizontal red
lines indicate limit or reference points for SSB/SSB <sub>MSY</sub> and F/F <sub>MSY</sub> 95
Figure A1: Fits to the PSLS CPUE index from one of the sensitivity runs ('6a_PSlong_2area') -
SURVEY 5 (PSLS long index 1N, region 1N)
Figure A2: Fits to the PSLS CPUE index from one of the sensitivity runs ('6a_PSlong_2area') -
SURVEY 6 (PSLS long index 1S, region 1S)104
Figure A2: Fits to the length composition data when LL2 & LL3 fleets' selectivity is estimated to be
logistic. For model '6_sL'105
Figure A3: Estimates of biomass for different growth curves used in sensitivity runs. CAAL =
'conditional-age-at-length' - growth is internally estimated in the model Lmin = age at length min is
fixed; Lmax = age at length max is fixed, otherwise von Bertalanffy parameters are estimated 106
Figure A4: Estimates of growth curves for different growth curves used in sensitivity runs. CAAL =
'conditional-age-at-length' - growth is internally estimated in the model. Lmin = age at length min is
fixed; Lmax = age at length max is fixed, otherwise von Bertalanffy parameters are estimated 106
Figure A5: Biomass estimates when the instantaneous rate of natural moratliy (M) is changed in the
model, highlighting the sensitivity of the model to these parameters. When estimated internally in the
model (MLorHam6Q), estimates of biomass changed significantly. Changing the maximum age of fish
(MHamel15 (Age $_{max}$ = 14.7 yr); MHamel17 (Age $_{max}$ = 17 yr)), had less of an effect on the overall
estimates of biomass, although the trend in biomass depletion changed107

# LIST OF TABLES

Table i: STOCK STATUS INDICATORS FROM MODEL ENSEMBLE9
Figure iv: Annual joint standardised catch rates (CPUE) for the frozen longline fleets of Japan, Korea,
and Taiwan, China from 1975-2024 for each model region. The grey line shows the longline CPUE
indices that were included in the 2022 model
Table 1: Definition of model fleets within the SS3 model for bigeye tuna in the Indian Ocean, including
the gear types used, and region that data are assigned to in the model
Table 2: Recent bigeye tuna catches (metric tonnes, t) aggregated by model fleet that have been included
in the stock assessment model. The annual catches are presented for 2020- 2024
Table 3: Tag recoveries by year of recovery (box), region of release (number released in bracket), and
region of recovery. Region of recovery is defined by the definitions of the fisheries included in the
model.
Table 4: Description of the sequence of model runs to update the 2022 base model
Table 5: Main structural assumptions of the bigeye tuna <i>base</i> model and details of estimated parameters.
Changes to the 2022 reference model are highlighted in red
Table 6: Description of various data inputs and biological parameters that were varied to test model
sensitivity to them.
Table 7: Description of the proposed final model options for the 2025 assessment. The final models
consist of a full combination of options below, making a total of 18 models. The options adopted within
the reference (base) model ('7_PSlong_LLq') are highlighted54
Table 6: Estimates of management quantities for the step-wise updates of the 2022 stock assessment
reference model ('0_base_2022') to the 2025 reference models ('6_update_bias' and
'7 update cpue LLq')
Table 9 (next page): Estimates of management quantities for the sensitivity testing from the base model
options. Current catch (2024) is estimated at 101,722 t. Base models are highlighted green. Internal
estimation of M (MLorHam6Q results in varying outcomes – very high estimates of SSB <sub>0</sub> , and
$SSB_{2024}/SSB_0$ and lower than expected estimates of $F_{2024}/F_{MSY}$ (yellow highlighted fields). Mbase also
produced similarly high SSB <sub>0</sub> but other values were similar to base models (blue highlighted fields).
All models (except 6d_PSlong_MLorHam6Q_hi) estimated C <sub>MSY</sub> at values lower than current catch.
87 Million (cheeps 64_1 storig_Million tamove_m) estimated clim51 at values tower than earlier earlier.
Table 10 Estimates of management quantities for the stock assessment model options. Current yield
(mt) represents yield in 2024 corresponding to fishing mortality at the FMSY level
Table 11: STOCK STATUS INDICATORS FROM MODEL ENSEMBLE

## **EXECUTIVE SUMMARY**

#### Introduction

Bigeye tuna (*Thunnus obesus*) is a large pelagic predatory fish found mainly in tropical waters throughout the Indian Ocean where they form a single genetic stock. Bigeye tuna can live for up to 15 years, and reach a maximum size of approximately 250 cm, with a maximum weight of over 210 kg. Sexual maturity is reached at between 100 to 125 cm (approximately three to four years of age).

The stock assessment for bigeye tuna in the Indian Ocean is commissioned every three years, according to the schedule set out within the workplan of the Working Party for Tropical Tunas (WPTT) within the Indian Ocean Tuna Commission (IOTC). In 2025, the stock assessment is based on an update of the 2022 stock assessment model and is a spatially structured age-based integrated model that uses catch rate indices, length-compositions, and tagging data to inform estimates of spawning stock biomass (SSB) and fishing mortality (F), relative to estimated maximum sustainable yield (MSY).

The assessment was completed using Stock Synthesis 3.30 and incorporates all newly available data since the previous assessment, including updated abundance indices, and updated age and length data that informs a newly estimated growth curve for bigeye tuna in the Indian Ocean.

#### **Methods**

The Stock Synthesis 3.30 (SS3.30) assessment model covers the period 1975-2024 and assumes that the Indian Ocean bigeye tuna constitute a single genetic stock, modelled as spatially disaggregated four regions, with 24 fleets. Standardised catch per unit effort (CPUE) series from the main longline fleets (1975-2024), and two purse seine fleets (1991-2024) were included in the model as relative abundance indices of exploitable biomass in each region. Tagging data from a regional tagging program were included to inform abundance, movement, and mortality rates.

Several sensitivities were run as outlined in the data preparatory meeting in May 2025 (27th Meeting of the WPTT) to explore the effects of alternative model assumptions (e.g. changes to estimation methods for natural mortality (M), and growth model parameterisation), and the impact of the inclusion or exclusion of specific datasets (e.g. the inclusion or not of the purse seine CPUE). After sensitivity analyses, and running of diagnostics, including running retrospectives, and age-structured production models (ASPM), the most internally consistent model was chosen as a base model, and the grid run using this model ('7\_update\_cpue\_LLq').

To account for uncertainty within specific model parameters, several model options were then run using the base model in a 'grid' of models using a combination of plausible options for these parameters. This included three options for the steepness parameter (h), three options for the instantaneous rate of natural mortality (M), and two options for selectivity in two frozen longline fleets (LL2 and LL3). This led to a total of 18 model options in the grid runs that cover an appropriate range of uncertainty in the base model parameterisation.

#### Results

In 2025, the overall stock status for bigeye tuna in the Indian Ocean is that the stock is **overfished** and **subject to overfishing** with a likelihood of 58.7 % (Figure i, Table i) over an ensemble of 18 models that encompass the main uncertainties within the model. The base model in the figure is 'io\_h80\_Gnew\_MHamel15\_sD'.

Table i: STOCK STATUS INDICATORS FROM MODEL ENSEMBLE

Catch in 2024:	101,722 t
Average catch 2016–2024:	88,965 t
MSY (1000 t) (plausible range):	94 (89 –99)
F <sub>MSY</sub>	0.26 (0.21–0.31)
SSB <sub>0</sub> (1000 t) (80% CI):	1677 (744-2609)
SSB <sub>2024</sub> (1000 t) (80% CI):	470 (222–719)
$SSB_{MSY}$	441 (194–689)
SSB <sub>2024</sub> /SSB <sub>0</sub> (80% CI):	0.28 (0.26–0.30)
SSB <sub>2024</sub> / SSB <sub>MSY</sub>	0.99 (0.84–1.15)
F <sub>2024</sub> / F <sub>MSY</sub>	1.22 (1.03-1.42)

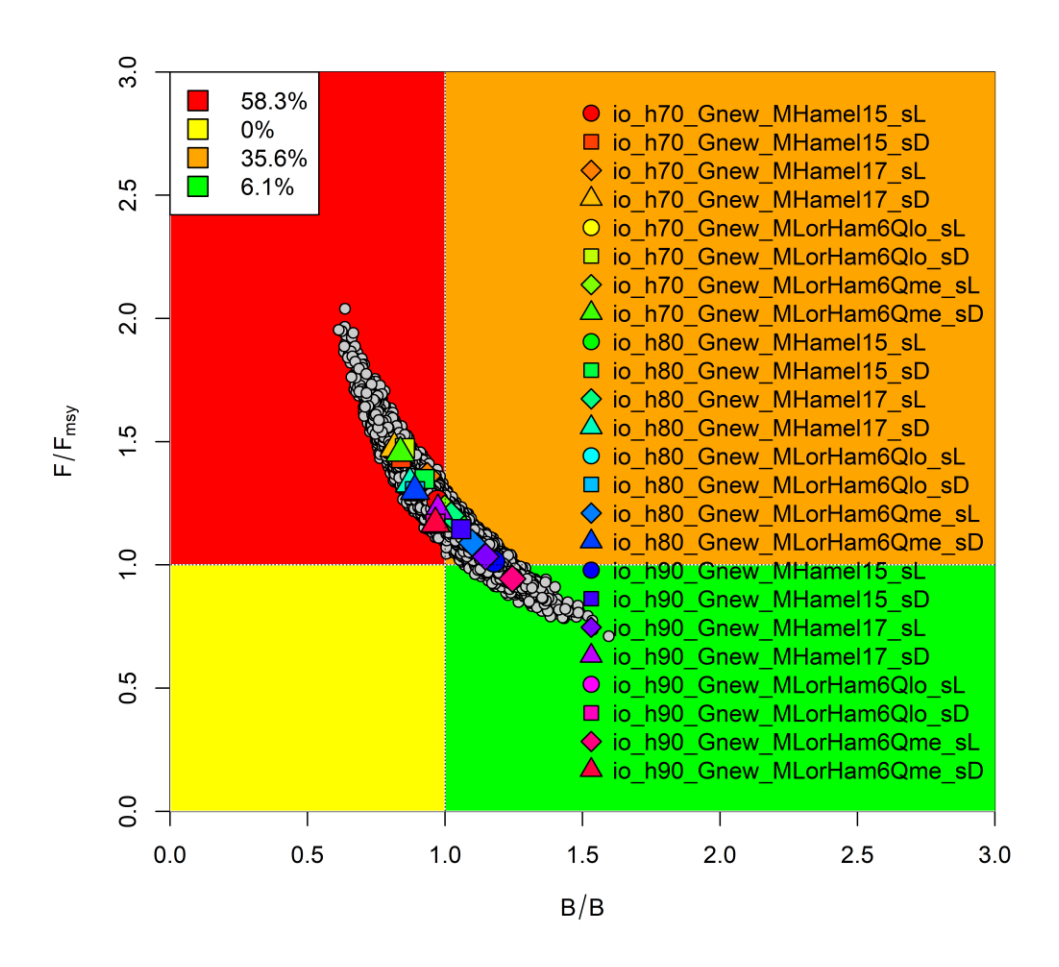


Figure i: Output from the KOBE plots from the ensemble of models in the grid.

In the 2022 assessment (using data up to 2021) the model ensemble estimated that the stock was **overfished** and **subject to overfishing** in 2021, this was a change from the 2019 assessment when the stock was estimated to be **not overfished** but subject to **overfishing**.

The estimated biomass trajectory shows a decline from exploited but equilibrium spawning stock biomass levels in 1975 to 2021 (Figure ii). Biomass levels appear to have stabilised and are increasing in the final years of the model, providing a more positive outlook for the stock, despite several years of increased catches that are estimated to be above MSY, and fishing mortality continuing to increase above that of  $F/F_{MSY}$ . As there is a significant lack of representative biological data (length data, and representative ages), the model is forced to fit closely to the main abundance indices from the longline fleets. As there have been increases in these indices in the three most recent years (2022-2024 inclusive), alongside increased catches, it is likely that the CPUE indices are driving the increase in estimated biomass in the model.

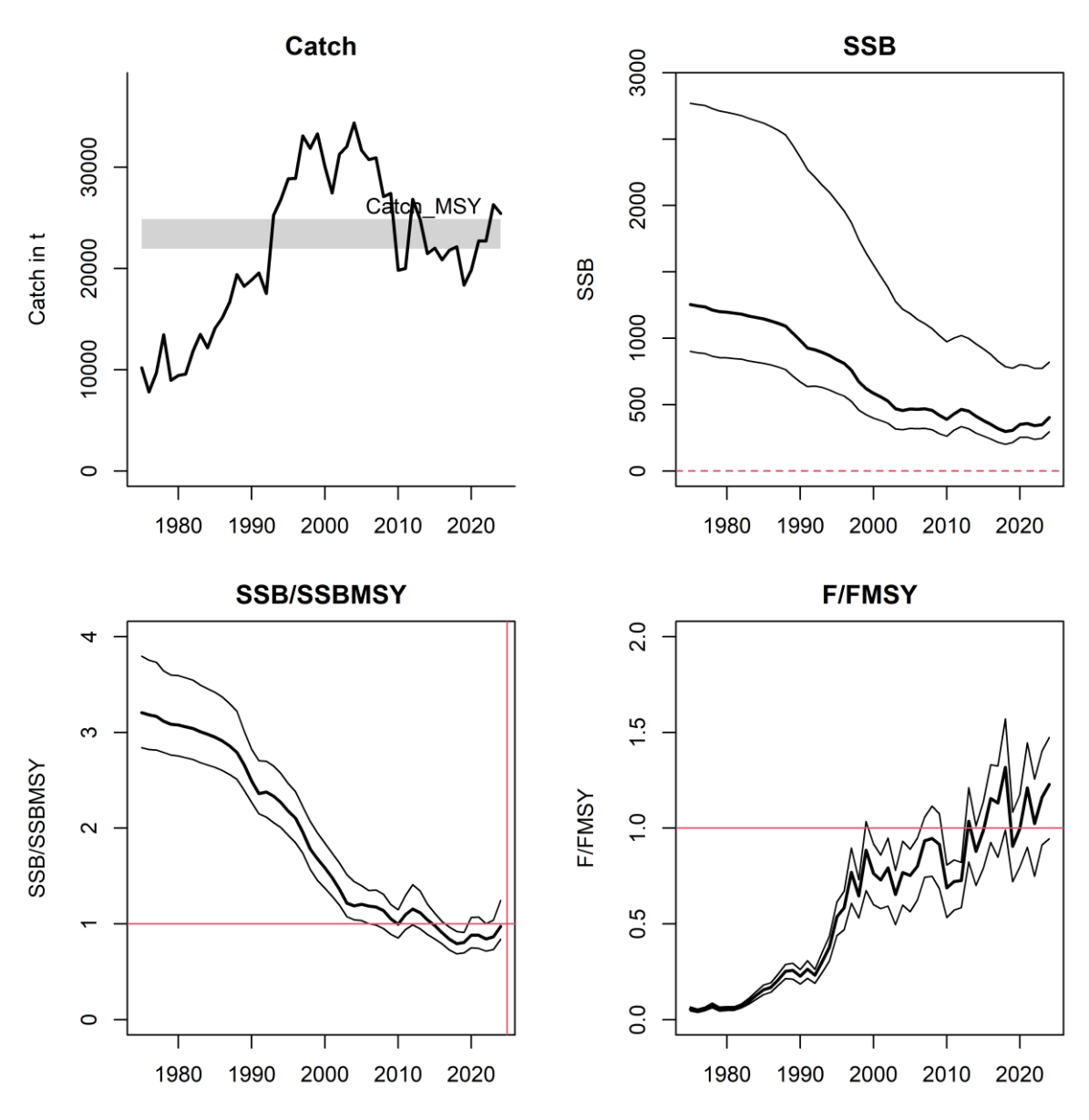


Figure ii: Management outputs from the ensemble of models (grid) used in 2024. Bounds around the main darker line represent the highest and lowest values from the grid of models. The grey band on the catch graph represents estimated optimal catch at MSY (80 % confidence interval). The horizontal red lines indicate limit or reference points for SSB/SSB<sub>MSY</sub> and F/F<sub>MSY</sub>. The red vertical line shows the current year (2025).

#### Catch

In the three years since the previous assessment, total catch has averaged 99,257 tonnes per year from all fleets within the fishery (Figure iii). Approximately 24 % of catch was taken by frozen longliners (LL) and 29 % by PSLS vessels in 2024.

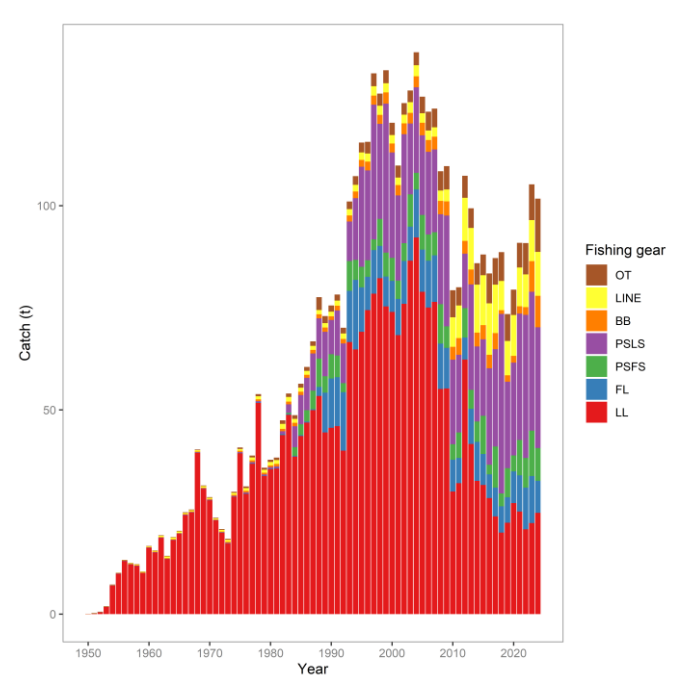


Figure iii: Estimated raised catches for the Indian Ocean bigeye tuna fishery from 1975-2024.

## Catch rates

Standardised catch rates included in the base model are a joint-CPUE provided by Japan, Taiwan (China), and Korea, based on catches from frozen longline fleets (Figure iv). Detailed methods for these indices can be found in the documents provided at the 27th Working Group for Tropical Tunas (Data Preparatory) in May 2025.

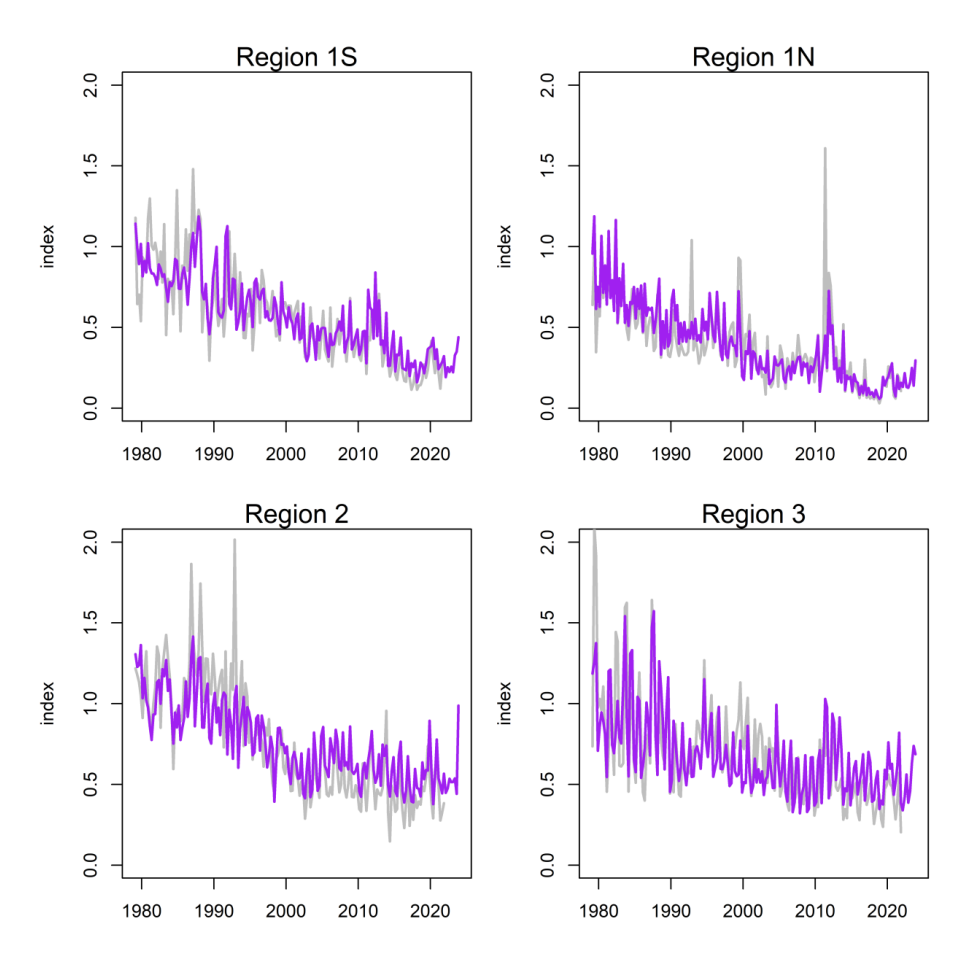


Figure iv: Annual joint standardised catch rates (CPUE) for the frozen longline fleets of Japan, Korea, and Taiwan, China from 1975-2024 for each model region. The grey line shows the longline CPUE indices that were included in the 2022 model.

## **Key sensitivities**

The model was sensitive to changes to the estimated instantaneous rate of natural mortality, and a change in the growth estimation to the newer estimates of age-at-length for bigeye tuna provided in 2025. The addition of the most recent longline CPUE indices also provided a more positive outlook on the stock than the previous indices. The model was relatively insensitive to the addition of the purse seine CPUE indices.

#### Recommendations for future assessments

A summary of recommendations for future assessments of bigeye tuna in the Indian Ocean are provided below. This can be added to during the assessment meeting.

- Improved quality and quantity of length composition data: It is recommended that improvements in both quantity and quality of length frequency data are provided to the Secretariat prior to the next assessment of bigeye tuna in 2028, and that any length data omitted in this assessment are reassessed for suitability and inclusion in 2028. Results from a recent consultancy with Dr. Paul Medley may inform the next BET assessment, alongside other tropical tuna stock assessments.
- Further development of additional abundance indices: as with other tuna assessments in the IOTC, the abundance indices are not representative of the total extent of the tuna fishery and associated catch data used in the assessment. There is additional concern regarding the contracting spatial extent of Korean and Japanese frozen longline fleets. It is recommended that other CPCs develop CPUE series for consideration in stock assessment of bigeye tuna. Standardised CPUE indices can either be included in an integrated modelling platform or contribute to overall knowledge of various components of the stock. Development of appropriate CPUE standardisations can be supported by the Secretariat or completed by the Secretariat (if appropriate operational data are provided).
- Ageing data: Currently there are a total of 253 data points for BET within the assessment model. This represents a minute percentage of the fish being caught. The samples cover only a few years of fishing, all within the last 10 years. It is strongly recommended that more fish are aged, encompassing both male and female fish, from all length-bins across the spatial extent of the fishery, to build a reasonable timeseries of biologically informative data. Age data should be accompanied by detailed information on the source of the fish (e.g. time, date, location, sex, fishing gear, vessel flag etc.) if the data are to be used to either estimate age-at-length within the model (as data need to be allocated to appropriate timesteps, model areas, and model fleets) or to account for changes in age-at-length over time or space (due to population dynamics, environmental factors, such as climate change or high fishing effort).

## **ACKNOWLEDGEMENTS**

This stock assessment was informed by previous assessments of bigeye tuna (*Thunnus obesus*) in the Indian Ocean, and from reading reports of recent assessments undertaken by the International Commission for the Conservation of Atlantic Tunas (ICCAT), the Western and Central Pacific Fisheries Commission (WCPFC), and the Inter-American Tropical Tuna Commission (IATTC) in the Atlantic, Western Pacific, and Eastern Pacific Oceans respectively. The 27th meeting of the Working Group for Tropical Tunas in May 2025 (Data Preparatory meeting) provided the starting input parameters, and various scenarios to test for model sensitivities, alongside possibilities for the final grid of models presented in this report, that will be discussed and finalised at the 28th meeting of the Working Group for Tropical Tunas (Assessment meeting) in October 2025, in Seychelles.

The assessment benefited greatly from updated ageing data provided by Dr. Paige Eveson, Dr. Jessica Farley, and the team at the Commonwealth Scientific and Industrial Research Organisation of Australia (CSIRO), and from updated abundance indices (catch per unit effort (CPUE)) from longline vessels (joint CPUE from Japan, Taiwan(China), and Korea), and purse seine vessels (CPUE lead by European Union (Spain), at ASZTI).

The abundance index for the longline fleet was developed as a collaborative effort between three nations, and the presence of observers (Dr. Gorka Merino, Dr. Simon Hoyle, Dr. Genevieve Phillips), and the authors of the assessment would like to acknowledge the efforts of this group in developing, reviewing, and producing three separate species' abundance indices in one year.

The assessment was greatly assisted by active discussions at the 27th meeting of the Working Group for Tropical Tunas in May 2025 (Data Preparatory meeting), and we acknowledge the preparation, and on-going active participation of all participants for the 28th meeting of the Working Group for Tropical Tunas (Assessment meeting) in October 2025.

We thank all the observers who collect and provide biological data for the assessment of tuna stocks in the IOTC Area of Competence, the IOTC Data Team for providing data to allow for a complete assessment of the stock, and previous stock assessment scientists at the IOTC for their code, and previous models which form the basis of this assessment.

## 1. INTRODUCTION

This paper presents the preliminary 2025 stock assessment of bigeye tuna (*Thunnus obesus*; BET) in the Indian Ocean (IO). As in previous assessments, the objectives of the 2025 bigeye tuna assessment are to estimate population level parameters which indicate the stock status and the impacts of fishing, such as time series of recruitment, spawning stock biomass, biomass depletion, and fishing mortality. The stock status is summarised using reference points that are adopted by the Indian Ocean Tuna Commission (IOTC).

The current assessment is carried out using the stock assessment framework Stock Synthesis 3.30 (Methot, 2013, Methot & Werner, 2013) using a length-based, age- and spatially structured population model. Previous stock assessments have also been conducted using Stock Synthesis (Shono et al. 2009; Kolody et al. 2010, Langley et al., 2013a, 2013b, 2016; Fu, 2019, Fu et al, 2022) and ASPM (Age-Structured Production Model) in 2011 (Nishida & Rademeyer, 2011). A summary of previous models from the last four stock assessments follows.

In 2013, there was a thorough examination of the key model assumptions, and the outputs from the assessment provided the basis for the management advice for bigeye tuna during the 15<sup>th</sup> Working Party for Tropical Tunas (WPTT15). However, the spatial dynamics of these models were not considered to adequately represent the dynamics of the stock, specifically the regional distribution of biomass, and the movement dynamics. Sensitivity runs suggested the model was sensitive to the spatial structure of the model (one or three regions), the tag mixing period (four or eight quarters), and the relative weighting of the length-frequency data. The final assessment models did not incorporate the available tagging data due to these issues.

In 2016, therefore, the stock assessment included a review of the spatial stratification and parameterisation of the models so that the tagging data could be integrated into the model [Langley, 2016; IOTC 2016]. The 2016 assessment model utilised the new composite longline catch per unit effort (CPUE) indices derived from the main distant water longline fleets, replacing the Japanese longline CPUE indices used in the previous assessment. A range of sensitivity runs were conducted, relating to natural mortality (M), selectivity and stock-recruitment (h) steepness. As such, the final assessment captured the uncertainty in the stock recruitment relationship (SRR), and the influence of the tagging data on the outputs. In 2016, the model estimated spawning stock biomass (SSB) to be above the SSB at maximum sustainable yield (MSY;  $SSB_{MSY}$ ). Fishing mortality (F) was estimated to be below the level that can be sustained at maximum sustainable yield ( $F_{MSY}$ ).

In 2019, the assessment adopted a new regional weighting scheme for the longline CPUE indices based on comprehensive analyses, and also adopted a revised procedure to correct for tag loss and reporting. The assessment model estimated a significant increase in fishing mortality (F) in 2018, driven by an increase in catches from the European Union (EU) purse seine fish aggregating device associated (FAD) fishery in 2018. The Working Party for Tropical Tunas (WPTT) considered this was primarily due to a change in the estimation of species composition for catches reported by the EU purse seine fleet in 2018, rather than an increase in bigeye tuna catch specifically (IOTC 2019a). The magnitude of catch increase was not considered accurate.

To incorporate catch from EU (Spain) purse seine fisheries in 2018 into the model, the catch was revised by attributing the species composition recorded in the EU (Spain) purse seine catches in 2017 to the total catches of bigeye from the EU (Spain) in 2018 see IOTC 2019a for further details.

The final assessment adopted an ensemble of 12 models that covered major components of structural uncertainty to characterise the stock status and predict future scenarios (IOTC 2019a). In 2019, the assessment estimated that the spawning stock biomass in 2018 was above  $SSB_{MSY}$ , but the fishing mortality was above  $F_{MSY}$ . The stock was determined to be **not overfished** but **experiencing overfishing**.

In 2022, the IOTC adopted a Management Procedure (MP) for recommending the Total Allowable Catch (TAC) for bigeye tuna [Resolution 22/03]. The MP contains a harvest control rule that determines the TAC for the next three years, is based on pre-agreed data inputs, and is required to be run by the Scientific Committee (SC) along a pre-arranged schedule (Williams 2021a; Resolution 22/03). As such,

the stock assessment no longer provides TAC advice, but does provide information on bigeye tuna stock status, which can be used to evaluate the performance of the MP (Williams et al., 2021b). The MP was run in 2025 (Williams et al., 2025), and an evaluation of the exceptional circumstances was presented at the same meeting (Preece et al., 2025).

In the 2025 assessment, there are only a few changes and/or improvements to the analysis in addition to the usual updates to the data. The changes are discussed in detail in the relevant sections of the report and included here briefly for clarity. The model development included testing various methods, including:

- Internal estimation of natural mortality, and application of the Lorenzen form of natural mortality (recommendation in the 2023 CAPAM Tuna Good Practices Workshop). This was carried out by the WCPFC assessment of bigeye tuna in 2023 and the ICCAT assessment of bigeye tuna in 2025.
- An update to growth parameters from a new ageing study (Eveson et al., 2025) that builds on the results presented prior to the 2022 assessment, including changing the model structure from a von Bertalanffy growth model with age-specific *k* parameters to a classical von Bertalanffy growth model.
- Internal estimation of growth parameters was tested to understand the sensitivity of the model to this method (using conditional-age-at-length, CAAL within Stock Synthesis), and to check for any potential model misspecification with relation to growth parameters currently estimated externally.
- Inclusion of both the updated joint CPUE longline indices from Japan, Korea, and Taiwan (China), and European (Spain) purse seine CPUE indices from tuna associated sets in two regions of the model.

In February 2025, the MP for bigeye tuna was run (Williams et al., 2025), and the TAC was increased and endorsed by a special convening of the Scientific Committee. The TAC increase was capped by the 15 % rule, within the MP, whereby the TAC cannot be increased by more than 15 % of the prior TAC to provide precaution within the harvest control rule.

In summary, this report documents the 2025 iteration of the stock assessment of the Indian Ocean bigeye tuna stock for consideration at the 25<sup>th</sup> WPTT due to be held in Seychelles, in October 2025. The stock assessment is based on the 2022 modelling framework and has incorporated revised and updated data up to the end of 2024, and newly available biological information. The assessment implements a length-based, age-structured and spatially explicit population model fitted to catch per unit effort (CPUE, abundance indices), length composition data, and tagging data. The assessment is implemented in Stock Synthesis (v3.30).

## 2. BACKGROUND

#### 2.1. Stock structure

Bigeye tuna (*Thunnus obesus*, Lowe 1839) is distributed across tropical and subtropical waters across the Atlantic, Indian, and Pacific oceans, while being absent from the Mediterranean. Indian Ocean bigeye tuna are genetically distinct populations from those in the Atlantic, with minimal mixing of adults (Chow et al., 2000, Grewe et al., 2019).

Tagging data from the Regional Tuna Tagging Project-Indian Ocean (RTTP-IO) phase of the Indian Ocean Tuna Tagging Programme (IOTTP) suggest that bigeye tuna migrate quickly and there may be some basin-scale movements, however the limited distribution of tag releases, and small number of returns from vessels external to the European Union (EU) and Seychelles (SEY) purse seine fleets operating in the western equatorial Indian Ocean makes it difficult to quantify large-scale population movements. While there may be some relatively discreet sub-populations, or slow mixing rates among sub-regions, there is no evidence that this is the case in the core area where most of the catch is taken, and presumably where the bulk of the population is located.

Current differences in estimates of growth between oceans supports the hypothesis of separate bigeye tuna stocks in the Indian and Pacific Oceans (Farley et al. 2004). Genetic studies indicate that bigeye tuna form a single stock in the Indian Ocean, which is not connected to stocks in the Pacific or Atlantic Oceans (Appleyard et al. 2002; Chiang et al. 2008; Díaz-Arce et al. 2020). Based on tagging data, and current genetic knowledge, the current assessment assumes the Indian Ocean bigeye tuna consists of a single stock.

In the Pacific Ocean, there have been extensive tagging and genetic studies lead by the Secretariat of the Pacific Community (SPC) and the Inter-American Tropical Tuna Commission (IATTC) (Schaefer et al., 2015; Moore et al., 2020). The tagging studies identify that most tagged fish remained within the general area of release (within 1,500 nautical miles), however some fish move large distances across the Pacific Ocean (> 4,000 nautical miles) presumably mixing with individuals from other regions and thereby reducing the probability of broad-scale genetic structure (Day et al., 2023). There is some evidence of differences in population dynamics across the Pacific Ocean (e.g. growth rates increase from west to east) which would be important to account for in stock assessment structure, however a review of all genetic and non-genetic information on bigeye tuna stock structure in the Pacific found there to be one stock within the Pacific Ocean (Hamer et al., 2023). Similar data are not available for the bigeye tuna in the Indian Ocean as of 2025, however the assessment would benefit from increased information on population structure.

Although there is no population structure within the Indian Ocean bigeye tuna stock assessment, the model partitions the data into regions to account for differences in fishery dynamics (Figure 1).

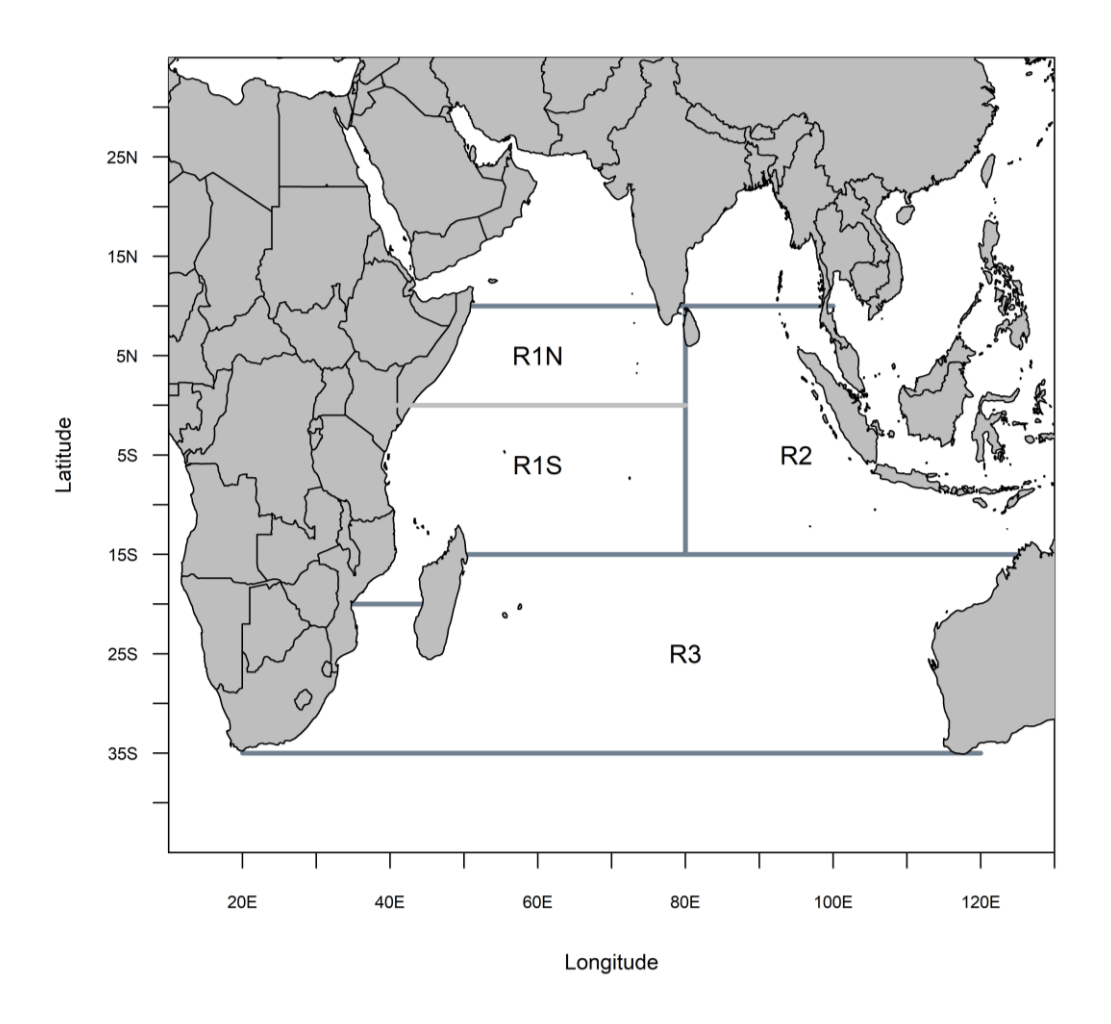


Figure 1: Spatial stratification of the Indian Ocean for the four-region assessment model.

## 2.2. Biology

Bigeye tuna, *Thunnus obesus* (Lowe, 1839) are large, highly migratory pelagic-oceanic fish within the *Scombaridae* (mackerels, tunas, bonitos). They are relatively fast-growing and have a maximum fork length (FL) of approximately 200 cm (Aires-da Silva et al., 2015; Farley et al., 2017) with an estimated average maximum length of between 169.2 to 172.7 cm in the Indian Ocean (Eveson et al., 2025). There have been two recent studies into growth information for bigeye (Farley et al., 2021; Eveson et al., 2025) which build on initial studies of otoliths (Eveson et al., 2012) and the most recent results presented at the  $27^{th}$  Working Party for Tropical Tunas (Data Preparatory) are incorporated into this assessment, with sensitivity runs to test the impact of changing the form of the growth curve (from a VB log k growth model in 2022 to a von Bertalanffy model in 2025).

The most recent study of age-at-length used ages from 253 tuna, mostly from the north-west Indian Ocean (142 samples) and builds on a study from 2021 where otoliths were collected as part of the 'GERUNDIO' project, using a new method developed to estimate the age of tuna from daily and annual growth zones within otoliths. The new estimates again represent a size-at-age that is slightly larger than the previous assessment, with a slightly longer mean asymptotic length ( $L^{\infty}$ =169.2-172.7 cm compared to 168 cm FL). There was some evidence of differences between male and female growth curves (Eveson et al., 2025), however more data are required to understand whether this is a true difference, or an artefact of sampling design. This is an area of which requires more research to fully understand the population variation in growth in bigeye tuna.

Bigeye tuna are assumed to attain maturity from 100 cm FL and reach full sexual maturity at 125 cm FL (Shono et al., 2009). Bigeye tuna are hypothesised to be continuous spawners, meaning that when conditions are suitable, they spawn almost daily (Sun et al., 2013). Peaks in spawning have been recorded during the first and fourth quarters of the calendar year (Kume et al., 1971; Sun et al., 2013).

Eggs and larvae are pelagic, presumably allowing for genetic mixing throughout the Indian Ocean as tagging studies in both the Indian and Pacific Oceans have showed that adult tuna only really mix with adjacent individuals (Schefer et al., 2015; GERUNDIO Project, IOTC).

Bigeye recruitment remains uncertain as the areas where larvae and early juveniles are concentrated have never been sampled nor studied by scientists (Fonteneau 2004). While the temperate regions are generally believed to be feeding grounds, recruitment is assumed to occur in all regions (hence differentiating between recruitment into the population, vs. spawning.)

The natural mortality (M) rate of bigeye tuna is likely to vary with size, as with other tropical tunas (Fonteneau & Pallares, 2004), with a relatively high natural mortality for younger fish, and a lower natural mortality for older fish. From the Regional Tuna Tagging Project (RTTP) data, many tagged fish were captured after 7–8 years at liberty, indicating a considerable proportion of the tagged fish had reached an age of 8–10 years; 8 tags were recovered after 10 years at liberty and a few tags were recovered during the last year (2015), corresponding to an age at recovery of 11–12 years. An aging study of bigeye tuna in the eastern and western Australia waters suggested the longevity of bigeye is more than the 8–10 years which were the maximum age commonly thought (Farley et al. 2004).

There is no additional information on the oldest bigeye tuna since the previous assessment, so this remains at 14.7 years old (Farley et al., 2020).

## 2.3. Indian Ocean bigeye tuna fishery overview

Bigeye tuna is an important species within tuna fisheries in the Indian Ocean. As with other tuna fisheries, larger individuals are targeted by longliners, while smaller individuals are caught by purse seine vessels utilising Fish Aggregating Devices (FADs) (Fonteneau 2004). The distant-water longline fishery for bigeye tuna started operation in the Indian Ocean during the early 1950s.

The distant-water longline fishery commenced operation in the Indian Ocean during the early 1950s. At the start of the fishery, bigeye tuna represented a significant component of the total catch from the longline fishery and catches increased steadily over the subsequent decades, reaching a peak in the late 1990s—early 2000s. The purse-seine fisheries and fresh-chilled longline fisheries developed from the mid-1980s, and total bigeye tuna catches peaked at about 150,000 t in the late 1990s (Figure 2). During the mid-2000s, the total annual bigeye catch declined considerably, primarily due to a decline in the longline catch in the western equatorial region in response to the threat of piracy off the Somali coast. The total annual catch declined to around 85,000 t in 2010 but recovered somewhat over the following years, reaching around 125,000 t in 2012. The total annual catch has declined since then and was 96,000 in 2018 (there were exceptionally high catches from the purse seine fisheries during 2018 which were potentially biased by changes in data processing methodologies confirmed by the EU (Spain) for its purse seine fleet for that year, see IOTC 2019 a, b). The annual catch decreased in 2019, but increased in 2020, and was around 95 022 t in 2021 before revisions to catch by Indonesia. The revised total catch for 2021 is approximately 90,882 t, and this remained steady in 2022 at 90,836 t before increasing significantly in 2023 (105,209 t) and 2024 (101,722 t).

The 2023-2024 catches are in the same range as peak catches seen between the late 1990s and 2008, although the catch is more evenly distributed among different fishing gears compared to the domination of the frozen longline fleets previously.

During the mid-1970s, the target species of Japanese longliners rapidly shifted from yellowfin to bigeye, accompanied by the introduction of deep-freezing technology that increased the value of Sashimi-grade bigeye (Okamoto 2005). However, since the 1990s, the bigeye component of tropical tuna catches has decreased, and the catch of yellowfin now exceeds that of bigeye. These changes in catch composition were thought to be caused by fleet dynamics whereby a shift in spatial effort occurred and the fishery moved to the yellowfin-dominant region of the western Indian Ocean. Most of the bigeye tuna catch from the Indian Ocean line fisheries is caught within the latitudinal range 35° S to 10° N.

## 3. DATA INPUTS

#### 3.1. General notes

Data used in this stock assessment consist of catch and length composition data, longline, and purse seine CPUE indices, and tag-recapture data. In this iteration of the assessment, conditional age-at-length data from a recent study (Eveson et al., 2025) are also used directly as data in the assessment model, for one of the sensitivity runs as was recommended by the review of the 2024 yellowfin tuna assessment and suggested by the participants of the data preparatory meeting. Data are continually being improved and as such catch and length composition datasets may not be identical to those in previous assessments. Where data inputs have substantially changed, it is noted in the sections below, and links to relevant methods papers are provided for further detail.

Model input files along with reproducible code to run the assessment, and all sensitivities are stored by the Secretariat and are available on request.

## 3.2. Spatial stratification

Stock assessment models often adopt regional structures to account for differences in biological characteristics of the species, regional exploitation pattern, or the level of mixing amongst subpopulations (Vincent, et al. 2018). In the 2013 bigeye assessment (Langley *et al* 2013a), the assessment model was stratified into three regions: western equatorial region (region 1), eastern equatorial region (region 2) and southern region (region 3). Most of the longline catch is taken within the two equatorial regions (regions 1 and 2; 15° S to 10° N), while the purse seine catch is predominantly taken within the western equatorial region (region 1).

A seasonal longline fishery operates in the southern region (region 3). The longitudinal partitioning of the equatorial area subdivides the distribution of tagged fish recoveries from releases that occurred in region 1. There are also some differences in the temporal trends in the longline CPUE indices from the three regions. The regional restructure was further refined in the 2016 assessment where the western equatorial region (region 1) was subdivided to account for differences in the distribution of tags within this region (see section 2.5 of Langley 2015). Region 1 was therefore partitioned at the equator into the area south of the equator and the area north of the equator, denoted as Region 1S and Region 1N, respectively (Figure 1). The four-region structure was adopted in the 2019 assessment, was used in the 2022 assessment, and is also used in the current assessment.

#### 3.3. Temporal stratification

The model covers the time period from 1975 – 2024, and assumes an exploited, equilibrium initial state in 1975. Within the model period, annual data are compiled into quarters (Jan–Mar, Apr–Jun, Jul–Sep, Oct–Dec), and the model is iterated using a quarterly time step (representing a total of 192 time steps) which as treated as a model year in Stock Synthesis (SS3). The quarterly timesteps were used to approximate the continuous recruitment of bigeye.

#### 3.4. Definition of model fleets

In SS3, data are required to be aggregated or defined in "fleets" within the overall fishery. Individual fleets represent relatively homogenous fishing units, with similar selectivity and catchability characteristics that do not vary significantly over time. Twenty-four (or twenty-two, depending on whether the purse seine CPUE indices were included) fleets were defined in the model (Table 1), of which, there are six "survey" fleets, for which only CPUE indices were assigned. The use of "survey" fleets for the CPUE indices was chosen as these indices are based on aggregated datasets and allow for separate estimation of selectivity and catchability within the model framework. Fleets were defined based on the fishing gear type, fishery type (e.g. fresh vs. frozen or free school vs. fish aggregating device (FAD) associated sets for purse seiners), and fleet dynamics (e.g. spatial and temporal extent of the fishery).

The definitions of model fleets were the same as those used in the previous two iterations of the SS3 stock assessment. The main longline fishery was split into two main fleets based on vessel type (fresh vs. frozen). Freezing longline fisheries are defined as vessels using drifting longlines for which one of

the following conditions apply: (i) the vessel hull is made of steel; (ii) vessel length is 30 m or longer; (iii) most of the catch of target species are frozen. A composite frozen longline fleet was defined in each region (LL1N, LL1S, LL2, LL3) aggregating the longline catch from all freezing longline vessels.

The fresh tuna longline fishery is comprised of vessels those using drifting longlines for which one of the following conditions apply: (i) the vessel has a fibreglass, Fibre-Reinforced Plastic (FRP), or wooden hull; (ii) vessel length is less than 30 m; (iii) the catch of target species remains fresh or in refrigerated seawater. Most fresh-tuna longline vessels operate in region 2, therefore the fresh-tuna longline fleet is comprised of vessels principally from Indonesia and Taiwan (China) in region 2 (FL 2).

The purse seine catch fisheries are defined into two groupings based on the fishing methods used: catches from sets on FAD-associated schools of tuna (purse seine log school; PSLS) and from sets on free schooling tuna (purse seine free schools; PS FS). Purse seine fisheries operate within region 1N, region 1S, and region 2. Individual purse seine fleets were therefore defined for each region separately.

A single bait boat fleet was defined within region 1N. The fishery included the pole-and-line and small seine fisheries (so-called as they catch smaller fish). Most of the catch associated with this fleet occurs in region 1N, with small amounts of catch from regions 1S and region 2, for the stock assessment, all catch is assigned to the bait boat fleet in region 1N.

An additional line-based fleet was defined within region 2, representing a mixture of fisheries that use handlines, small longlines, and the gillnet and longline combination fishery of Sri Lanka. Although some handline catch is taken from a fishery in region 1, all catch data were assigned to the line fleet in region 2.

For region 1N and region 2, a miscellaneous ("Other") fleet was defined comprising catches from artisanal fisheries other than those specified above (e.g. gillnet, trolling and a range of small gears).

Table 1: Definition of model fleets within the SS3 model for bigeye tuna in the Indian Ocean, including the gear types used, and region that data are assigned to in the model.

Code	Method	Region	Notes
FL2	Longline, fresh tuna fleets	2	
LL1N	Longline, frozen tuna	1N	
LL1S	Longline, frozen tuna	1S	
LL2	Longline, frozen tuna	2	
LL3	Longline, frozen tuna	3	
PSFS1N	Purse seine, free schooling	1N	
PSFS1S	Purse seine, free schooling	1S	
PSFS2	Purse seine, free schooling	2	
PSLS1N	Purse seine, FAD associated sets	1N	
PSLS1S	Purse seine, FAD associated sets	1S	
PSLS2	Purse seine, FAD associated sets	2	
BB1N	Bait boat and small-scale encircling gears (PSS, RN)	1N	Primarily catch from the Maldives bait boat fishery.
LINE2	Mixed line gears (handline, gillnet/longline combination)	2	Gears grouped on the basis that primarily catch large bigeye tuna.
OT1N	Other (trolling, gillnet, unclassified)	1N	
OT2	Other (trolling, gillnet, unclassified)	2	

## 3.5. Catch data

#### 3.5.1. General notes

Catch data were compiled based on the fleet definitions in Table 1. An update of quarterly catches by fleet was provided by the IOTC Secretariat, including catches since the last assessment (2022–2024 IOTC-WPTT27-AS-BET-CEraised\_1950-2024.

The catch time series was very similar to that of the previous assessment, except for the case of the Indonesia data where revised estimates of data from all fisheries has caused differences in the total catch of bigeye tuna.

Total annual catches for 2022, 2023 and 2024 included in the updated catch history are 90,832, 105,210, 101,722 t respectively (Table 2). The total catch in 2023 is the highest amongst the last five years, with only a slight drop in 2024 (Figure 2, Table 2).

Table 2: Recent bigeye tuna catches (metric tonnes, t) aggregated by model fleet that have been included in the stock assessment model. The annual catches are presented for 2020-2024.

Fleet	2020	2021	2022	2023	2024
FL2	7,772	8,885	10,205	11,518	7,846
LL1S	14,255	14,729	8,635	10,352	13,407
LL2	4,228	5,008	4,370	4,135	4,875
LL3	3,102	3,144	2,641	2,868	2,957
PSFS1S	3,176	2,257	6,190	9,659	5,753
OT1N	2,990	1,709	2,191	3,363	7,600
OT2	3,225	4,310	5,471	5,385	5,463
PSLS1S	10,886	10,236	13,294	12,721	10,543
PSLS2	2,351	3,308	6,867	10,480	10,473
BB1N	1,664	1,771	1,901	7,501	7,702
LINE2	9,989	9,521	8,020	10,050	10,756
LL1N	5,568	2,208	5,114	4,917	3,530
PSFS1N	742	6,393	1,065	1,456	2,265
PSLS1N	9,473	17,403	14,872	10,804	8,552
Total	79,421	90,884	90,832	105,210	101,722

## 3.5.2. Longline, frozen (LL1N, LL1S, LL2, LL3)

The frozen longline fleets operate throughout the Indian Ocean although catches are concentrated in the equatorial region. Catches were primarily from Japanese, Korean and Taiwanese (China) distant-water longline vessels. Most (62%) of the frozen longline catch has in the past been taken from the western equatorial region and annual catches from the LL1 fishery (LL1S and LL1N) steadily increased from the early 1950s to reach a peak of 64,000 t in 2003–2004. Catches of approximately 55,000 t were maintained during 2005–07, before declining rapidly to  $\sim$  15,000 t in 2010–2011. In 2012, catch increased again to  $\sim$  50,000 t, before again declining to  $\sim$  14,000 t in 2018 (Figure & 3). The catch from LL1N and LL1S in 2024 has increased to 16,937 t.

Annual catches from the LL2 fleet fluctuated between  $\sim 10-15{,}000$  t from 1975 to 2011. In the subsequent years, catches have declined sharply to  $\sim 3-4{,}000$  t between 2017 and 2021 (Figure ,3). The catch in 2024 has increased slightly to 4,875 t.

Annual longline catches from the LL3 fleet were comparatively low, averaging  $\sim 3,000$  t from 1960 to 1990 (Figure ,3). Catches then increased to a significant peak of 22,000 t in 1995, before declining steadily to  $\sim 5,000$  t in 2007, remaining at that level until around 2018 when catches again declined to  $\sim 3,000$  t between 2018 - 2021, and have remained steady at approximately 3,000 t in the years since the last assessment (2022-2024).

#### 3.5.3. Longline, fresh (FL2)

The fresh tuna fleets developed in the late 1980s, and annual catches rapidly increased to reach a peak of  $\sim 30-35{,}000$  t in the late 1990s to early 2000s. Catches declined sharply in 2003 and then again in 2010, as some vessels moved south to target albacore tuna (*Thunnus alalunga*). Annual catches were  $\sim 12{,}000-15{,}000$  t between 2011 and 2015 and declined to  $\sim 7{,}000-9{,}000$  t during 2017–2021 (Figure ). Catches increased to  $> 10{,}000$  t in 2022 and 2023, before declining to 7,846 t in 2024.

## 3.5.4. Purse seine (PSFS1N, PSFS1S, PSFS2, PSLS1N, PSLS1S, PSLS2)

Almost all of the industrial purse-seine catch was taken within the western equatorial region and catches were dominated by the FAD associated schools (PSLS1N and PSLS1S) (Figure 3). Annual catches from

the PSLS1 (N and S) fisheries reached a peak of  $\sim 30,000$  t in the late 1990s and have fluctuated at 15 - 25,000 t over the last decade, except for 2012, when lower catches occurred. Since the late 1990s, annual catches from the purse-seine free-school fishery (PSFS1N and PSFS1S) have fluctuated between 50-100,000 t. While the activities of purse seiners have also been affected by piracy in the western Indian Ocean, the decline in catches were not as marked as for longline fleets (IOTC 2018a, b). Relatively minor catches were taken intermittently by the purse-seine fisheries in the eastern equatorial region.

There was a marked increase of reported catches on the purse seine FAD-associated schools in 2018. The WPTT21 considered this magnitude of increase of catches is not credible and is likely to have reflected several changes related to the methodologies to produce catch statistics by EU,Spain in 2018. The WPTT21 identified a methodology to revise the bigeye tuna catches reported by EU,Spain in 2018 (limited to their log-associated school component), which applied the species composition recorded for the log-associated component of EU,Spain purse seine catches in 2017 to the total catches (log-associated) reported in 2018 by the same fleet (IOTC 2019a). The method was subsequently developed further during the WPDCS15 (IOTC 2019b), which applied a spatial-temporal re-estimation procedure, based on several proxying scenarios. The WPTT24(DP) in 2022 agreed to use the proxying scenario number four (as recommended by the WPDCS15) to re-estimate Spanish purse seine catch for the 2022 stock assessment model (IOTC 2022). This approach caused marked reductions in catches of bigeye tuna reported by the EU purse seine fleet component in 2018 (~ 12,000 t). The purse seine FAD-associated sets' catch significantly increased in 2021, with catches from region 1N more than doubling those of the previous year (Table 2).

Annual catches for each fleet are outlined in Table 2.

### 3.5.5. Bait boat (BB1N)

Bigeye tuna catch from the Maldives bait boat fishery are assigned to the BB1N fleet in the model. They are estimated to have increased steadily from minimal catches in the late 1970s to  $\sim$  6-7,000 t in recent years (FIGURE 4). Catches decreased to  $\sim$  5,000 t in 2018 but then increased significantly to a peak of 8,600 t in 2020, declining again to 7,000 t in 2021. Catches increased in 2024 to 7,702 t.

#### 3.5.6. Line, small-scale (LINE2)

This fleet encompasses small-scale fisheries that use handlines, small longlines, and the gillnet/longline combination fishery of Sri Lanka. Similarly to the BB2 fleet, catches increased from a minimal level in the 1970s to a peak of 12,000 t in 2020. Catches in 2023 were 10,756 t.

## 3.5.7. Other (OT1N, OT2)

The fisheries included in the 'other' fleets are gillnet, trolling, and other minor artisanal gears not covered in the other fleets. Data are split into two regions within the equatorial ocean. Within the western Indian Ocean, the OT1 fleet is primarily comprised of the Iranian driftnet fishery that operates on the high seas. Total catches were negligible prior to 2005 but have increased to 3,363 t (OT1N) and 5,385 t (OT2) in 2023 (Figure 3). Catch increases are attributed to major changes within the fisheries, including gear creep (increase in boat size, development of fishing techniques) and a change in fishing areas (IOTC 2018). The OT2 fleet is primarily comprised of the Indonesian troll and gillnet fisheries.

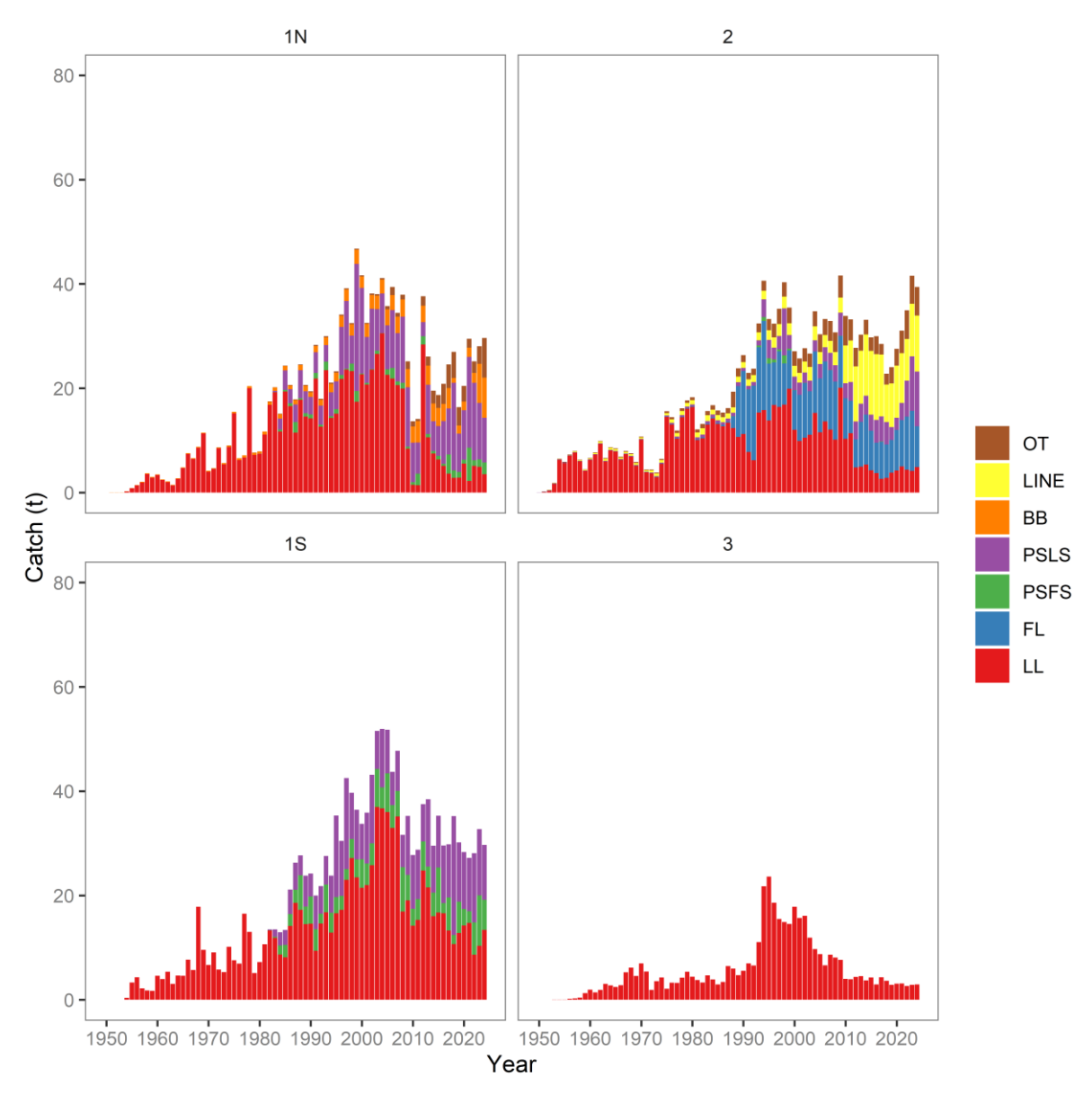


Figure 2: Fishery catches (x 1000 metric tonnes) aggregated by model region and coloured according to fishing fleet in the model.

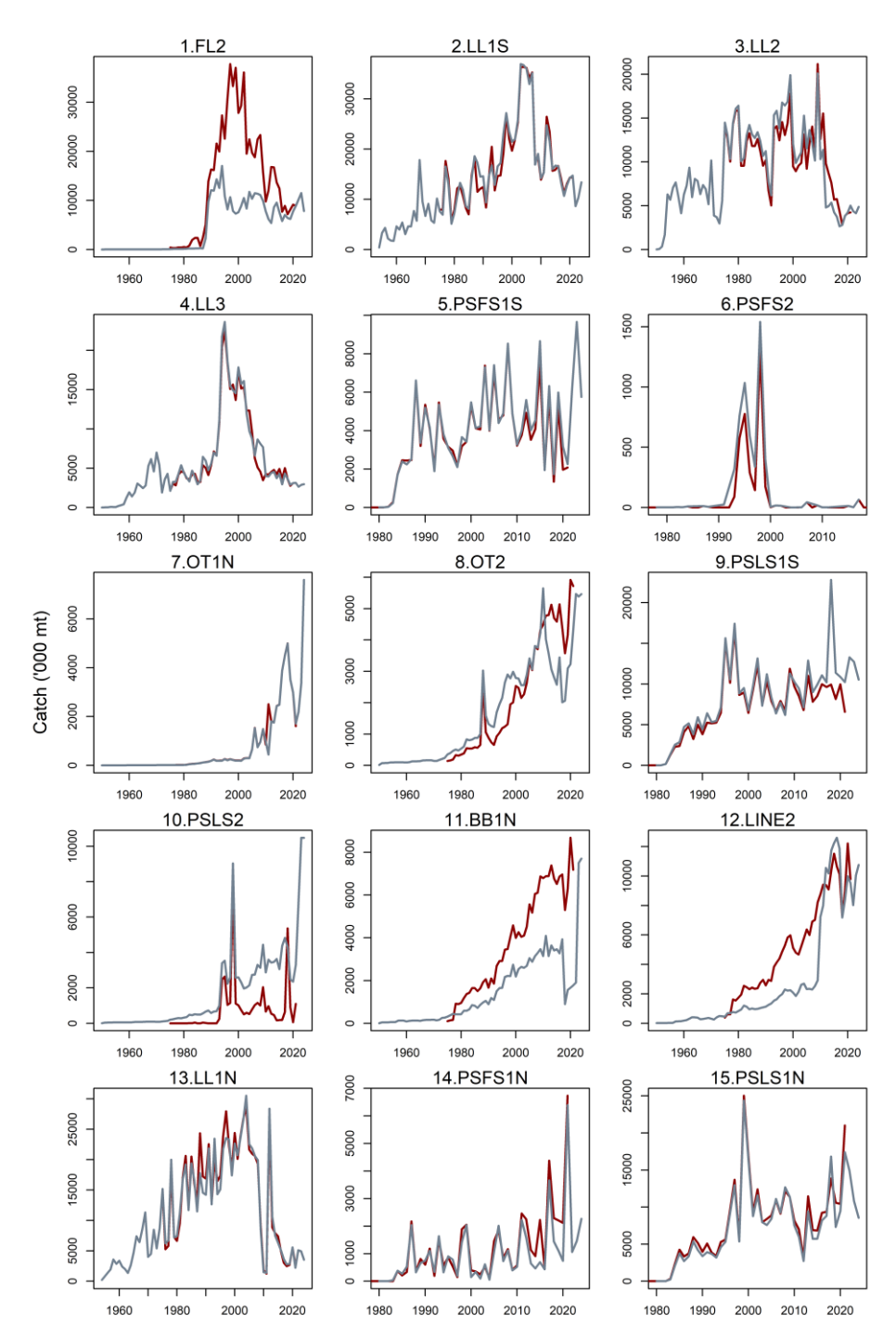


Figure 3: Fishery catches (metric tonnes) aggregated by year. Note the y-axes differ between plots. Red lines are catches used in the 2022 assessment. The differences in catch are mainly due to the revision of catch data by Indonesia, although some changes will be due to general improvements in the data quality over time.

#### 3.6. Abundance indices

## 3.6.1. Longline CPUE

The 2022 assessment used longline CPUE series provided by Japan, Korea, and Taiwan (China) developed during a joint-CPUE workshop (Kitakado et al., 2022) and the 2025 assessment includes longline CPUE series that have been developed by the same collaborative effort between Japan, Korea, and Taiwan (China). The series were presented at the 27<sup>th</sup> Working Party for Tropical Tunas (Data Preparatory) (IOTC-2025-WPTT27(DP)-09) alongside a report detailing the methods (Kitakado et al., 2025). The CPUE series were developed at a joint workshop where there were outside observers, but only the three nations had access to the operational data.

The CPUE standardisation included operational data on catch numbers by species, spatio-temporal data (1° latitude and longitude; daily records), vessel identification (vessel ID), number of hooks used, hooks between floats (HBF – for regions 1N, 1S and 2), and clustering outcomes for region 3 to account for changes to target species during fishing operations. Data covers the period 1979 - 2024 (Japan and Korea), and 2005 - 2024 (Taiwan, China). Data screening took place to ensure only relevant data were included – e.g. vessels needed to have  $\geq 20$  data points; with  $\geq 10$  positive (e.g. non-zero) CPUE data; and data were subjected to 20 % sub-sampling in each of the spatio-temporal covariates.

Generalised Linear Models (GLMs) were used to standardise the CPUE using the following covariates: time (quarters); location (5  $^{\circ}$  latitude x longitude grid); vessel ID; cluster category (e.g. target species); HBF as a mean value, allowing for depth stratification (shallow:  $\leq$  7 HBF; medium: 8 – 13 HBF; and deep water:  $\geq$  14 HBF).

The indices produced show broadly the same trends as the analyses in 2019, and 2022, despite differences in the methods used (see Kitakado et al., 2025 for more details; Figure 4). There has been a slight increase in standardised CPUE in 2025 for the final few years, which is especially evident in region 2. It is unclear whether this is due to changes in abundance, or differences in the data available for this region.

The CPUE time series is used as the main abundance index from 1979 to 2024 for each of the four model regions (1N, 1S, 2, and 3).

The earlier assessment used the indices developed from the longer time series (1953–2015) but excluded the years prior to 1979 for several reasons: the decline in the indices during the late 1960s—early 1970s is inconsistent with the relatively low level of catch. The 2–3-fold increase in the indices during 1976–1978 was considered to be related to factors other than abundance (Kolody et al 2010, Langley et al 2013b, Langley 2016, Hoyle et al. 2017a).

\_

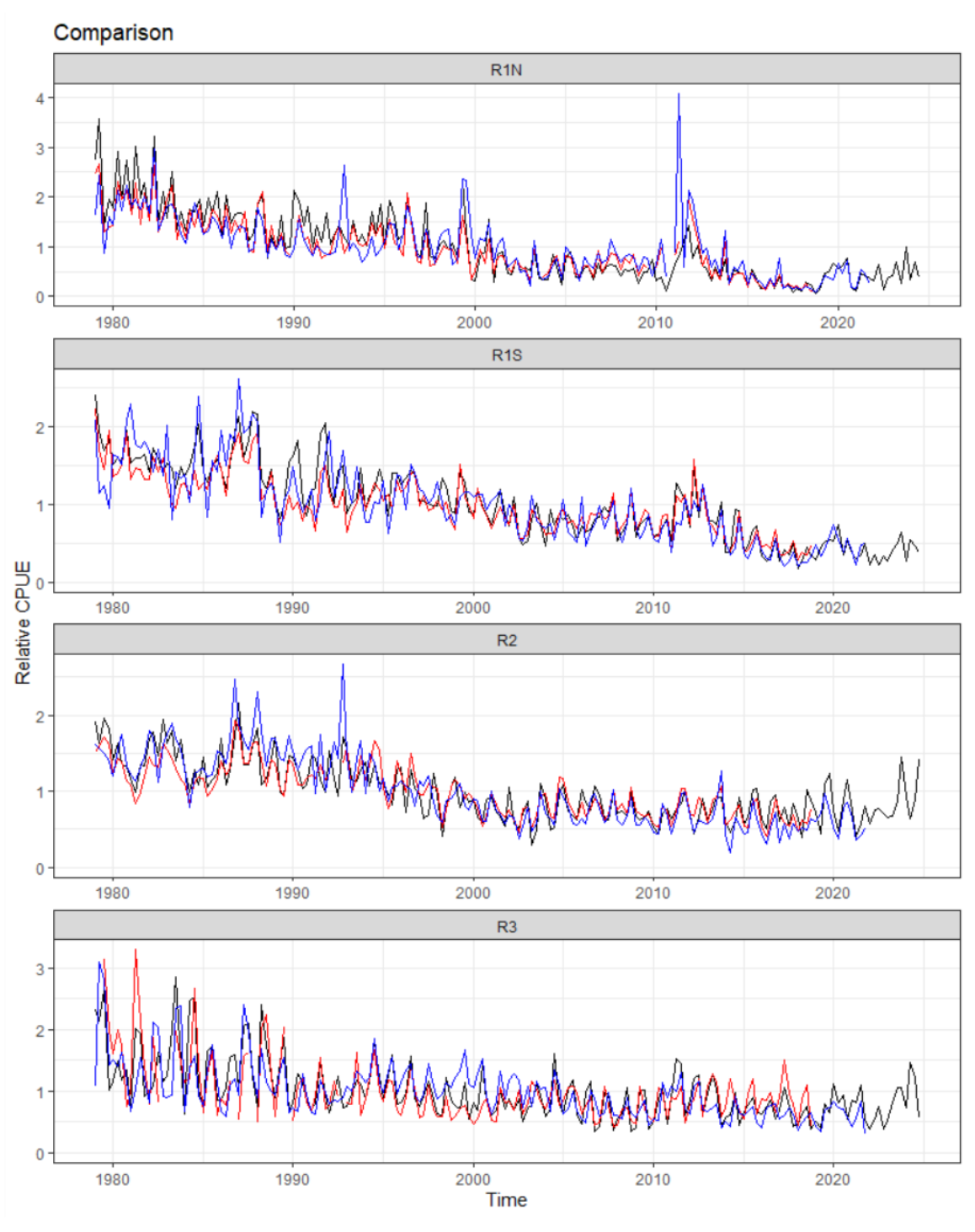


Figure 4: Standardized CPUE series produced in 2019 (red), 2022 (blue), and 2025 (black). Operational-level data were used in the 2019 and 2025 analyses, while aggregated data were used in 2022.

The standardised quarterly CPUE indices used as inputs to the assessment are shown in Figure 4 . The CPUE indices from the four regions exhibit broadly comparable trends, declining by about 65-75% from the early 1980s to 2010s. In the western equatorial regions (regions 1N and 1S), the decline from 1979 to the early 2000s is greater in the northern subregion (region 1N), but this region started from a higher starting CPUE. Both regions have standardised CPUEs that are at the lowest mean point over the entire timeseries of the fishery. The indices in both R1N and R1S peaked in 2011 when the main fleets returned to the main fishing ground but declined rapidly to the lowest level in 2018. Both indices, however increased moderately during 2019 – 2021, and have stabilised around this level up to 2024.

In the eastern tropical region (region 2) there is also a general decline in CPUE since 1980, although the CPUE is relatively stable until the mid-90s when the CPUE remains relatively stable until 2018 when fluctuations in CPUE increase, leading to a relative increase in CPUE from 2021-2024 to levels not seen since the mid-1990s, considering the general reduction in both catch and effort in this area (for Korea and Taiwan, China, for which data are provided), this increase may not be reflective of an increase in abundance, but more an artefact of data availability, and should be treated with caution.

The index in region 3 (temperate region) has remained relatively stable since the start of the timeseries, although again there is an increase in CPUE in the final three years since the last assessment (2022-2024.

In each region, the annual trend in the indices is generally very consistent among all quarters. The CPUE indices from region 3 exhibit considerable seasonal variation, with lower CPUE in the first and fourth quarters (austral summer), and relatively high CPUE in the second and third quarters (austral winter). This seasonality is also somewhat reflected in the longline length composition data, with large fish caught in the third quarter and smaller fish in the first and second quarters. SS3 does not have the flexibility to estimate seasonal catchability or movement dynamics when the model is configured based on a quarterly time step. Consequently, to account for the seasonal variation in the CPUE indices, the Region 3 CPUE indices were incorporated in the model as four separate sets of abundance indices (i.e. one series for each quarter). This follows the same method used in 2022 as there was no evidence to support a different structure within the model.

For the regional longline fleets, a common catchability coefficient was estimated in the assessment model, thereby, linking the respective CPUE indices among regions, as was done in the 2022 model. This significantly increases the power of the model to estimate the relative (and absolute) level of biomass among regions. However, as CPUE indices are essentially density estimates it is necessary to scale the CPUE indices to account for the relative abundance of the stock among regions. The approach used was to determine regional scaling factors that incorporated both the size of the region and the relative catch rate to estimate the relative level of exploitable longline biomass among regions (Hoyle & Langley 2018, Table 3). The relative scaling factors are R1N: 0.799, R1S: 1.000, R2: 0.373+0.486 (0.859), R3: 0.626. These factors are the same as those used in the previous assessment <sup>1</sup>. For each of the principal longline fisheries (LL1N, LL1S, LL2, LL3), the standardised CPUE index was normalised to the mean of the period for which the region scaling factors were derived (i.e. the GLM index from 1979–1994). The normalised GLM index was then scaled by the respective regional scaling factor to account for the regional differences in the relative level of exploitable longline biomass among regions. This follows the same methods as in the 2022 assessment.

Overall, the 2025 CPUE indices show similar trends to the 2022 assessments (Figure 5).

29

<sup>&</sup>lt;sup>1</sup> The values quoted in the report for the assessment were not the values implemented in the assessment model runs.

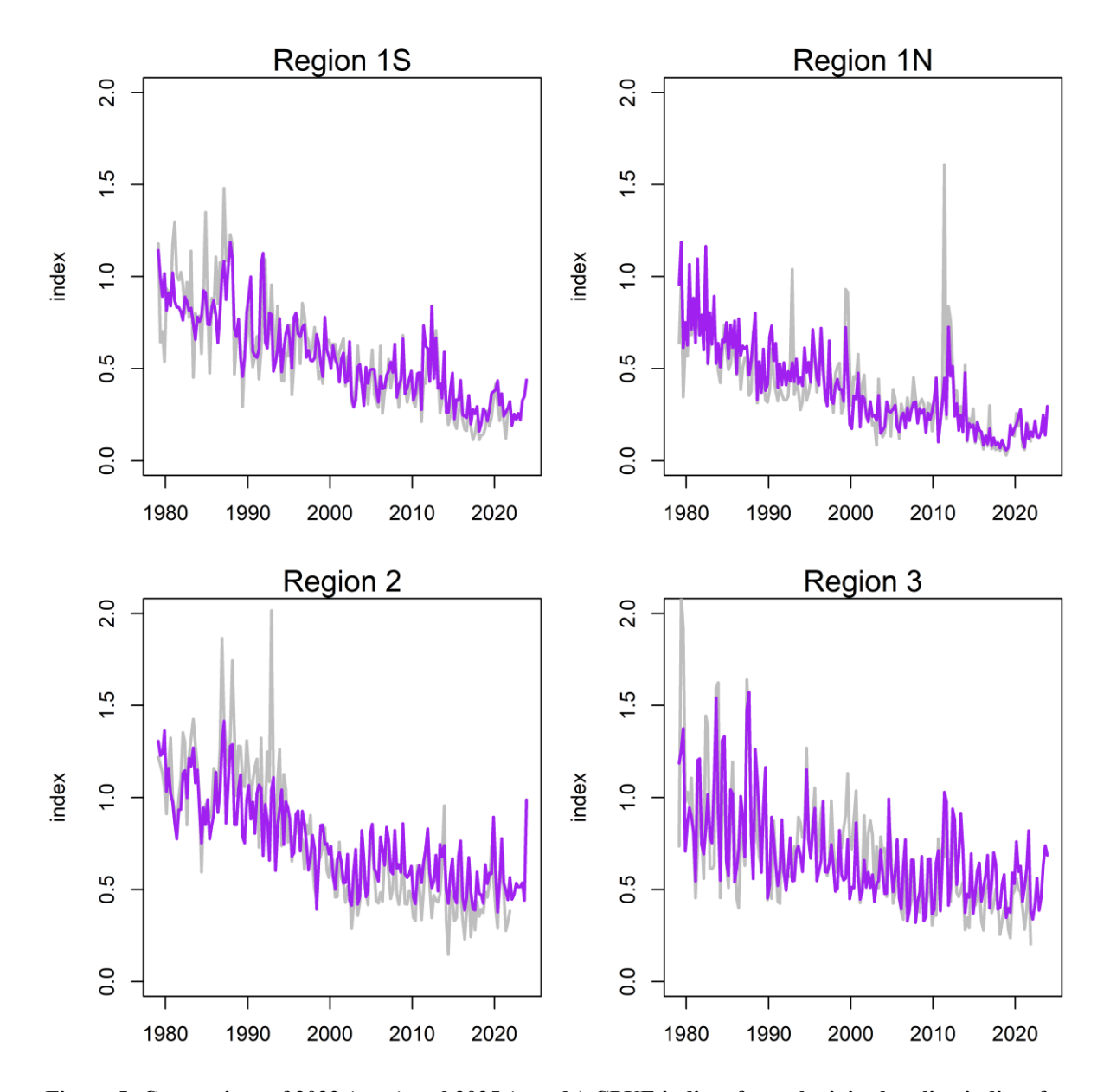


Figure 5: Comparison of 2022 (grey) and 2025 (purple) CPUE indices from the joint longline indices from Taiwan (China), Korea, and Japan.

#### 3.6.2. Purse seine CPUE

The European Union (EU) purse seine fishing vessels in the Indian Ocean have benefitted from observer sampling, and extensive logbook reporting from 1991-2024, and as such there is sufficient data from which to perform CPUE standardisation. As in 2022, standardised indices of bigeye tuna CPUE were developed by the European Union (Spain) (Correa et al., 2025). As purse seine vessels primarily capture smaller individuals, it is hypothesised that CPUE indices from these data can provide abundance indices for juvenile bigeye tuna and therefore likely provide some information on recruitment into the fishery.

Two sets of regional (region 1N and region 1S) indices were developed for two separate timeframes. The 'short' indices were based on data from 2010-2024 using detailed covariates that account for the use of drifting FADs (dFADs) by vessels, and 'long' indices that were based on data from 1991-2024 that do not include these additional covariates. Both indices show similar trends and overlap well over the time period covered by both sets of indices (2010-2024; Figure 6). Although the shorter indices include more covariates that could help with standardisation and explanation of CPUE trends, the authors found that dFAD covariates 'generally had significant impacts on BET (bigeye tuna), but there

[sic] impacts were often contradictory and quite small'. They hypothesise that the bycatch nature of bigeye tuna may go some way to explain the equivocal impact of dFAD covariates on CPUE standardisation.

Sea surface temperature (SST) was found to be the most important environmental explanatory variable, and this was included in both the short and long indices, perhaps confounded with time of day, as juvenile bigeye tuna are known to migrate vertically diurnally (Hino et al., 2019).

For these reasons, although both the long and short indices were tested in the model as sensitivities, the final base model includes the long index as it provides data across a longer time period, and the current scientific estimates show that including dFAD covariates as yet have little impact on the CPUE standardisation, and environmental variables likely have more impact on the abundance and density of juvenile / sub-adult bigeye tuna.

The purse seine CPUE indices were implemented in the SS3 framework as two additional 'survey' fleets, with mirrored selectivity to the PSFS1N and PSFS1S fleets respectively.

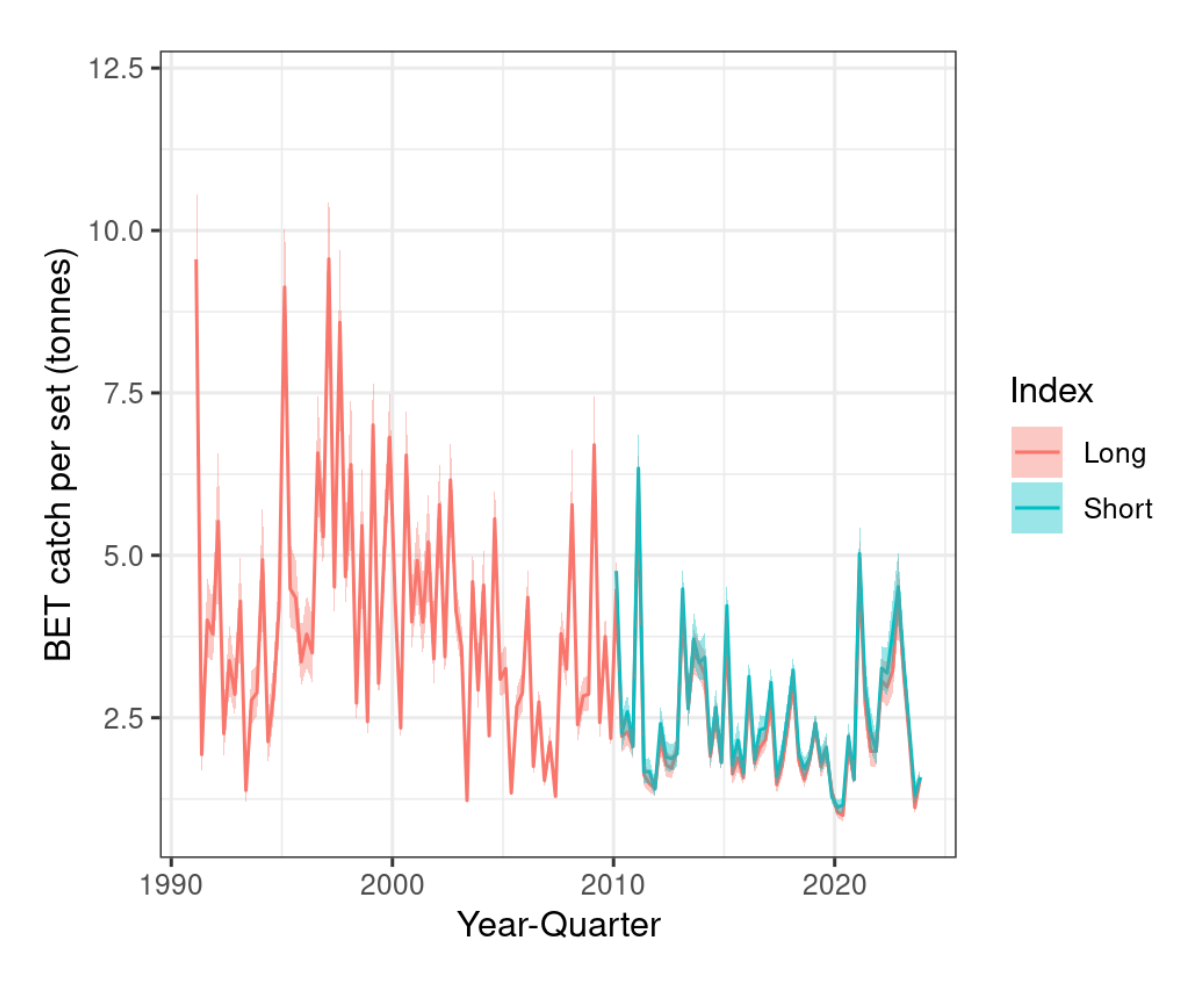


Figure 6: Quarterly standardized CPUE index for the long and short time series superposed (Correa et al., 2025).

To ensure that there was no conflict introduced into the model by including the purse seine CPUE indices, a quantitative comparison between the longline and purse seine CPUE trends was completed using methods developed elsewhere but used within other IOTC Working Parties. This analysis confirmed that all CPUE indices showed similar trends and therefore could be included within the base model (Appendix B).

## 3.7. Length frequency data

Available length-frequency data for each of the defined fisheries were compiled into 95 2-cm size classes (10–12 cm to 198–200 cm) and were aggregated to provide a composite length composition for each year/quarter. Each length frequency observation for purse seine fisheries represents the number of fish sampled raised to the sampling units (sets in the fish compartment) while for fisheries other than purse seine each observation consisted of the actual number of bigeye tuna measured. Each aggregated length sample was assigned an initial sample size. The sample size was determined based on the number of fish included in the aggregated sample, up to a maximum of 1000. The sample size was then divided by 100 resulting in a maximum initial sample size of 10. Purse seine length samples were also assigned an initial sample size of 10. A graphical representation of the availability of length samples is provided in Figure 7. The model structure allocates data to 4-cm length bins.

## 3.7.1. Longline, frozen (LL1N, LL1S, LL2, LL3).

Size frequency data are available for the LL1–3 fisheries from 1965 to 2024. Prior to 1995, the length compositions were dominated by sampling from the Japanese longline fleet, while in the subsequent period the size data were increasingly dominated by data collected from the Taiwanese (China) frozen tuna longline fishery. In recent years, length frequency data were also collected from locally based longline fleets (e.g., Seychelles).

Length and weight data were collected from sampling aboard Japanese commercial, research and training vessels. Weight frequency data collected from the fleet have been converted to length frequency data via a processed weight-whole weight conversion factor and a weight-length key (Chassot et al., 2016). While in recent years most of the samples available have come from scientific observers on commercial vessels, in the past, samples came from training and research vessels, and commercial vessels. Matsumoto (2016) suggested that length distribution was similar between sampling sources (commercial and non-commercial vessels) or platform (fishermen, scientists, observers) in the Indian Ocean. Length frequency data from the Taiwanese (China) longline fleet are also available from 1980–2024. Length samples from this component come from commercial vessels and include lengths recorded by fishermen and, to a lesser extent, lengths measured by scientific observers on some of those vessels.

Previous assessments of Indian Ocean bigeye tuna have highlighted the temporal variability in the length composition data from the main longline fisheries. Langley (2016) examined the longline length data to investigate potential sources of variation in fish length. For the LL1 fleet, there were marked differences in the sizes of fish sampled from the various longline vessels during the late 1980s and early 2000s. There were also divergent temporal trends in the lengths of fish sampled amongst the fleets (see Figure A1 of Langley 2016). A similar trend is also apparent in the length composition data from the eastern equatorial region. Langley (2016) restricted the length data to the main area of catch from the bigeye tuna longline fishery for each model region to minimise potential variation in length composition attributable to the collection of length samples from the periphery of the fishery.

The lengths of fish sampled from the Taiwanese (China) fleet increased markedly during the early 2000s and the length compositions of the samples from catches of most fleets were comprised of larger fish during 2005–2015 (see Figure A1 Appendix 1 of Langley 2016). The increase in Taiwanese (China) fish sizes during the period coincided with a large shift in the ratio of the Taiwanese (China) bigeye and yellowfin longline catches in the region during the same period; the ratio of bigeye in the longline catch increased during the late 2000s and remained at a higher level in the subsequent years (Hoyle et al 2015, see Figure 20). A review of the recent Taiwanese length composition data by Geehan & Hoyle (2013) recommended excluding from stock assessments the size data for BET, YFT and ALB from the Taiwanese DWLL fleet after the early-2000s, until the cause of changes in the size frequency data have been determined by the WPTT". A more recent review shows that the sampling behaviour of Taiwanese and Seychelles fleets (mostly reflagged Taiwanese vessels) have changed over time, with patterns in the logbook length data inconsistent with other vessels (Hoyle et al. 2021), and as such the WPTT27 (DP) recommended omitting all Taiwanese and Seychelles logbook length data from the current assessment

(IOTC 2025). However, the length data collected by the scientific observers on Taiwan (China) vessels in the period 2005–2024 were included in the assessment.

In the 2024 dataset, most of the measurements from the SCY length frequency data were incorrectly entered into a database and so ended up being converted into very large fish (all fish were > 400 cm TL). To ensure this was not biasing the model outputs, all 2024 length data from SCY were excluded. Additionally, there were other rows of data (mainly from SCY data) that only included measurements from very large fish (last four length bins), and no other measurements. These were removed from the assessment based on information from the data team (E. Chassot, pers. comms.).

For the final data sets used in the model, the length compositions of the LL1N, LL1S, LL2, and LL3 fleets are dominated by fish in the 90–150 cm length range (Figure 8). The average lengths of fish in the sampled catch fluctuated over the study period, with regions 2 and 3 having smaller average sizes than regions 1N and 1S, particularly in the early years (Figure 9).

## 3.7.2. Longline, fresh tuna fleet (FL2).

Length and weight data were collected during the unloading of catches at several ports, primarily from fresh-tuna longline vessels flagged in Indonesia and Taiwan (China) (IOTC-OFCF sampling). Length data from 2012-2021 were included in the previous assessment, and for the current assessment, an additional three years of data are included (2012–2024).

The composite length composition of the catch is similar to the distant water longline fleet (Figure ) and remained relatively stable over the sampling period except in 2012 when there are larger fish in the samples (Figure ).

## 3.7.3. Purse seine (PSFS1N, PSFS1S, PSFS2, PSLS1N, PSLS1S, PSLS2).

Length-frequency samples from purse seiners have been collected from a variety of port sampling programmes since the mid-1980s. The samples are comprised of large numbers of individual fish measurements and represent comprehensive sampling of the main period of the fishery (Figure 8). Limited size data are available from the purse-seine fisheries within region 2.

The FAD-associated purse-seine fishery (PSLS) primarily catches smaller bigeye tuna, while the size composition of the catch from the free-school fishery is bimodal, being comprised of the smaller size range of bigeye and a broad mode of larger fish (Figure ). There was a general decline in the average length of fish caught by the PSLS1 fishery from 1990 to 2018 (Figure ). The average size of fish sampled from the free-school fishery was variable among quarters, although fish sizes tended to have increased through the 1990s and the early 2000s (Figure ). It is unknown whether the trends in the length composition of the purse seine catch are representative of the population or reflect changes in the operation of the fishery.

#### 3.7.4. *Bait boat (BB1N)*

Limited length samples are available from the fishery (Figure ) and the sampled catch was dominated by fish in the smaller length classes (50–70 cm) (Figure and Figure ). These samples are not used in the assessment, following previous assessment methods (Fu et al., 2022).

## *3.7.5. Line, other (LINE2)*

Negligible length frequency data are available from the fishery although the available data indicate that the catch was predominantly composed of larger fish (Figure ). Fish sampled from this fishery are generally larger than the fish sampled from the other main longline fisheries. In 2020–21 and 2021, the Indonesian line vessels sampled a considerable number of small fish (around 50 cm). It is not known how well these small fish are representative of this fishery therefore these samples are not included in the current assessment.

## 3.7.6. Other fleets (OT1N, OT2)

While catches from the OT1N fleet are dominated by the Iranian driftnet fleet, there are no length samples available from this component of the fishery. Instead, the available OT1N length samples were

collected from the 'other' fisheries that operated prior to 2005 (Figure ). The aggregate length samples encompass a broad length range (Figure ). For the Other 2 (OT2) fleet, limited length samples were collected from the Indonesian small purse seine and troll fisheries. The aggregate length frequency data available include two size modes from the small-scale purse seine samples (Figure ). This is probably due to different sizes of fish taken by different modes of fishing (e.g., fishing at night with light, around anchored FADs, etc.). Due to concerns around the representativeness of these samples, they are not included in the assessment, following previous assessments (Fu et al., 2022).

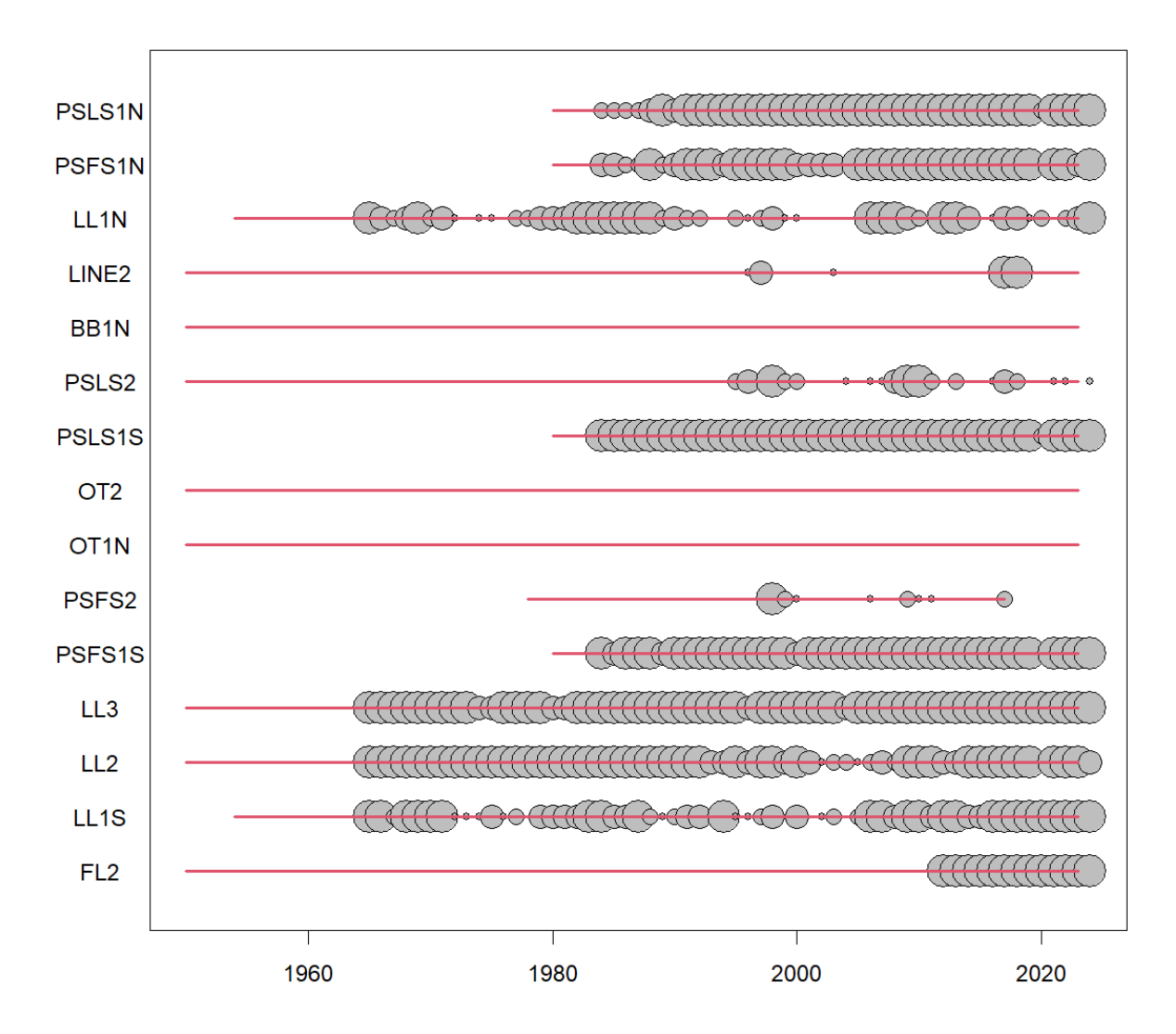
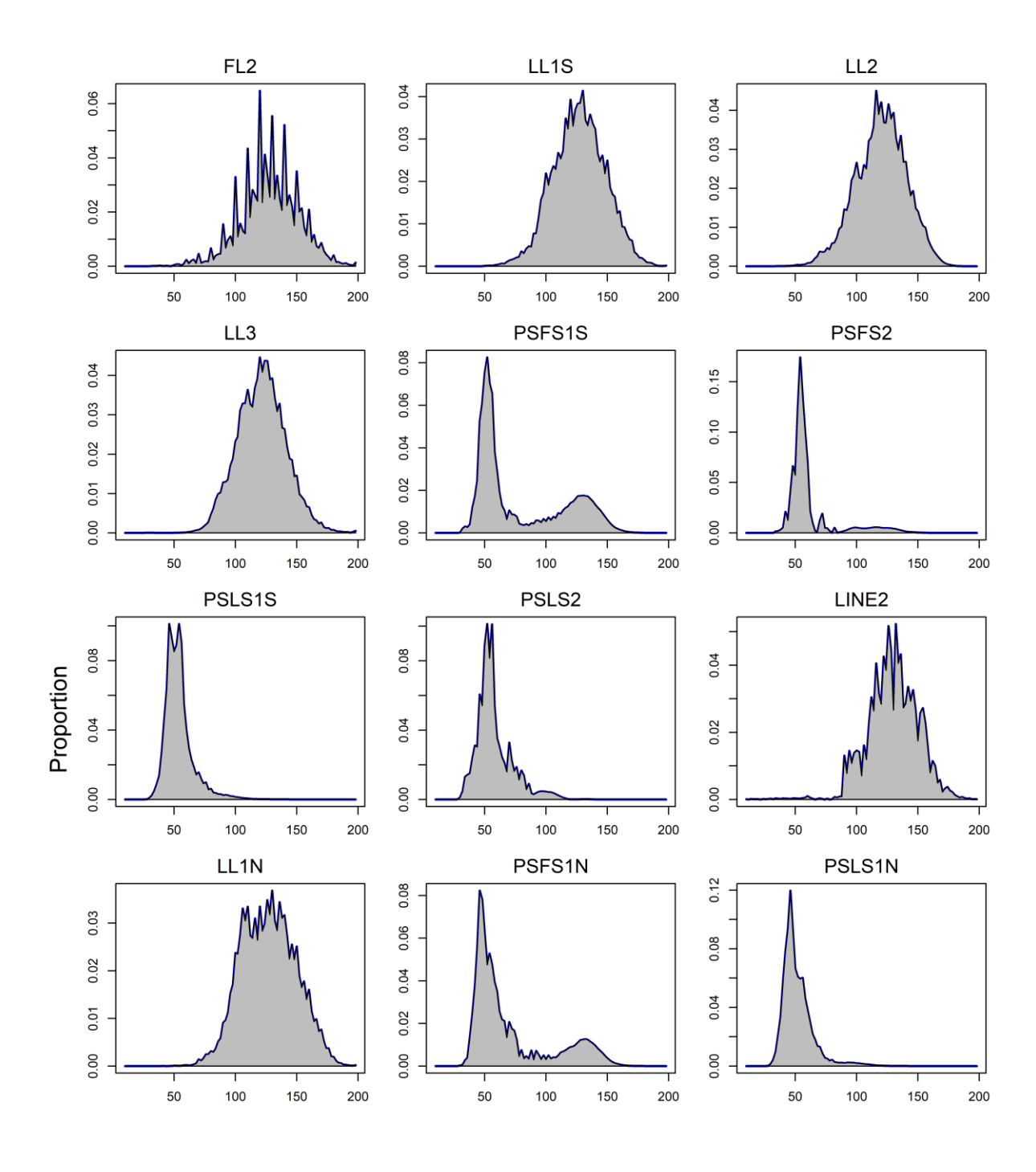
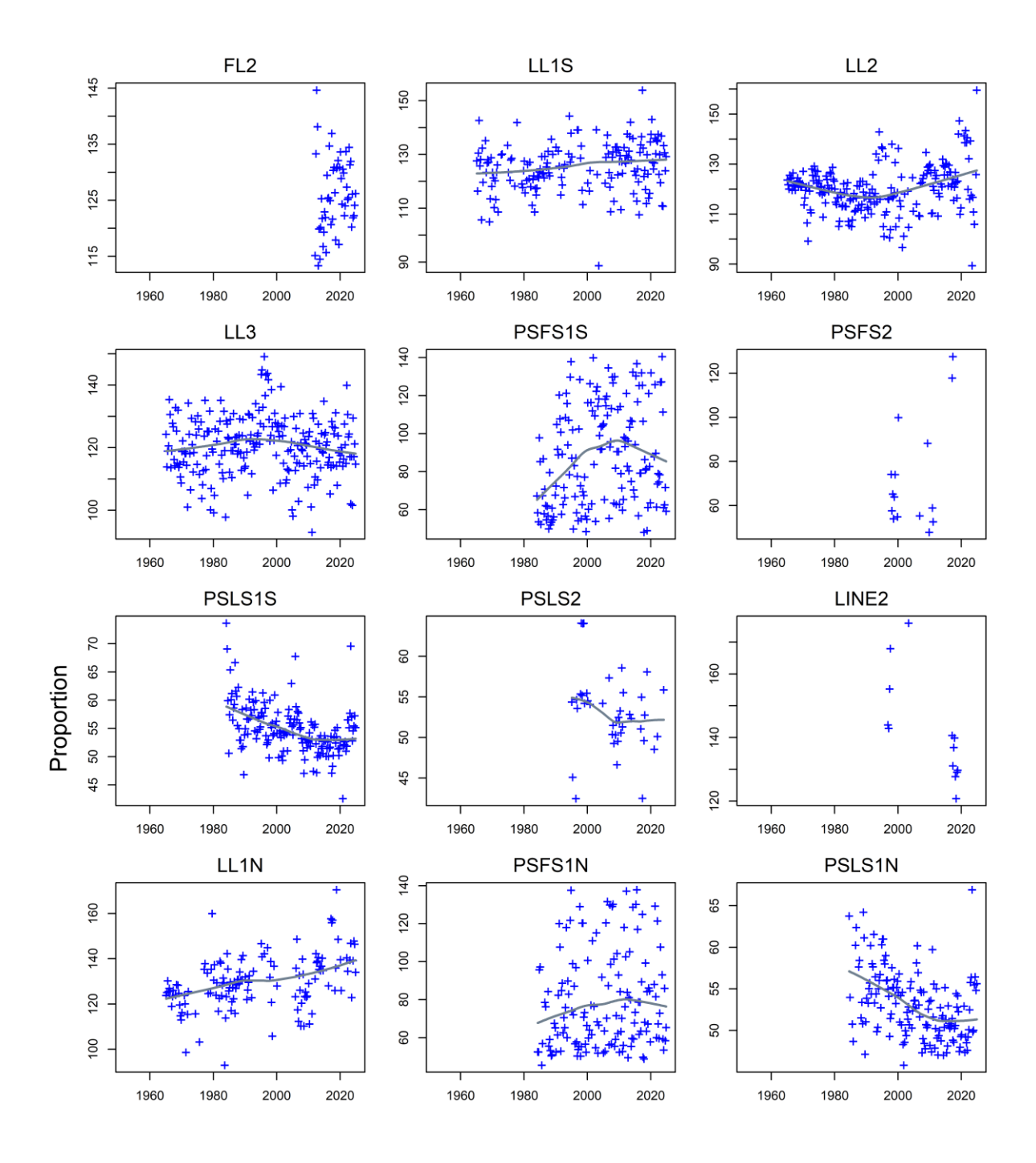


Figure 7: The availability of length sampling data from each fishery by year. The grey circles denote the presence of samples in a specific year (the size indicate number of quarters being sampled). The red horizontal lines indicate the time period over which each fishery operated.



Length (cm)

Figure 8: Length compositions of bigeye tuna samples aggregated by model fishery.



Length (cm)

Figure 9: Mean length (fork length, cm) of bigeye sampled from the principal fisheries by year quarter. The grey line represents the fit of a loess smoother to the dataset.

### 3.8. Tagging data

Tagging data have not been updated since the 2022 assessment model. The data used consist of bigeye tuna tag releases and returns from the Regional Tuna Tagging Project-Indian Ocean (RTTP-IO) phase of the Indian Ocean Tuna Tagging Programme (IOTTP). Tags were released during 2005–2007 and recoveries were monitored by the IOTTP during 2005–2009 and by the IOTC in the subsequent years.

A total of 34,478 bigeye tuna were released by the RTTP-IO program (removed tagged fish with unknown length). All the bigeye tag releases of the RTTP-IO occurred in a localised area off the Tanzanian coast within the western equatorial region (region 1S) (Figure 10). Most of the releases occurred during the second and third quarters of 2006 and the third quarter of 2007 (Figure 11). In total, 5,674 tag recoveries (removed tags with unknown recovery dates) could be assigned to the fleets included in the model. A relatively high proportion of tag recoveries occurred in the vicinity of the main release location (Table 3). There were also a relatively large number of tags recovered from bigeye tuna catches in the Mozambique Channel. Overall, most of the tags were recovered in the home region, some recoveries occurred in adjacent regions, particularly region 1N. A very small number of tags were recovered in regions 2 and 3 (less than 1%) Figure 10).

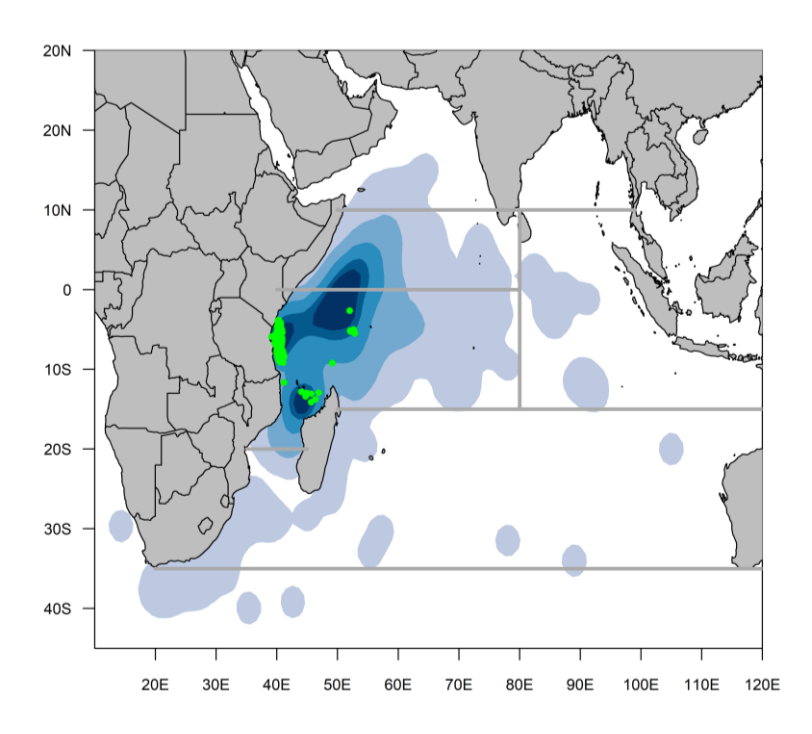


Figure 10: Location of releases (green) and density of recoveries for the bigeye tuna RTTO-IO tag

Program

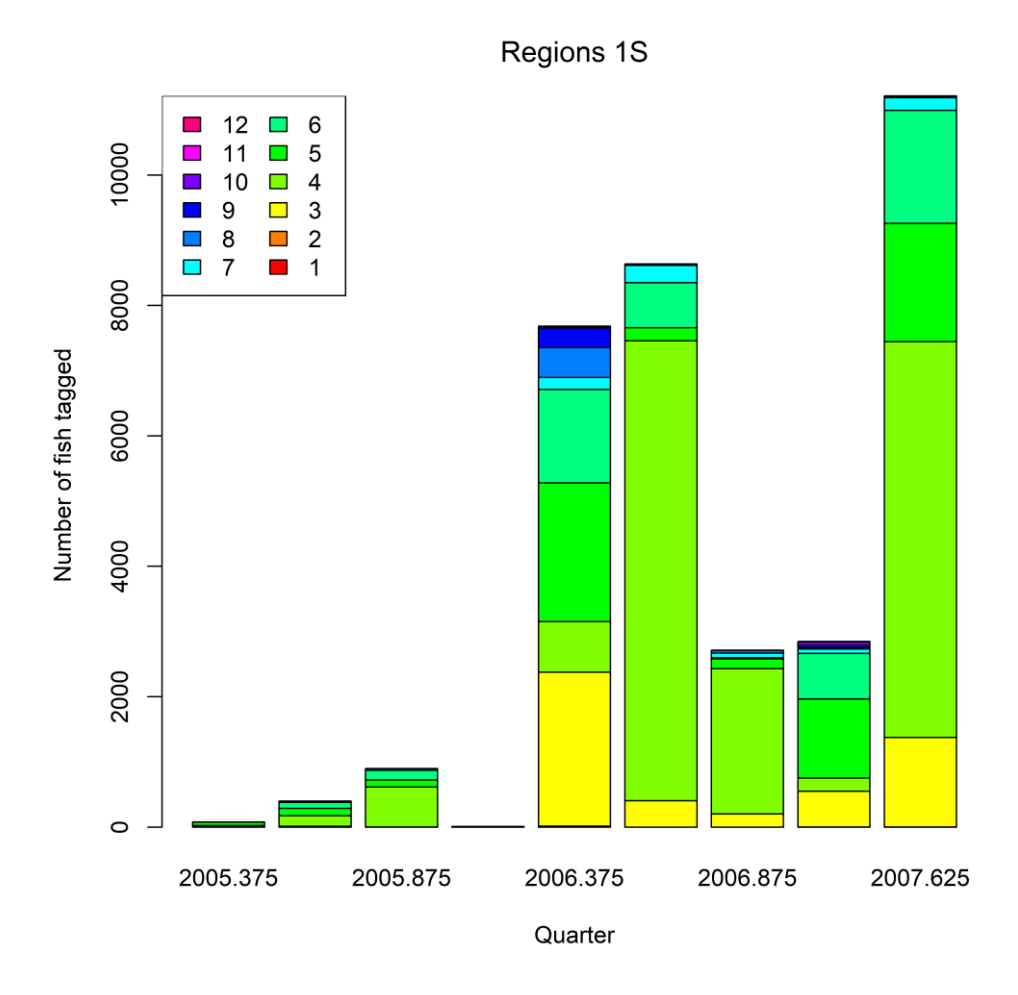


Figure 11: Number of tag releases by quarter and age class (year) included in the assessment data set. All tag releases occurred in region 1S. Ages (year) were assigned based on the length of the fish, and updated growth model from Eveson et al. (2025).

Table 3: Tag recoveries by year of recovery (box), region of release (number released in bracket), and region of recovery. Region of recovery is defined by the definitions of the fisheries included in the model.

Year	Release region (n releases)	Recoveries by region (n)					
		1S	1N	2	3		
2005	1S (1,375)	6	5				
2006	1S (19,042)	478	256	4	1		
2007	1S (14,061)	2,407	613		3		
2008		1,191	160		9		
2009		178	18	3	13		
2010		107	8	2	15		
2011		36	17	2	15		
2012		72	14		5		
2013		13			1		
2014		11					
2015		10			1		

Most of the tag recoveries occurred between mid-2006 and 2008 (Table 3). The number of tag recoveries started to attenuate in 2009 although small numbers of tags were recovered up to the end of 2015. Most of the recaptures near main release locations were from purse seine FAD-associated sets during 2007 and were comprised of tagged fish that had been at liberty for 6–12 months. Recoveries from the purse seine fishery for fish at liberty for at least 12 months were more evenly distributed over the main area fished by the purse seine fleet.

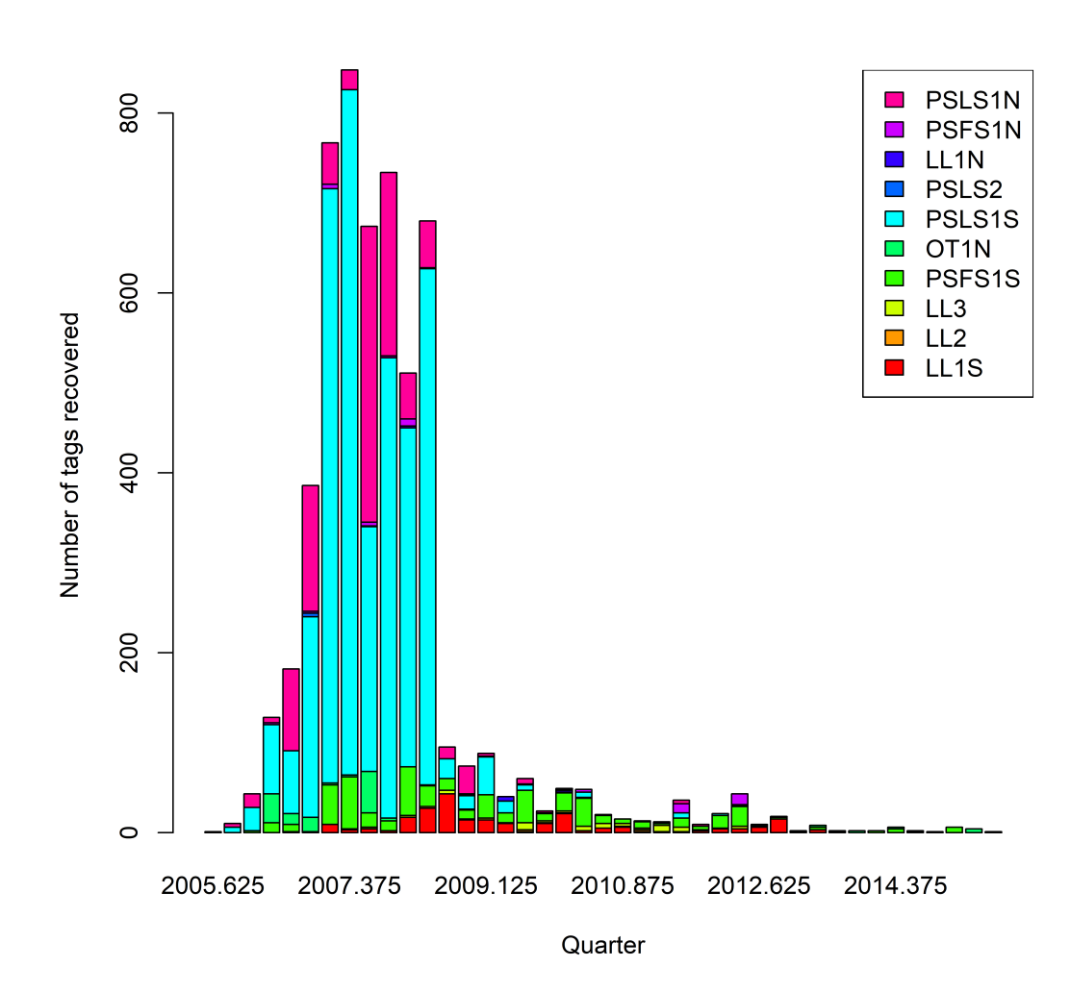


Figure 12: Bigeye tag recoveries by year/quarter and fishery included in the assessment model. Purse seine tag recoveries have not been corrected for reporting rate.

A significant proportion of the tag returns from purse seiners were not accompanied by information concerning the set type. These tag recoveries were assigned to either the free-school or FAD-associated fleets based on the assumed age of the fish at the time of recapture, i.e. based on the age assigned to the release group and the period at liberty. Fish "older" than 12 quarters were assumed to be recaptured by the free-school fleets; "younger" fish were assumed to be recovered by the FAD-associated fleets.

Langley (2016) identified several differences in the recovery rate (number of tags per tonne of catch) from the PSLS fleets between latitudinal zones for tags at liberty for at least 12 months (Tag recovery rates south of 2°S were consistently higher than north of 2°S during the main recovery period). The difference in tag recovery rates between the two main areas of the fishery indicates that the dispersal of tagged bigeye during the 12 month "mixing period" was insufficient to redistribute tagged fish

throughout the bigeye population resident within the western equatorial region (Region 1N and 1S). Consequently, the distribution of PSLS fishery effort (and catch) would have strongly influenced the number of tags recovered from the fishery. Following Langley (2016), the western equatorial region has been partitioned into two regions (Region 1N and Region 1S) in the assessment model account for the potential incomplete mixing of tagged fish.

For incorporation into the assessment model, tag releases were stratified by release region, time period of release (quarter) and age class. The returns from each tag release group were classified by recapture fishery and recapture time period (quarter). The tag data were further adjusted for tag losses and reporting rates to minimize the bias on estimates of fishing mortality and abundance in the assessment model. The procedure is described in below.

# 3.8.1. Age assignment of tag releases

In the current assessment, the age at release was converted based on the mean growth function. In the previous assessment, the use of an age-length key approach that admits the uncertainty in the size distribution at age had been explored. In the 2025 model, as the growth function has been updated, the tag releases and recaptures have been reassigned to different age groups, based on the new growth function.

## 3.8.2. Tag mortality

As in the 2022 assessment, the number of tags in each release group was reduced by 30% to account for initial tag mortality. The initial tag mortality estimates of 20.5% was increased by a further 10% to account for an assumed level of tag mortality associated with the best (base) tagger (Hoyle *et al* 2015). The total number of tags released was 34,427 and processing the tags in this way reduced the number to 24,109 tags.

### 3.8.3. Tag reporting rate

The results of the tag seeding experiments conducted during 2005–2008, have revealed considerable temporal variability in tag reporting rates from the Indian Ocean purse seine fleets (Hillary *et al.* 2008a). Reporting rates were lower in 2005 (57%) compared to 2006 and 2007 (89% and 94%). Quarterly estimates were also available and were similar in magnitude (Hillary *et al.* 2008b). This large increase over time was the result of the development of publicity campaign and tag recovery scheme raising the awareness of the stakeholders (e.g. stevedores and crew). SS3 assumes a constant fishery-specific reporting rate. To account for the temporal change in reporting rate, the number of tag returns from the purse-seine fishery in each stratum (tag group, year/quarter, and length class) were corrected using the respective estimate of the annual reporting rate (Langley 2016).

The approach to correct the number of tag returns for the reporting rate follows Kolody (2011), Fu (2017), and Fu et al. (2018): tags recovered at-sea are assumed to have a 100% reporting rate; tags recovered from landings in Seychelles were corrected for the quarterly estimates of reporting rates from Hillary *et al* (2008b). The tag recoveries were further increased by the proportions of EU PS catches landed outside the Seychelles, to account for purse-seine catches that were not examined for tags. For example, the adjusted number of observed recaptures for a PSLS fleet as input to the model,  $R_L'$  was calculated using the following equation:

$$R_L' = R_L^{sea} + \frac{R_L^{sez}}{P^{sez}r^{sez}}$$

where

 $R_L^{sea}$  = the number of observed recaptures recovered at sea for the PSLS fleet.

 $R_L^{sez}$  = the number of observed recaptures recovered in Seychelles for the PSLS fleet.

 $r^{sez}$  = the reporting rates for PS tags removed from the Seychelles

 $P^{sez}$  = the scaling factor to account for the EU PS recaptures not landed in the Seychelles.

The adjusted number of observed recaptures for a PSFS fleet was calculated similarly. A reporting rate of 94% was assumed for the correction of the 2009–2015 tag recoveries. The numbers of tag recoveries were also adjusted for long-term tag loss (tag shedding) based on an analysis by Gaertner and Hallier (2015). Tag shedding rates for bigeye tuna were estimated to be approximately 1.7% per annum.

A total of 24109.4 releases were classified into 50 tag release groups (a reduction from 68 in 2022 using the previous growth model). Most of the tag releases were in the 4–6-year age classes (Figure 6) A total of 5,666 actual tag recoveries were included in the tagging data set. The cumulative effect of processing the tag recovery data increased the number of recoveries to 6,928 tags.

# 4. MODEL DESCRIPTION

The model was implemented in Stock Synthesis 3.30. A detailed description of the model and the general assumptions, alongside detailed technical descriptions of various components can be found in the SS3 User Guide, and associated webpage, and publications. Most of the structure of the model has remained the same since the 2022 model, and as such the sections are the same as in the previous stock assessment report. There have been updates in 2025 to both the growth and natural mortality.

## 4.1. Population dynamics

The model population structure is comprised of 41 quarterly age classes; the first age class represents fish aged 0–3 months (age 0) and the last age class accumulates all fish age 40+ quarters. The population is aggregated by sex and partitioned by region.

The model commences in 1975 and extends to the end of 2024 in quarterly intervals (192 timesteps).

The initial (1975) age structure of the population was assumed to be in an exploited, equilibrium state. The four main LL fleets were operating prior to 1975, and initial fishing mortality parameters were estimated for each of these fleets, based on early catches and size structure in the commercial catches in the early years. The resulting fishing mortality rates are applied to determine the initial numbers-atage in each model region.

#### 4.1.1. Recruitment

Recruitment of age 0 fish occurs in each quarterly time step of the model. Recruitment was estimated as deviates from the Beverton-Holt (BH) stock recruitment relationship (SRR). The recruitment deviates were estimated for the period that corresponds to the operation of the PSLS fleet which provides catch and length data for the smaller fish and, hence, may be informative regarding the variation in recruitment (1985–2023 (156 deviates; year quarters 232-388)). Recruitment deviates were assumed to have a standard deviation ( $\sigma_R$ ) of 0.6. The final model options included three (fixed) values of steepness of the BH SRR (h 0.7, 0.8 and 0.9). These values are considered to encompass the plausible range of steepness values for tuna species such as bigeye tuna and are routinely adopted in tuna assessments conducted by other tuna RFMOs.

The recruitment for bigeye remains uncertain as the areas where larvae and early juveniles are concentrated have never been sampled nor studied by scientists (Fonteneau 2004). While the temperate regions are generally believed to be feeding grounds, recruitment is assumed to occur in all regions (hence differentiating between recruitment into the population *vs.* spawning.) The overall proportional distribution of recruitment among the four regions was estimated by the model. There is little information to indicate that there are significant differences in the pattern of recruitment between the regions, i.e. the CPUE trends are broadly comparable between the equatorial regions and the length composition data from the longline fleets do not appear to be informative regarding recruitment. Length composition data from the fleets targeting smaller fish are available from the western equatorial regions only. The relative distribution of recruitment between the four regions (1N, 1S, 2, 3) was previously assumed to be temporally invariant. However, in 2022 regional recruitment distribution was allowed to vary for 2001–2019 (year quarters 297-372) in the basic model, to account for as the divergent regional CPUE trends in more recent years. As the LL CPUE indices in 2025 are no longer diverging in trends, and all are increasing, the regional recruitment distribution was fixed to revert to being temporally invariant.

A full log-bias adjustment factor  $(-\frac{1}{2}\sigma^2)$  is applied to the recruitment deviates (as recruitment variability is assumed to be lognormally distributed, see Methot et al. 2013). Potential underestimation of recruitment variability due to uninformative data implies further bias correction may help ensure that the population scaling parameter R0 represent the long-term average recruitment. The optimal bias correction  $(-\frac{1}{2}b\sigma^2,b\leq 1)$  can be determined from the relationship between the assumed and estimated recruitment variability (Methot and Taylor 2011). With this approach, bias correction was applied to the recruitment deviations in the period that is sufficiently informative about the full range of recruitment variability based on the suggested values in the SS3 output.

#### 4.1.2. Growth

In the previous assessment, growth was estimated using data from two studies of bigeye tuna otolith-derived age data, and tag release / recovery data (Eveson *et al* (2012); Farley et al., 2021). This year, additional estimates of age and growth derived from otoliths collected in the Indian Ocean as part of the 'GERUNDIO' project were used to update the previous estimates of Farley et al., (2021) (Eveson et al., 2025). The latest dataset includes estimates of age from both daily and annual growth zones (opaque zones) from 253 bigeye tuna from across the size spectrum found in the Indian Ocean. Preliminary age validation work using otoliths and data from the IOTTP provided evidence that the methods used in the study are accurate. The new estimates represent a length-at-age that is slightly larger than estimated in the 2021 study ( $L^{\infty}$ =172.7 cm vs 168 cm FL) and, as there was little difference between the different parameterisations of the von-Bertalanffy growth curves, it was agreed by the 27<sup>th</sup> WPTT to use a traditional VB within SS3 due to the difficulties of establishing accurate ages at which to have age-based k values. (Figure –left).

In this assessment, continuity runs tested the impact of moving away from Eveson (2012) growth (as agreed by 27WPTT(DP)), and sensitivity runs were completed to examine the impact between using Farley (2021) and Eveson (2025) estimates.

Although data were split into two sexes in the analyses presented by Eveson et al. (2025) at the 27<sup>th</sup> WPTT(DP), there are insufficient data to fully understand whether the differences in growth curves within this dataset are due to differences in biology between males and females, or due to artefacts in the data due to a paucity of representative spatial and temporal variation in the datasets (e.g. to know whether the growth curves are different between male and female fish, sufficient samples from across the range of the species, and from several cohorts (e.g. samples from several years) is necessary to account for other sources of variation).

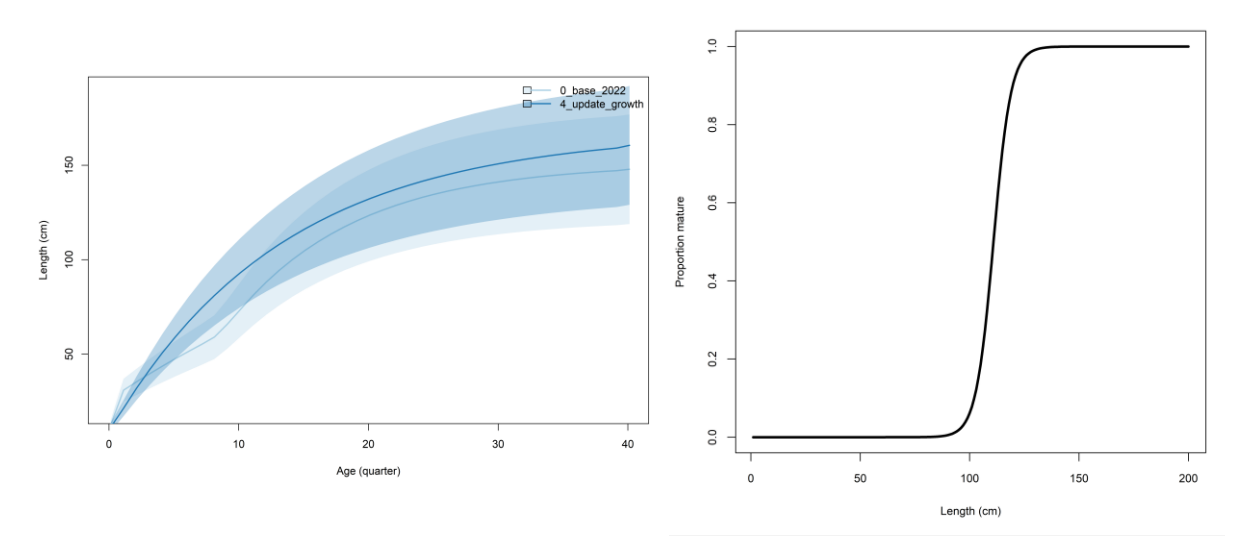


Figure 13: Fixed growth functions for bigeye tuna from the 2022 and 2025 assessments ( $\theta_base_2022$  and  $\theta_aupdate_growth$  respectively) by Farley et al. 2021 and Eveson et al. 2025 (left), and length-based maturity Ogive following Shono et al (2009) (RHS). For the growth functions, the shaded distributions represent the assumed variability of mean size-at-age in the assessment models.

As has been suggested in reviews of tuna stock assessments, and following other tuna RFMO's testing this feature, it was decided by the 27th WPTT(DP) to test the impact of estimating growth internally within SS3 by using the conditional-age-at-length feature. To implement this in SS3, all age data, with associated length are incorporated into the model, and assigned to relevant fleets, regions, and timesteps within the model. For many of the age samples there was sufficient information to assign data to a fleet, region, and timestep. For all samples information was partially missing (e.g. month of capture, or specific gear type used to capture the fish), therefore data were assigned to a fleet based on the most likely scenario (e.g. if only gear type was missing, but all other data matched that of a 'purse seine

vessel in the NWIO', the data would be assigned to a 'purse seine vessel in the NWIO' and then assigned to a relevant model fleet).

A total of 253 aged fish were included in the dataset: all purse seine related fish were assigned to PSLS fleets (FAD-associated sets), and all line associated fish were assigned to LL fleets (frozen tuna). Allocation of data to fleets, regions, and timesteps was imperfect due to limited data being available. In the future, it is recommended that all relevant information (date of collection, location of collection, gear type used, vessel flag state) are recorded alongside the otolith data to improve the quality and reliability of data within the assessment model if this method is to be used in final model options.

The length-weight relationship is based on estimates by Chassot et al. (2016) ( $a=2.217 \times 10^{-5}$ , b=3.01211).

## 4.1.3. *Maturity*

The size of sexual maturity was equivalent to that applied by Shono et al (2009) and the same as has been used in all subsequent BET assessments as no new information is available for bigeye tuna in the Indian Ocean. Female fish were assumed to attain sexual maturity from 100 cm (F.L.) with full sexual maturity at about 125 cm (Figure –right). Zudaire et. al (2022) estimated reproductive parameters for bigeye tuna in the Indian Ocean as part of the 'GERUNDIO' project. The shape of the preliminary maturity ogive obtained is very different to the ogive currently used in the stock assessment, although the estimates of length at 50% maturity are similar (112.7 cm versus 110.9 cm FL). The proportion mature at length does not reach 100% as expected in the larger length classes and requires further investigation and as such has not been used in this assessment, as in 2022.

#### 4.1.4. Natural mortality

The instantaneous rate of natural mortality (M) varies with age and consists of an average over age classes and age-specific deviations from the overall average M. In many fish stock assessments, M is fixed at a pre-specified value for all ages or sizes and is often not based on data related to the species or fishery being assessed. Incorrectly specifying M within stock assessments (and therefore having a mis-specified model) has been shown to have significant impacts on the relevant estimations of management-relevant indicators (Punt et al., 2021; Maunder et al., 2015).

In previous IO bigeye tuna assessments, age-specific natural mortality has been estimated externally to the model, and input as a fixed M-at-age-function. Natural mortality can also be estimated internally within SS3, a method which allow the data to inform estimates of M within the model. This method requires careful review of the model diagnostics, and plausibility of the final model estimates (Hamel et al., 2023, Punt et al., 2023).

From the RTTP, a considerable number of tagged fish were captured after 7–8 years at liberty, indicating a considerable proportion of the tagged fish had reached an age of 8-10 years; 8 tags were recovered after 10 years at liberty and a few tags were recovered during the most recent year (2015), corresponding to an age at recovery of 11-12 years. The higher level of M estimated in previous stock assessments (e.g. 2019) would result in a very small proportion of the tagged fish reaching 12 years of age, suggesting that a lower level of M is more plausible. The lower level of M is also supported by ageing studies of bigeye tuna in the eastern and western Australia water which suggests the longevity of bigeye is more likely to be 14.7 years, higher than original estimates in the Indian Ocean, but lower than that in the Atlantic Ocean (Farley et al. 2004; Farley et al., 2025).

Hoyle (2022) reviewed approaches for estimating M for bigeye tuna and proposed an approach to provide estimates of age dependent M. The approach involves determining a target level of M based on the maximum observed age, and the relative M-at-age based on the Lorenzen functional form. The two components are then combined using the approach of Porch (2011) which rescale the Lorenzen curve so that the average mortality rate matches a target value over the relevant life history period. Using this approach, Hoyle (2022) provided four alternative values of target M based two alterative maximum observed ages for bigeye tuna (14.7 years in the Indian Ocean or 17 years in the Atlantic Ocean), and two empirical methods to estimate M (Then et al. (2015)). In the 2022 assessment, three estimates of M were used in the final ensemble of models ("Mbase", "MHamel15", and "MHamel17", Fu et al., 2022)

In the  $27^{th}$  WPTT data preparatory meeting, it was suggested that the "MHamel17" estimate was removed from the 2025 model, as it used an unrealistic estimate for maximum age (17 years) that has not been observed in the Indian Ocean. Additionally, it was suggested that internal estimation of M within SS3 was trialled, alongside "MHamel15". This follows the ICCAT 2025 bigeye tuna stock assessment. To internally estimate M inside SS3, adult tuna ages are specified (4-10 quarters), so M varies between age 0 to 4, then asymptotes from age 10 to maximum age in the model (40 quarters). The curve follows a Lorenzen functional form and has been named "MLorHam6Q" – age in the model is specified in quarters and uses option 6 within the M options in SS3 (see SS3 User Guide). Mean M at Age<sub>max</sub> estimated outside the model using the same methods and code as used in the ICCAT assessment. Code is available from the Secretariat.

Three starting values for M were used, following methods used in the ICCAT bigeye tuna assessment. The uncertainty grid was built with the values of 50% CI of estimates of M, and the weightings were estimated from the density function assuming lognormal distribution of M with SD=0.31. The three starting values for M were 0.30 (low), 0.37 (medium), 0.45 (high).

A comparison of the various M used in the 2022 base model ("Mbase"), and in the 2025 assessment can be found in Figure 14.

#### 4.1.1. Movement

In Stock Synthesis, movement is implemented as the proportional redistribution of fish amongst regions, including the proportion remaining in the home region. The redistribution of fish occurs instantaneously at the end of each model time step (quarter).

Movement of fish was estimated amongst the four model regions. Movement was parameterised to estimate differential movement from young (8 quarters) to old (≥15 quarters) fish to approximate potential changes in movement dynamics associated with maturation. For each movement transition, two separate movement parameters were estimated (for young and older fish). A linear interpolation between the age specific movement rates was applied to determine movement of the intermediate age classes. Fish younger than age 3 quarters were assumed to remain within the natal region. Movement rates were assumed to be temporally invariant.

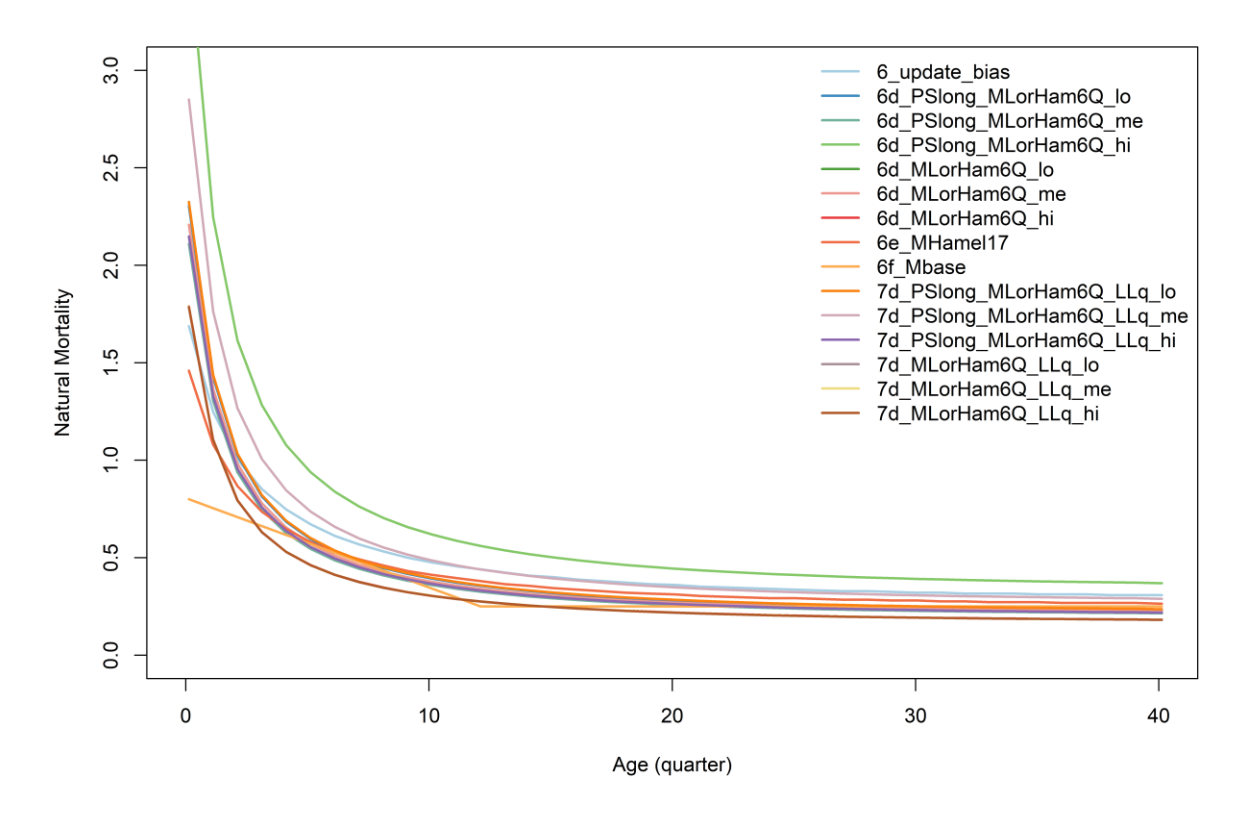


Figure 14: The different instantaneous rates of natural mortality (M) used in the 2022 ("0\_base\_2022", "6f\_Mbase") and 2025 assessment models. The model "5\_update\_M" uses the Hamel & Cope model, using 14.7 years as the Agemax, while "6e\_MHamel17" uses the Hamel & Cope model, using 17 years as the Agemax (for comparison). The models named "MLorHam6Q" are where M is internally estimated within the model, using Agemax at 14.7 years and 'adult' fish ages are from 4-10 years. Age in the graph is in quarters as this is how it is structured in the model.

## 4.1.2. Fleet dynamics

As in the 2022 model, age-based selectivity was assumed for all fleets. Selectivity is more likely to be a length-based process for most gears. However, as the model has adopted a quarterly resolution, the age-based selectivity is considered adequate in approximating the length-based process. Separate selectivity functions were estimated for each of the four main longline fleets where a logistic function was used for LL1N and LL1S fleets, and a double normal function was used for the LL2 and LL3 fleets. A logistic selectivity was assumed for the FL2 longline fleet.

The selectivity of the PSLS fleets were estimated using a double normal functional form. Separate selectivity functions were estimated for the PSLS1N and PSLS1S fleets. For the PSLS1N and PSLS1S fleets, there was a marked shift in the length composition of the fleet catch in the mid-2000s. The modelling option of accounting for the apparent change in the selectivity of the PSLS1 fleet was explored by incorporating a random walk on the estimation of the selectivity parameters related to the age of the peak selectivity and the width of the ascending limb of the selectivity. The temporal shift in selectivity was not included in the final model options.

To account for the bimodal length composition of the catch from the PSFS fleets, the selectivity was modelled using a cubic spline with six nodes. The selectivity of the PSFS1N and PSFS1S fleets was assumed to be equivalent.

Limited data were available to estimate the selectivity of either the PSLS2 or PSFS2 fleets. The selectivity of these fisheries was constrained (mirrored) to be equivalent to the corresponding fleet selectivity in the western equatorial region 1S.

Limited size data are available from the "Other" fleets. During the previous assessment, attempts to estimate independent selectivity for these fleets were not successful, partly due to the variability in the length composition between samples. In aggregate, the length compositions are bimodal and similar to the length composition from the PSFS fleets. On that basis, the selectivity for the two "Other" fleets (OT1N and OT2) were assumed to be equivalent to the PSFS fleets. Similarly, limited length data are available for the LINE2 fishery, and the selectivity was assumed to be equivalent to the main longline fleets. Further it has been suggested the length samples from the "bait boat" fleet (mostly from Maldives pole and line fishery) are thought to be of very poor quality; therefore the selectivity of this fleet was assumed to be equivalent to the PSLS1S fleet.

Fishing mortality was modelled using the hybrid method that estimates the harvest rate using Pope's approximation and then converts it to an approximation of the corresponding F (Methot & Wetzel 2013).

### 4.2. Dynamics of tagged fish

### 4.2.1. Tag mixing

In general, the population dynamics of the tagged and untagged populations are governed by the same model structures and parameters. The tagged populations (tag groups) are monitored over time intervals following release. The predicted number of tags in each region and subsequent time intervals are derived based on the movement parameters, natural mortality and fishing mortality. For each time interval, the number of tags recovered by a specific fleet is predicted based the modelled number of tags in each age class in the region, the selectivity of the fleet and the fishing mortality of the specific fleet. The predicted number of tag recoveries is also moderated by the fleet specific reporting rate.

The assessment framework assumes that the probability of capturing a tagged fish is equivalent to the probability of catching an untagged fish. Violation of the assumption of homogeneous mixing of tagged fish at the relevant spatial scale (i.e. region) is likely to introduce a bias in the estimation of fish abundance. In SS3, a mixing period is specified which partitions the tag data sets (by release group); tag recoveries (observed and predicted) from the mixing period are excluded from the tag likelihood and therefore do not influence the estimation procedure.

For bigeye tuna, almost all tags were released from a localised area of region 1S. The tagged bigeye were predominantly aged 4–8 quarters at release, while the selectivity of the PSLS1S is estimated to be 4–11 quarters. Consequently, there is likely to be a limited time (4–8 quarters) during which most of the tagged fish would be available to the PSLS fleets. Thus, a mixing period of four quarters was chosen on the basis that enough tagged fish remained available to the PSLS fleets during the post mixing period, albeit for a relatively limited period.

An analysis of the spatial distribution of the tag recoveries from the purse-seine fleets (see Appendix A of Fu 2019) suggested that the four quarter mixing period may be sufficient to allow for a reasonable degree of mixing of tagged fish within the south-western equatorial region (Region 1S). The dispersal of tags into the north-western equatorial region (Region 1N) will be mediated by the estimated movement rates (from region 1S), however, the distribution of tagged fish in this region is unlikely to be homogeneous and it is likely that tag densities would be higher in the southern area of region 1N (i.e. closer to the release location). Consequently, tag recoveries from the region may be influenced by the spatial distribution of the catch from the fleets.

Specifying a mixing period of 12 months (4 quarters) in the stock assessment model will effectively exclude 76% of all the FAD-associated tag recoveries, while retaining 69% of the free-school recoveries (reducing the total tag recoveries by 66%). This effectively reduces the potential bias introduced by the FAD-associated tag recoveries while maintaining most of the free-school tag recoveries. The remaining FAD-associated tag recoveries are predominantly comprised of fish larger than 80 cm and, arguably, these larger fish are likely to be more evenly distributed that the smaller size category.

# 4.2.2. Tag reporting

The observed number of tag recoveries for the purse seine fleets were already adjusted to account for the differential tag reporting rates. On that basis, the reporting rates for the purse seine fleets were fixed at 1.0. The model also incorporates the tag recoveries from the other fleets, most notably the LL fleets. There are no external estimates of tag reporting rates available for the longline fishery and, hence, the fishery specific reporting rates were estimated based on uninformative priors and were assumed to be temporally invariant. Tag recoveries from the longline fleets will be considerably less informative about stock abundance.

The tag mixing process is highly variable in time and space and is likely to vary by release group. Different release groups may experience different levels of tag loss and/or reporting due to tagger effects. Recent development in tag modelling has suggested the modelling of tags conditioned on the number returned, to minimise the bias due to the heterogeneity due to tag losses, reporting, or mixing amongst release groups.

### 4.3. Modelling methods, parameters, and likelihood

The total likelihood is composed of four main components: catch data, the abundance indices (CPUE), length frequency data and tag release/recovery data. There are also contributions to the total likelihood from the recruitment deviates and priors on the individual model parameters. The model was configured to fit the catch almost exactly so the catch component of the likelihood is very small. There are two components of the tag likelihood: the multinomial likelihood for the distribution of tag recoveries by fleets over time and the negative binomial distribution of expected total recaptures across all regions. Details of the formulation of the individual components of the likelihood are provided in Methot & Wetzel (2013).

The regional CPUE indices are assumed to represent the relative abundance (numbers of fish) of the proportion of the regional population that was vulnerable to the longline fishery. The weighting of the CPUE indices followed the approach of Francis (2011). Following previous assessments, and related analyses, CV of 0.1 was assigned to each set of longline CPUE indices in the base model, to ensure the stock biomass trajectories were broadly consistent with the CPUE indices while allowed for a moderate degree of variability in fitting to the indices. Purse seine indices were given a CV of 0.2 as suggested at the 27th WPTT(DP).

The relative weighting of the tagging data was controlled by the magnitude of the over-dispersion parameters assigned to the individual tag release groups. Following Langley (2016), the over-dispersion parameters for all tag release groups were estimated within the assessment model assuming a relatively uninformative beta prior (mean 10, sd 3). This prior reflected the variability in the tag-recapture data (variance of the standardised residuals) as determined from preliminary model runs (Langley 2016).

For all fleets, except for the PSLS fleets, the individual length frequency observations were assigned an effective sample size (ESS) of 1. For the PSLS fleets an ESS of 10 was assigned to all length observations. The higher weighting of the purse seine PSLS length frequency data reflects the comprehensive nature of the port sampling programme monitoring the catch. There is a high degree of variation in the length composition data from the PSFS fleets which appears related to the bimodal structure in the fishery length compositions; variation in the individual length samples may be attributable to sampling different proportions of the catch from each length mode. Based on the apparent level of sampling error an ESS of 1 was assigned to the length samples from the PSFS fleets.

## 5. ASSESSMENT MODEL RUNS

A base model was configured that represents a continuity run from the 2022 assessment with updated data and several revisions of the model. A range of sensitivity or exploratory models were later conducted explore alternative assumptions and parameter configurations. On basis of the analyses, final model options were tentatively proposed that include an ensemble of models running over permutations of plausible parameters and/or model settings, from which the stock status was estimated, and uncertainty was quantified (the Grid). The assessment was conducted using the 3.30 version of the Stock Synthesis software using R. Most diagnostic plots, and model updates were coded in R and generated using the *r4ss* and *ss3diags* packages. Stock status is reported for the terminal year of the model (2024).

#### 5.1. Base model

In the 2022 assessment, final model options selected to quantify stock status by the WPTT25(AS) included 24 models with alternative assumptions on selectivity (2 options), steepness (3 values), natural mortality

The 2022 reference model was re-run to ensure continuity, and some revisions were incorporated based on preliminary analyses. These revisions are to improve the assessment model, but they do not represent any major structural changes to the model. The revisions included:

- Updating growth parameters to those from Eveson et al. (2025)
- Updating the instantaneous rate of natural mortality (M) to 'MHamel 15' as the reference M
- Updating the recruitment deviations to the appropriate timeframe
- Updating the bias adjustment to recommended values in SS3

A sequential, stepwise approach was taken for the model updates (Table 4). The configuration of the resulting base model is summarised in Table 5.

Table 4: Description of the sequence of model runs to update the 2022 base model.

Model	Description				
Base_2022	2022 reference model with steepness = 0.8, tag lambda =0.1				
0_base_2022	Updated R and SS3 executable (same version – 3.30)				
1-update-catch	Updated and revised catch series, extended the model to 2024				
2-update-CPUE	Updated and revised longline CPUE indices				
3-update-LF	Updated and revised length-frequency data				
4-update-growth	Updated growth to Eveson et al. (2025).				
5-update-M	Update from 'baseM' to 'MHamel15' – maximum age of 14.7 yrs.				
6-update-bias (base_2025a)	Update bias adjustment values to those recommended by SS3.				
7-update-CPUE_LLq (base_2025b)	Same configuration as '6-update-bias' but with 0.5 % discount on LL CPUE to account for gear creep / changes in catchability.				

Table 5: Main structural assumptions of the bigeye tuna *base* model and details of estimated parameters. Changes to the 2022 reference model are highlighted in red.

Parameter	Assumptions	Values		
	Occurs at the start of each quarter as 0 age fish.			
	Recruitment is a function of Beverton-Holt stock-recruitment relationship (SRR).	$R_{\theta} \text{ Norm}(10,10); h = 0.80$		
Recruitment	Regional apportionment of recruitment to R1N, R1S, R2, and R3.	PropR <sup>2</sup> Norm(0,1.0)		
	Temporal recruitment deviates from SRR, 1985–2023.	Sigma ( $\sigma$ ) $r = 0.6$ . 156 deviates.		
	Proportion of recruitment allocated to regions is temporally invariant.			
Initial population	A function of the equilibrium recruitment in each region assuming population in an initial, exploited state in 1975.			
	Initial fishing mortality estimated for LL1N,1S,2,3 fisheries.	Norm(0.10,99)		
	41 quarterly age-classes, with the last representing a plus group.	0 – 40+		
	Growth based on von Bertalanffy growth model	$L^{\infty} = 167.54288 \text{ cm}, k = 0.300; L_{\min} = 0.200$		
Age and growth	SD of length-at-age based on a constant coefficient of variation of average length-at-age.	CV =0.10		
	Mean weights ( $W_j$ ) from the weight-length relationship $W = aL^b$ .	a = 2.217e-05, $b = 3.01211$		
Instantaneous rate of natural	Age-specific, fixed, estimated externally to model using Hamel & Cope (2022); and Age <sub>max</sub> of 14.7.	'MHamel15'		
mortality (M)	Estimated internally within the model – using age as quarters, option 6 in SS3, and $age_{max}$ of 14.7.	'MLorHam6Q'		
Maturity	Length specific logistic function from Shono et al (2009).	Maturity of 50% females = 110.888 cm		
Maturity	Mature population includes both male and female fish (single sex model).	Maturity slope = -0.25		
Movement	Age-dependent with two blocks; age classes 3-8 and 15-40+ (quarters).	12 movement coefs. Norm(0,4).		
	Ramp function age 8-15 (quarters)	12 movement coets. (voim(0,4).		
	No movement prior to age class 3 (quarters).			
	Constant among quarters.			

	Age specific, constant over time.				
Selectivity	<b>Longline – frozen:</b> Separate logistic selectivity parameters for LL1N, LL1S, LL2 and LL3				
	<b>Purse seine:</b> Separate selectivity for PSLS1N, common selectivity PSLS1S and PSLS2. Common selectivity for all PSFS fleets.	Logistic <i>p1</i> Norm(20,10), <i>p2</i> Norm(1,10)			
	Longline – fresh: LF2 fleet logistic selectivity.	Double Normal			
	Line: LINE2 share principal longline (frozen) LL selectivity.	Five node cubic spline			
	Bait boat: BB1N fleet: double normal selectivity.				
	Other: OT 1N & 2 share PSFS selectivity.				
	<b>CPUE:</b> Longline CPUE indices share principal LL selectivity; purse seine CPUE indices share principle PSLS selectivity.				
	Temporally invariant. Shared regional catchability coefficient.				
Catchability	No seasonal variation in catchability for LL or PS CPUE.	Unconstrained parameter LLq			
	LL2,3 CPUE indices have CV of 0.2; LL1N,1S CV 0.25.				
Fishing mortality	Hybrid approach (method 3, see SS3 User Guide (Methot & Wetzel 2013).				
Tag mixing	Tags assumed to be randomly mixed at the model region level four quarters following the quarter of release. Accumulation after 28 quarters				
	All (adjusted) reporting rates constant over time.				
Tag reporting	Common tag reporting rate fixed for all purse seine fleets.	PS RR 1.0			
	Non-purse seine tag reporting rates have uninformative priors.	Other fisheries Norm(-0.7,5)			
Tag variation	Over dispersion parameters estimated for each tag release groups.	Beta prior (mean 10, sd 3)			
	Multinomial error structure.				
Length composition	PSLS length samples assigned maximum effective sample size (ESS) of 10.				
	PSFS length samples assigned maximum ESS of 1.0.				
	LL and Other fisheries length samples assigned a maximum ESS of 1.0.				

### 5.2. Model sensitivity testing

The base models (6\_update\_bias and 7\_update\_cpue\_LLq) were the starting points for further analyses and exploration of potential sensitivities within the model. Within this phase, variations of key data inputs, biological parameters, and model structures were explored. In 2022, several structural components of the model were explored. In this year's assessment, no major structural changes were tested, and instead the model sensitivity to data inputs, and biological parameters was tested. The aim of doing these runs was to identify any major sources of uncertainty that would impact assessment outputs. If specific data inputs or biological parameters were found to impact the assessment output, the plausible variations in these values were kept in the final ensemble of models used in the 'grid' from which stock status is derived.

Initial sensitivity testing was discussed at the 27<sup>th</sup> WPTT data preparatory meeting, and some initial explorations agreed on. Further runs were included as model development continued. Table 6 below provides a brief description of the range of alternative model options explored in sensitivity testing.

As the 27<sup>th</sup> WPTT agreed that two sets of 'base' models should be used for sensitivity testing (one with a 5% discount on the longline CPUE indices, and one without), there is a suite of models with the longline CPUE indices as they were provided to the Secretariat (**6\_update\_bias**), and another suite of models that have a 5% discount on the longline CPUE indices (**7\_update\_cpue\_LLq**).

Table 6: Description of various data inputs and biological parameters that were varied to test model sensitivity to them.

Sensitivity	Description of test				
Addition of purse seine CPUE indices					
6_PSlong_2area	Addition of purse seine CPUE 'long' index; 2 areas (1S + 1N as				
	separate indices)				
7_PSlong_2area_LLq	As above, with 5% discount on longline CPUE indices.				
6b_PSshort_2area	Addition of purse seine CPUE 'short' index; 2 areas (1S + 1N				
	as separate indices)				
7b PSshort 2area LLq	As above, with 5% discount on longline CPUE indices.				
Internal estimation of growth: "C	Conditional-age-at-lengtn"				
6c_PSlong_CAAL	Estimation of growth curve internally in SS3, using conditional-				
6c CAAL	age-at-length with standard von Bertalanffy growth model. All				
_	parameters (age-at- $L_{min}$ ; age-at- $L_{\infty}$ ; $k$ ) estimated in the model.				
	With ( <i>PSlong</i> ) and without purse seine CPUE indices.				
7c PSlong CAAL LLq	As above, with 5% discount on longline CPUE indices.				
7c CAAL LLq	1 12 dec (3) (() una p / c una count on rongimo er ez murcos				
6c PSlong CAAL lmax	Estimation of growth curve internally in SS3 using conditional-				
6c CAAL lmax	age-age-length with standard von Bertalanffy growth model.				
oe_chill_imax	Age-at-L <sub>max</sub> fixed using Eveson et al. (2025) data. Age-at-L <sub>min</sub>				
	and $k$ estimated. With $(PSlong)$ and without purse seine CPUE				
	indices.				
7c PSlong CAAL lmax LLq	As above, with 5% discount on longline CPUE indices.				
_	As above, with 5% discount on longine of the indices.				
7c CAAL lmax LLq	Estimation of annual assumption (SC2 value and distance)				
6c_PSlong_CAAL_lmin	Estimation of growth curve internally in SS3 using conditional-				
6c_CAAL_lmin	age-age-length with standard von Bertalanffy growth model.				
	Age-at-L <sub>min</sub> fixed using Eveson et al. (2025) data. Age-at-L <sub>max</sub>				
	and $k$ estimated. With ( <i>PSlong</i> ) and without purse seine CPUE				
a pol carrier	indices.				
7c_PSlong_CAAL_lmin	As above, with 5% discount on longline CPUE indices.				
7c CAAL lmin	. 14. (10.				
Instantaneous rate of natural mo	ortanty (M)				
6d PSlong MLorHam6Qlo	Internal estimation of age-based M, based on the Lorenzen				
6d PSlong MLorHam6Qme	functional form, and estimation of the rate of M at age <sub>max</sub> = 14.7				
6d_PSlong_MLorHam6Qhi	yr using methods from (Hamel & Cope 2022), as used in the				
6d MLorHam6Qlo	ICCAT bigeye tuna assessment in 2025. With (PSlong) and				
6d MLorHam6Qme	without purse seine CPUE indices.				
6d MLorHam6Qhi					
7d PSlong MLorHam6Qlo LLq	As above, with 'lo', 'me', 'hi' options, with 5 % discount on				
7d PSlong MLorHam6Qme LLq	longline CPUE indices.				
7d PSlong MLorHam6Qhi LLq					
7d MLorHam6Qlo LLq					
7d MLorHam6Qme LLq					
7d MLorHam6Qhi LLq					
6e PSlong MHamel17	External estimation of age-based M, based on the Lorenzen				
6e MHamel17	functional form, and estimation of the rate of $M$ at age <sub>max</sub> = 17				
<u>-</u> <del>-</del>	yr using methods from (Hamel & Cope 2022),. Tested with				
	( <i>PSlong</i> ) and without purse seine CPUE indices.				
7e PSlong MHamel17 LLq	As above, with 5 % discount on longline CPUE indices.				
7e_I Stong_MITamet17_EEq 7e_MHamel17_LLq	The account of foliginic of the indices.				
6f PSlong Mbase	External estimation of age-based M, as used in the basic model				
6f Mbase	in 2022.				
oj_1viouse	111 4044.				

Selectivity of frozen longline fleets LL2 + LL3						
6g PSlong sL Alter estimated selectivity of fleets LL2 and LL3 (fr						
$\log sL$ longline fleets) from double normal to logistic (to be the sa						
	as LL1N + LL1S.					
	Tested with ( <i>PSlong</i> ) and without purse seine CPUE indices.					
7g_PSlong_sL_LLq	As above, with 5 % discount on longline CPUE indices.					
7g sL LLq						

# 5.3. Proposed ensemble models (Grid)

On basis of the sensitivity analyses, and discussions at the  $27^{th}$  WPTT (data preparatory meeting), further model options were configured to capture the main uncertainties in the model. From the results of the sensitivity analyses, the model was most sensitive to changes in growth, and the instantaneous rate of natural mortality (M), and to include uncertainty in the steepness (h) parameter associated with the stock recruitment relationship (SRR) in tropical tunas, different values of h are proposed for inclusion in the ensemble models. Therefore, the final models proposed for inclusion in the ensemble of models are:

- one option for growth;
- three options for M;
- two options for selectivity, and
- three options for *h*.

Table 7: Description of the proposed final model options for the 2025 assessment. The final models consist of a full combination of options below, making a total of 18 models. The options adopted within the reference (base) model ('7\_PSlong\_LLq') are highlighted.

Model options	Description					
Steepness (h) in SRR	• $h70: h = 0.70$					
	• $h80$ : $h = 0.80$					
	• h90: $h = 0.90$					
Growth	• Gnew: VB growth parameters estimated by Eveson et al. (2025)					
Natural Mortality	• Mhamel 5 – Lorenzen functional form <i>M</i> with adult M estimated from the Hamel & Cope (2022) estimator assuming a maximum age of 14.7, see Hoyle 2021-					
	• MLorHam6Qlo – Internally estimated <i>M</i> using 'option 6' within SS3 (see SS3 User Guide), with adult (4-10 quarters) <i>M</i> estimated using Hamel & Cope (2022), assuming a maximum age of 14.7 yr.					
	• MLorHam6Qme – Internally estimated <i>M</i> using 'option 6' within SS3 (see SS3 User Guide), with adult (4-10 quarters) <i>M</i> estimated using Hamel & Cope (2022), assuming a maximum age of 14.7 yr.					
	<ul> <li>Mhamel17 – Lorenzen functional form M with adult M estimated from the Hamel &amp; Cope (2022) estimator assuming a maximum age of 17, see Hoyle 2021.</li> </ul>					

Selectivity in LL2 + LL3	• sL: logistic selectivity for LL2 and LL3 (same as other frozen longline fleets)
	• sD: double normal selectivity for LL2 and LL3

### 6. MODELLING RESULTS

### 6.1. Continuity runs from 2022 model

Updating R had no impact on the model estimates. The previous assessment was also run using SS3.30, so there was no need to update the SS3 executable. Updating the 2022 base model with catch had some impact to historical estimates of spawning stock biomass (hereafter referred to as biomass), between the years 1990 to present, presumably due to re-estimation of catches by Indonesia. Biomass estimates in recent years (2020-2024) were very similar, noting that the recent catches (2022, 2023, 2024) continued to drive the biomass in a downward trajectory.

Updating the CPUE indices (joint frozen longline indices) significantly increased the historical biomass estimates, with a steeper decline in spawning stock biomass between 2000 and 2010 than previously seen. Current biomass estimates (~2012 onwards) show a divergence from the previous model, with biomass estimates decreasing slightly to 2020, but then increasing to 2024, in a more optimistic result than before (Figure 15).

Updating the length frequency composition had almost no impact on the biomass estimates, probably due to the relative paucity of information, but updating the growth and natural mortality estimates had significant impacts on the biomass estimates. The overall trends were similar between all models, but overall scale of biomass was increased by changing the growth parameters, and then markedly decreased by updating the natural mortality (Figure 15). The model is particularly sensitive to the estimate of natural mortality, as is demonstrated in the sensitivity runs.

The recruitment bias correction again reduced the overall scale of biomass slightly, and slightly reduced the historical initial biomass estimates, resulting in a flatter decline to current biomass levels. Accounting for catchability and / or gear creep in the longline indices had almost no impact on the estimated biomass levels, except in the final year of the model when the estimates diverge slightly.

Two base models were taken into the sensitivity testing one using the additional gear creep / catchability on the CPUE index (7\_update\_cpue\_LLq), and another without the CPUE creep (6\_update\_bias).

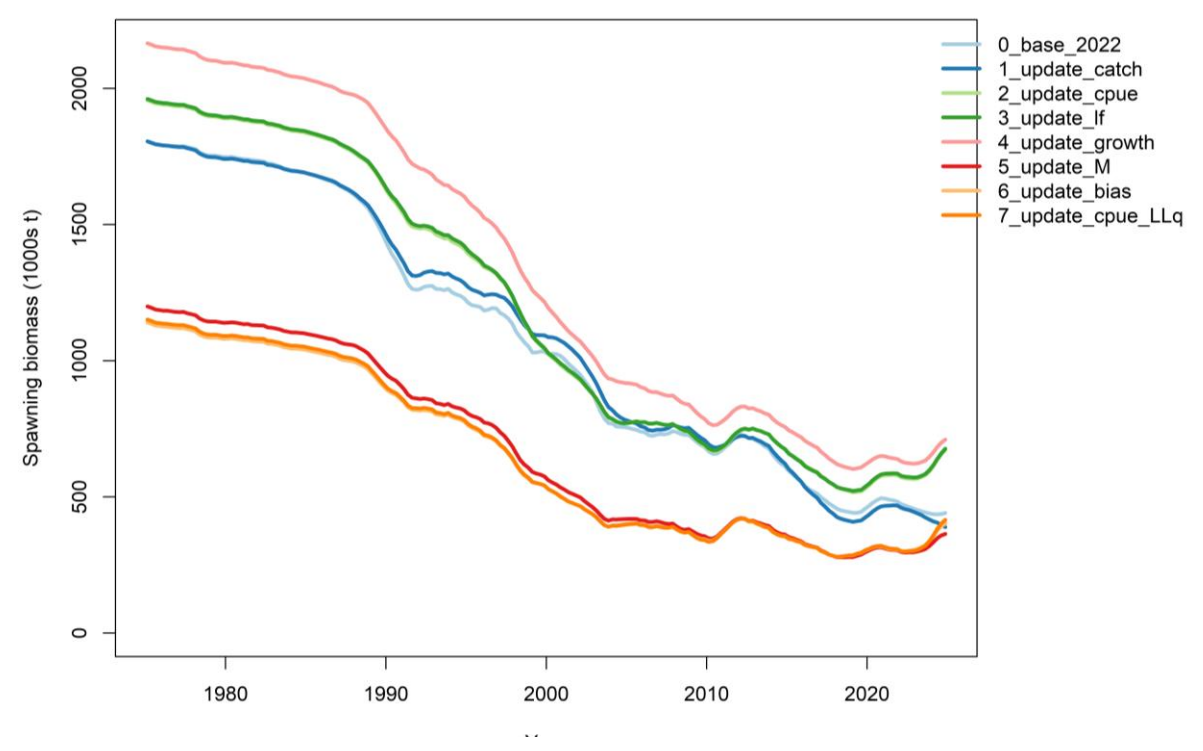


Figure 15: Spawning biomass trajectories for IO bigeye tuna from the stepwise model updates. (from the 2022 assessment reference model '0\_base\_2022').

Table 6: Estimates of management quantities for the step-wise updates of the 2022 stock assessment reference model ('0\_base\_2022') to the 2025 reference models ('6\_update\_bias' and '7\_update\_cpue\_LLq')

	SSB <sub>1975</sub> (t)	$SSB_{MSY}(t)$	SSB <sub>2024</sub> (t)	SSB <sub>2024</sub> SSB <sub>1975</sub>	SSB <sub>1975</sub> SSB <sub>MSY</sub>	F <sub>MSY</sub>	F <sub>2024</sub>	$F_{1975}F_{MSY}$	$C_{MSY}(t)$
0_base_2022	1,925,270	580,627	437,742	0.227367	0.753913	0.186898	0.165894	0.887616	91,646
1_update_catch	1,925,820	545,556	400,641	0.208037	0.734372	0.196945	0.346256	1.758133	91,267.6
2_update_cpue	2,076,520	587,376	644,521.5	0.310385	1.09729	0.203536	0.204629	1.005369	95,063.2
3_update_lf	2,081,580	582,991	648,034.8	0.311319	1.111569	0.21073	0.217157	1.0305	94,831.6
4_update_growth	2,305,810	714,255	689,056.5	0.298835	0.964721	0.2597	0.273666	1.053777	103,146
5_update_M	1,297,680	371,380	351,164.2	0.270609	0.945566	0.25275	0.296161	1.171753	105,391.6
6_update_bias	1,238,880	367,060	381,361.5	0.307828	1.038962	0.244544	0.294938	1.206074	100,594
7_update_cpue_LLq	1,249,740	371,339	389,702.2	0.311827	1.049451	0.245846	0.280407	1.140581	101,098.8

#### 6.2. Model fits

## 6.2.1. Base models (6 update bias and 7 update cpue LLq)

The base models fit the new CPUE indices for the three main fisheries (LL1N, LL1S & LL2) and the seasonal CPUE indices from LL3 well enough (Figure 16 a,b & 17a,b). The residuals did not reveal any obvious patterns in region 1N and region 3, however there is a significant downward trend in region 1S and a significant upward trend in the residuals in region 2 (Figures 18a,b & 19a,b). Overall, the variation in the residuals was broadly comparable to the S.E. initially assigned to the CPUE indices.

Overall, there was a good fit to the aggregated length frequency data for most of the main fisheries with comprehensive sampling (Figure a & b). For the purse seine free school fisheries (PSFS), the relative proportion of fish in the small ( $\leq$ 80cm) and large (>80cm) length mode is variable over time, probably due to size related schooling behaviour of adult bigeye tuna, resulting in less adequate fits to the length composition distributions, particularly in region 2 for small fish, and region 1S and 1N for larger fish. For the PSFS2 fishery this may also be due to the paucity of data available (Figures 19a & b).

The recent trends in the predicted average fish size for the main longline and purse seine fisheries are broadly consistent with the sampling data. The average length of fish from LL2 is still over-estimated by the model throughout the 1980s and 1990s despite the use of a more flexible, double normal selectivity function (Figures 20a,b). There is a marked decline in the average size of fish sampled from the purse seine FAD fisheries in both region 1S and region 1N (Figure 2a & b), particularly between 2010 to 2020. This trend is not as evident in the predicted average fish size derived from the model for region 2, however there are far fewer samples in this region.

The average length of fish sampled from the PSFS is highly variable (Figure 2a & b) probably reflecting the proportion of the catch sampled from the smaller and larger modes of the combined length composition. The model prediction of average length represents the length of fish in the intermediate length range (80–100 cm).

There is an improvement in the fits to the length data from the fresh tuna longline fisheries in region 2 as in the previous assessment. Although the selectivity in the LINE fishery was assumed to be the same as the frozen longline fisheries (Figures 20a,b), the model fitted the catch samples relatively well, despite the small number of samples. However, there are still insufficient samples to estimate a separate selectivity in this fishery.

The fit to the observed number of tag recoveries was examined for those fisheries which accounted for most of the tag returns (e.g., PSLS1S). The fit to the number of tag recoveries was examined by recombining the tags into individual release periods (i.e., aggregating the releases by age class) and excluding those recoveries that occurred during the mixing period. The fit to the tag recoveries was examined by time period (quarters) and by age at recovery, and by time at liberty (quarters) for the individual release periods and the aggregated data set (all releases combined).

The number of tag recoveries varied considerably amongst the release periods (Figure 1a,b & Figure a,b). The tags released in 2005 and the first quarter of 2006 had very low recoveries, probably due to the small number of releases and high tag mortality in the initial phase of the program.

Most of the observed tag recoveries in the post mix period were from the PSLS1S fishery and a high proportion of the total recoveries occurred during the first four quarters following the mixing period Figure a,b & Figure a,b). Longer-term recoveries were less vulnerable to the PSLS1S fishery (due to the age specific selectivity) and, hence, numbers of recoveries declined considerably (Figures 21a,b & Figure a,b).

The fit to the tag recoveries from the PSLS1S fishery by age class (at recovery) suggested that the model under-estimated the overall number of tags recovered from the fishery in younger and older age classes, to varying degrees. Fits were better to all fisheries other than the PSLS fleets (Figures 23a,b). This result indicates that the age-specific recoveries are inconsistent with the fishery selectivity functions. The tag recoveries from the PSLS fishery included a significant proportion of fish above 80 cm which generally were not vulnerable to the commercial fishery. Limited numbers of tags were also recovered by the PSFS1S and LL1S fisheries after longer periods at liberty (compared to PSLS1S). The model tends to

underestimate the number of tag recoveries throughout the age classes from the PSFS1S fishery as in 2022. This may be indicating inadequate mixing of the tags with the fish population vulnerable to the PSFS fishery.

Overall, there was a reasonable fit to the tag recoveries from the PSLS 1S fishery during the main tag recovery period (to 2011), as in 2022, but the model no longer over-estimates the number of longer term tag recoveries from the older age classes (at recovery), i.e. those fish at liberty for a longer period, which could reflect the better specification of natural mortality within the base models in 2025, or could still be a reflection of mis-reporting in tag recoveries. A small number of tags were recovered in region 1N and the model predicts a correspondingly low number of tag recoveries from the region, as in 2022.

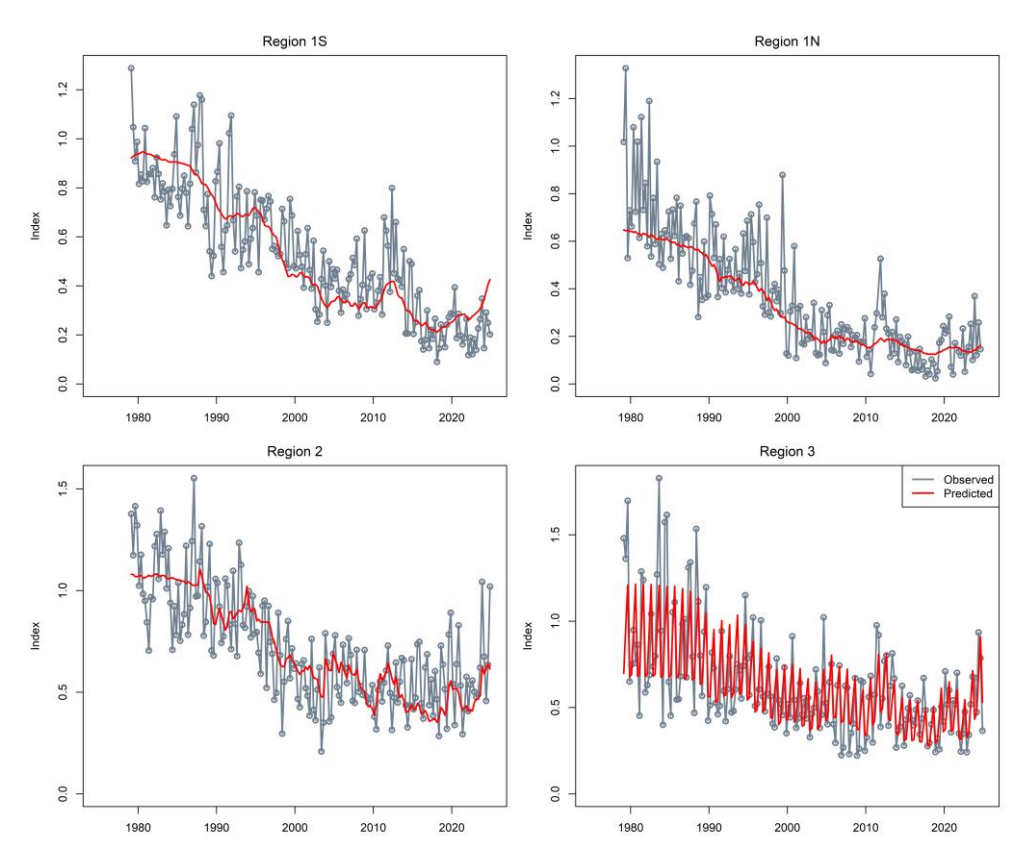


Figure 16a: Fits to the joint regional frozen longline CPUE indices 1979-2024 in the base model '6\_update\_bias'.

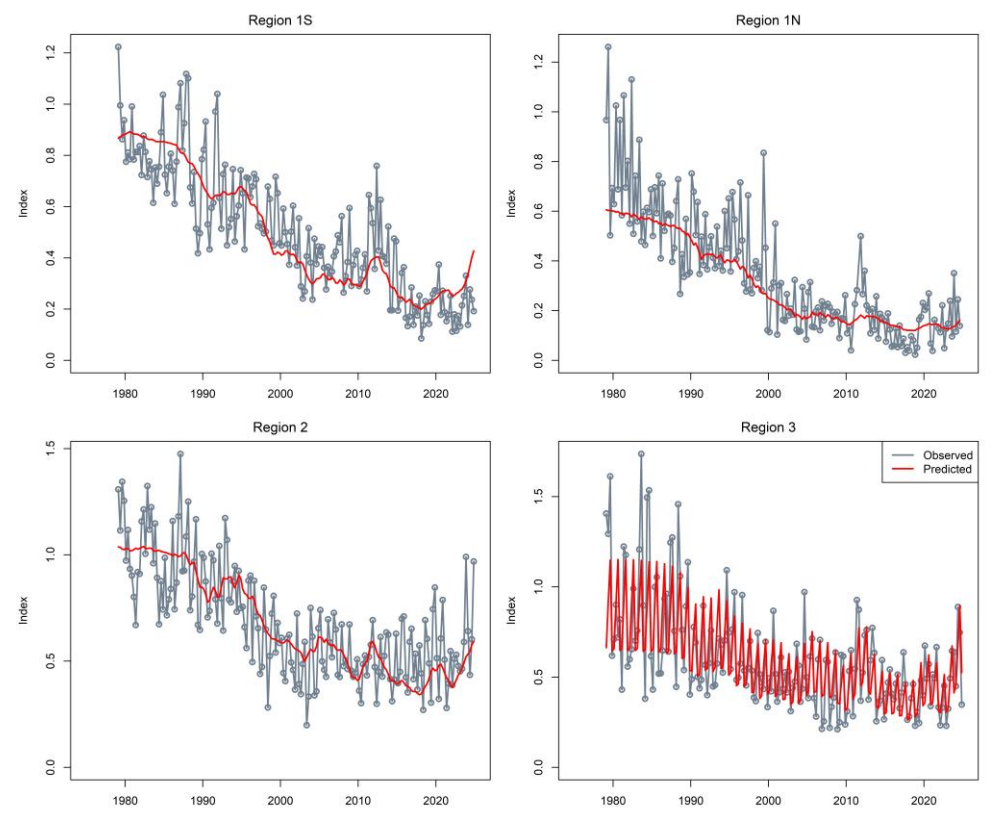
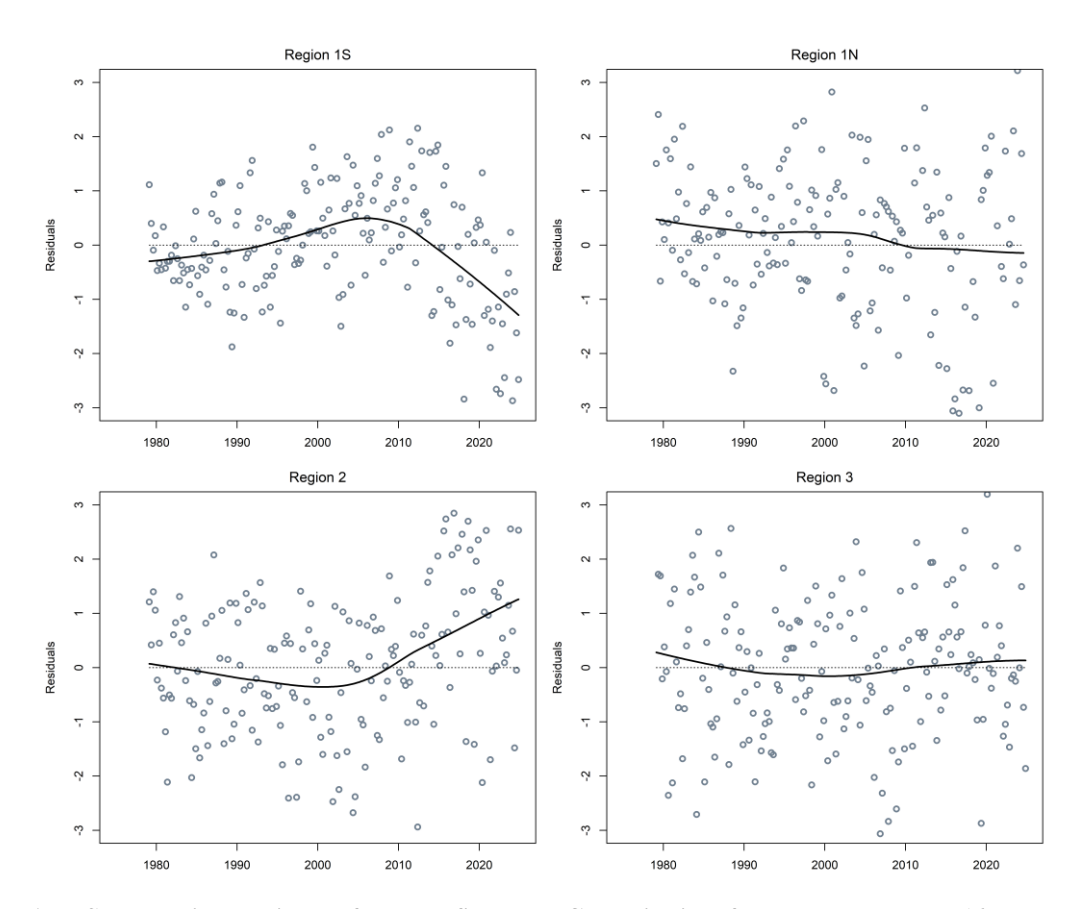
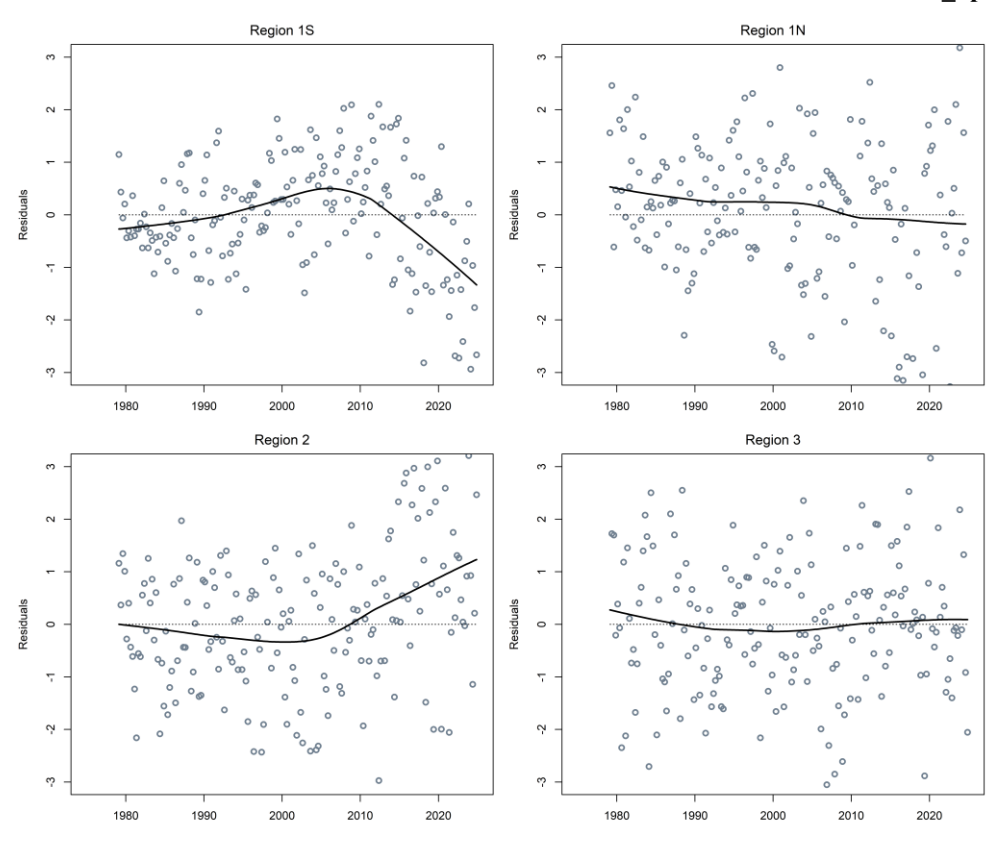


Figure 16b: Fits to the joint regional frozen longline CPUE indices 1979-2024 in the base model  $'7\_update\_cpue\_LLq'$ .



 $Figure\ 17a:\ Standardised\ residuals\ from\ the\ fits\ to\ the\ CPUE\ indices\ from\ the\ base\ model\ `6\_update\_bias'.$ 



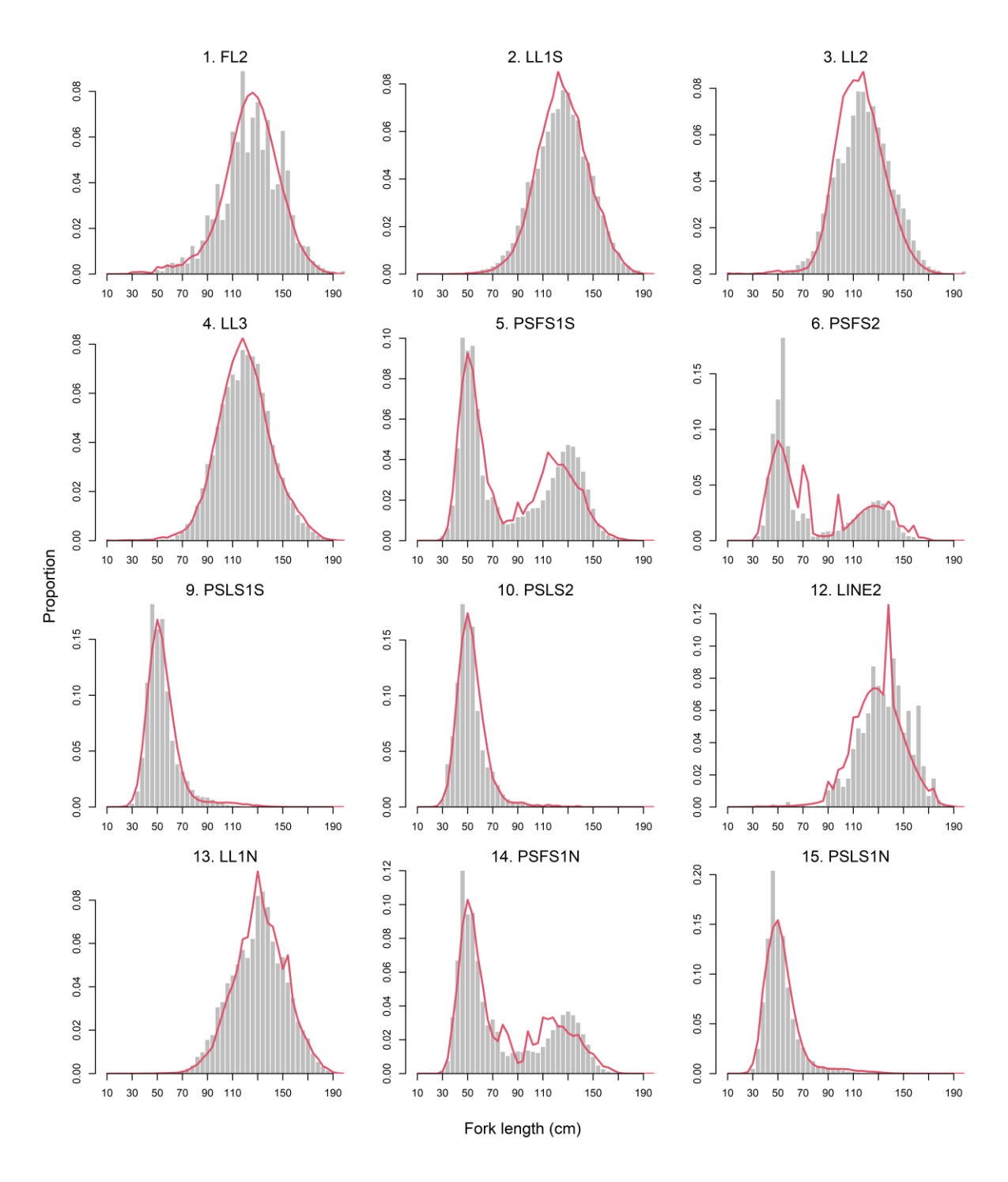


Figure 18a: Observed (grey bars) and predicted (red line) length compositions (in 4 cm intervals) for each fishery of bigeye tuna aggregated over time for the base model '6\_update\_bias'.

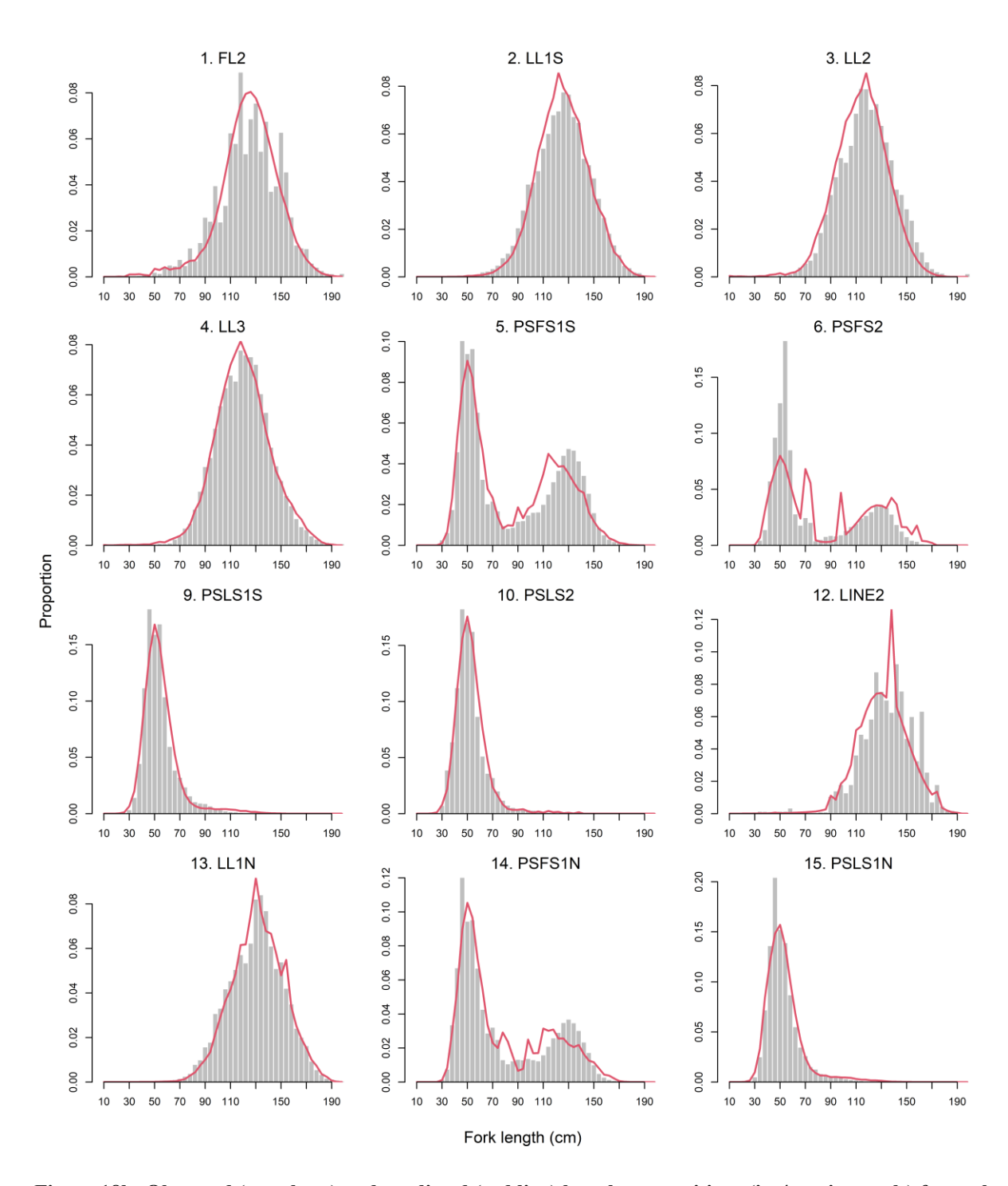


Figure 18b: Observed (grey bars) and predicted (red line) length compositions (in 4 cm intervals) for each fishery of bigeye tuna aggregated over time for the base model '7\_update\_cpue\_LLq'.

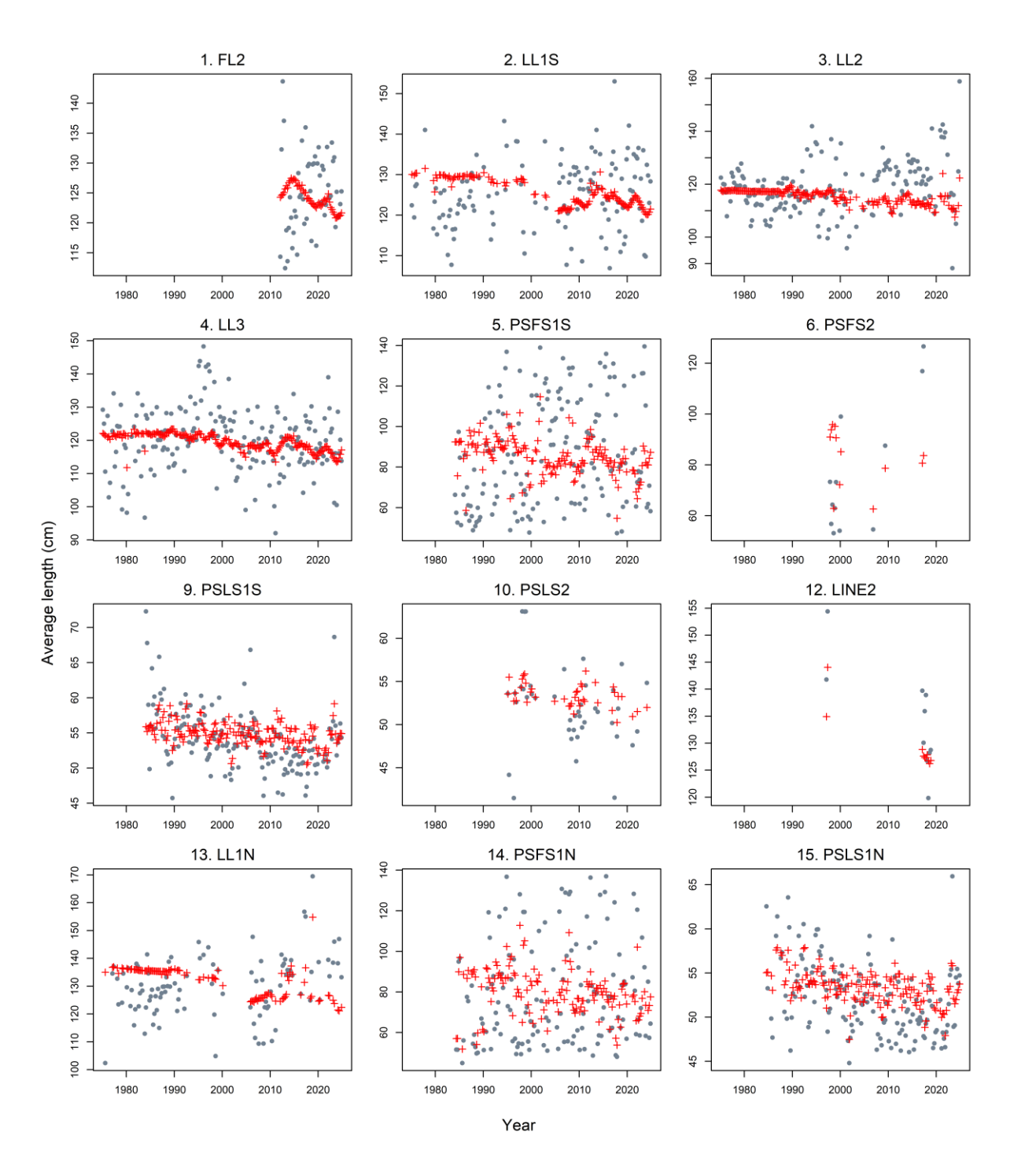


Figure 29a: A comparison of the observed (grey points) and predicted (red points and line) average fish length (FL, cm) of bigeye tuna by fishery for the main fisheries with length data for the base model '6\_update\_bias'.

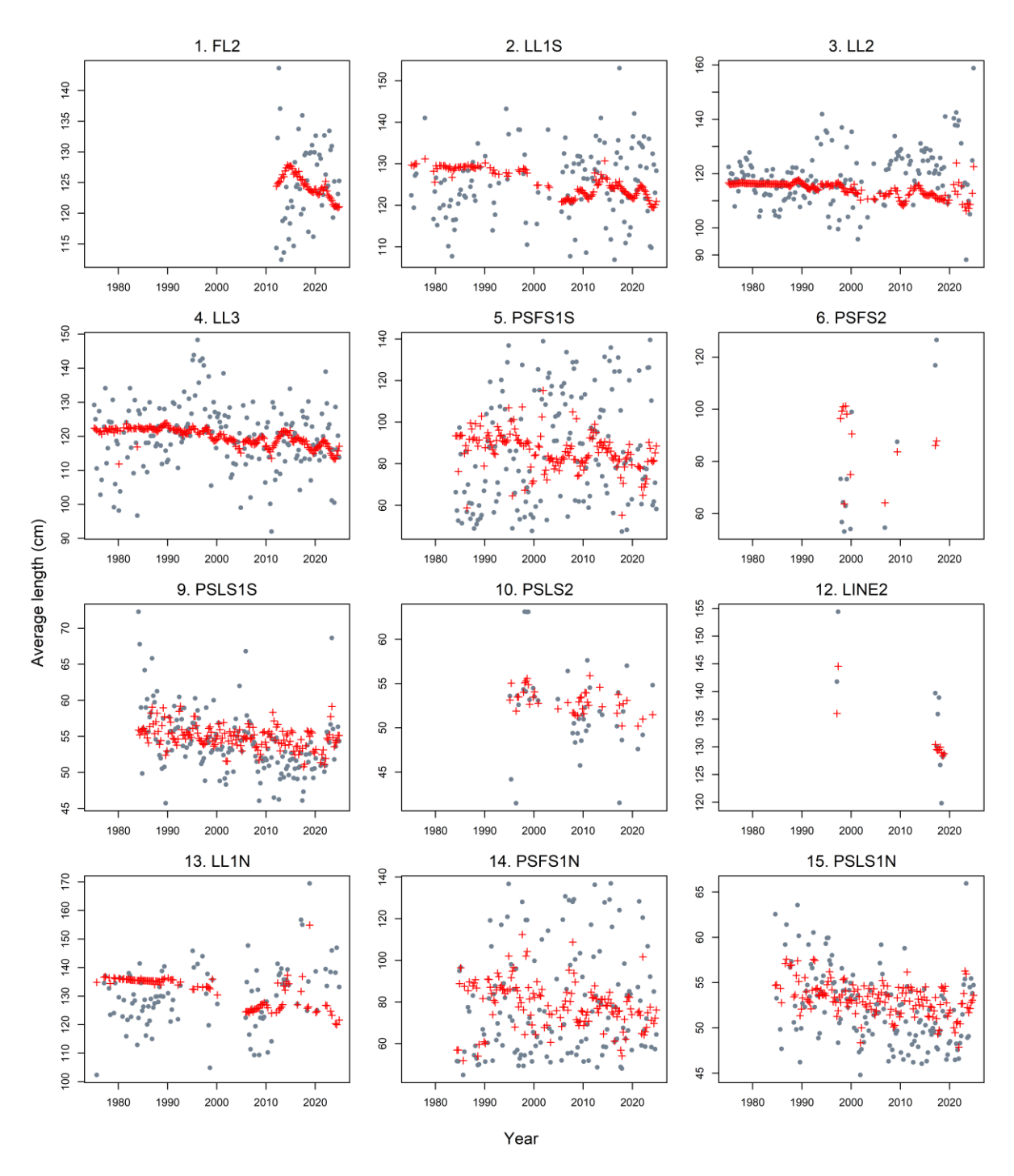


Figure 19b: A comparison of the observed (grey points) and predicted (red points and line) average fish length (FL, cm) of bigeye tuna by fishery for the main fisheries with length data for the base model '7\_update\_cpue\_LLq'.

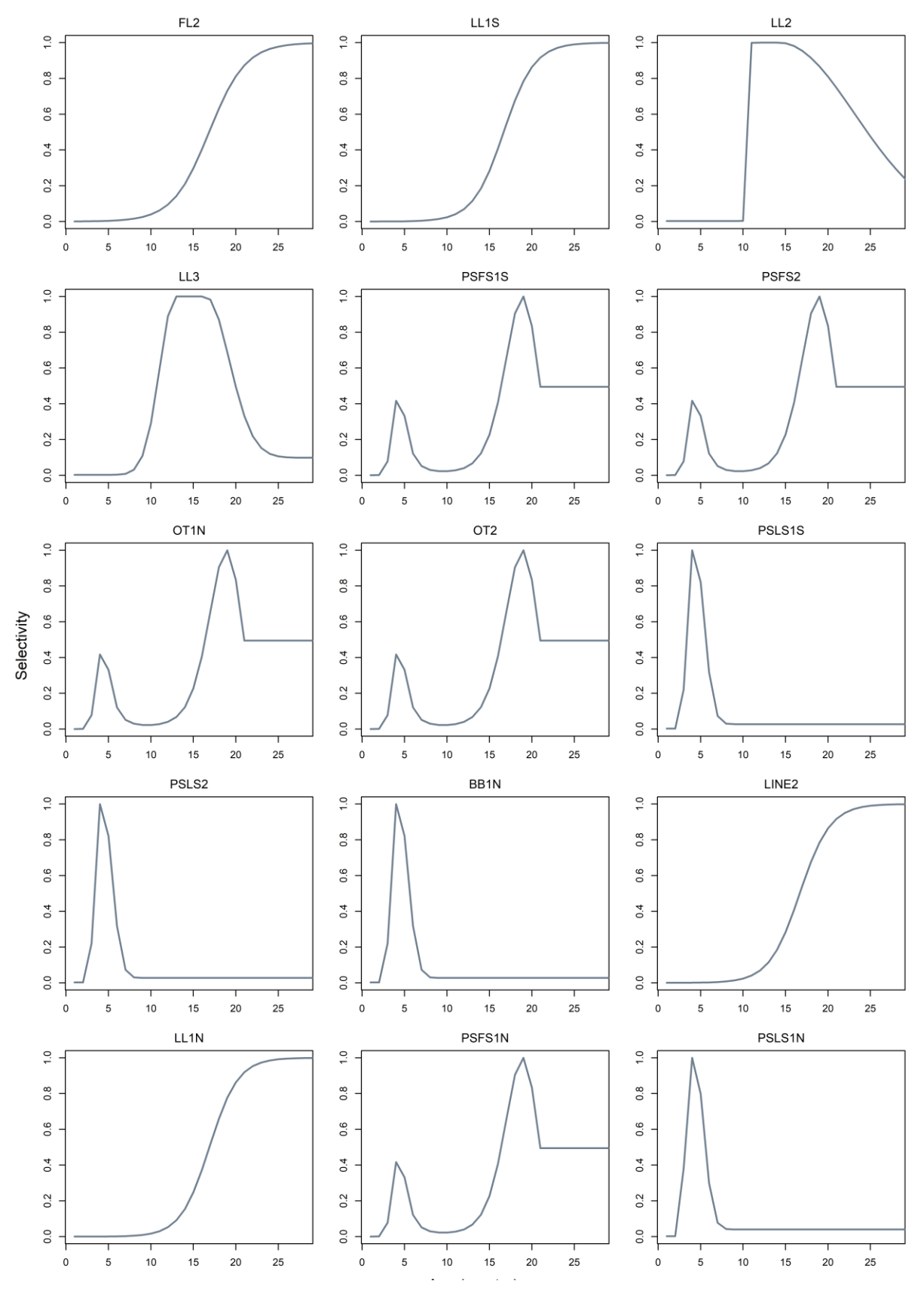


Figure 20a: Estimated age-based (quarters) selectivity for model fleets within the base model '6\_update\_bias'.

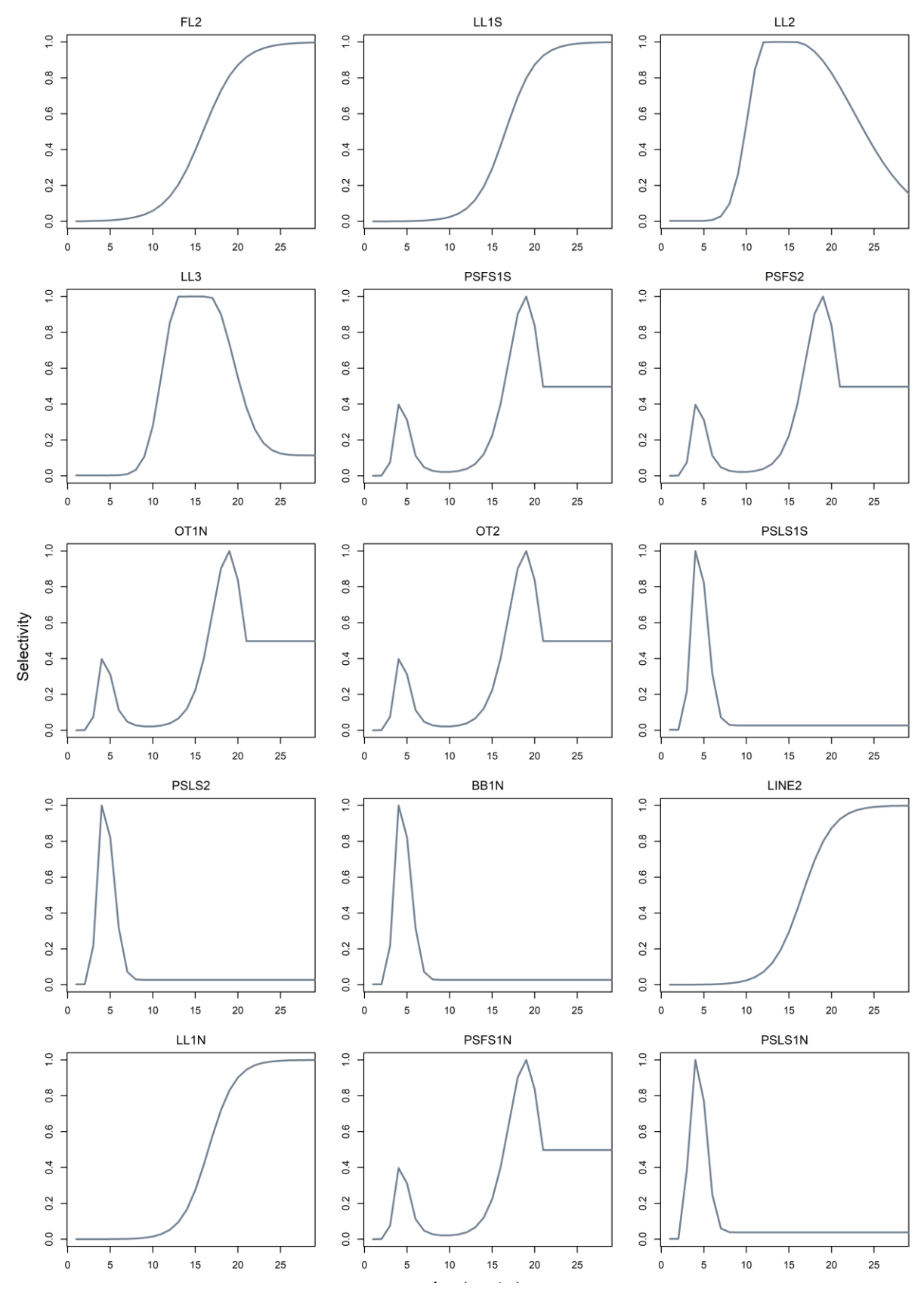


Figure 20b: Estimated age-based (quarters) selectivity for model fleets within the base model '7\_update\_cpue\_LLq'

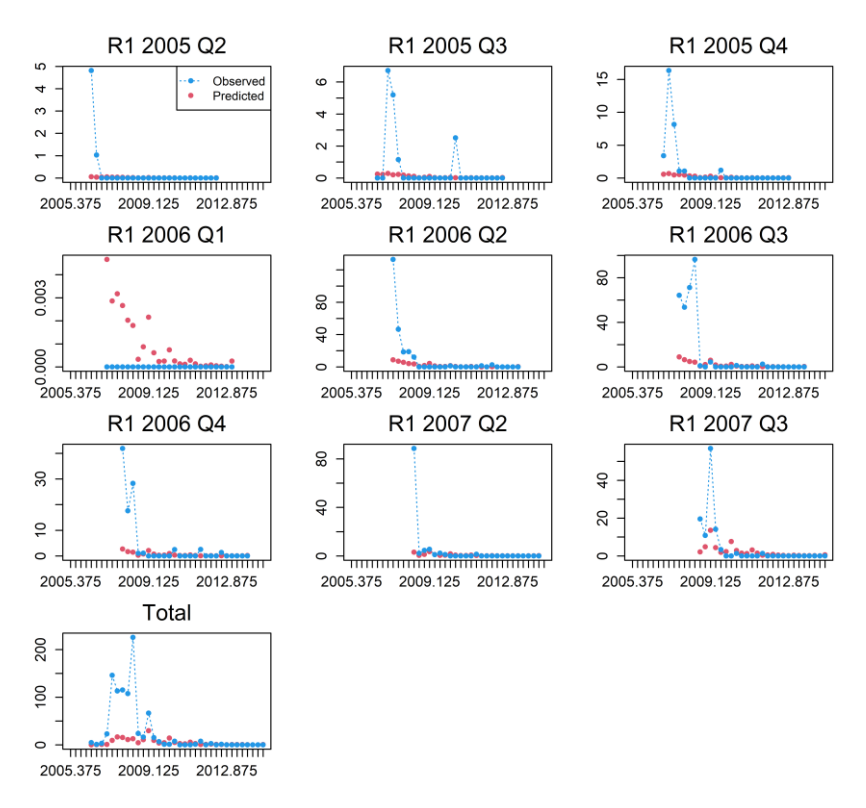


Figure 21a: Observed and predicted number of tags recovered by quarter for the PSLS fishery in region 1S (PSLS 1S). Only tags at liberty after the four quarter mixing period are included. Tag recoveries are aggregated for each release group. Base model '6 update bias'.

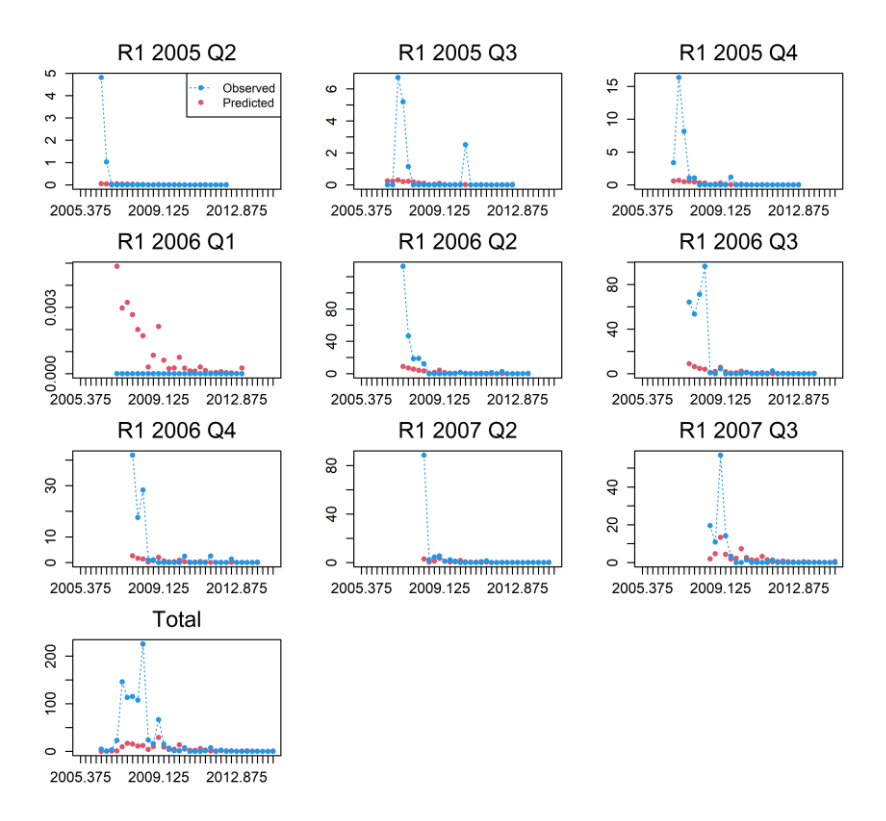


Figure 21b: Observed and predicted number of tags recovered by quarter for the PSLS fishery in region 1S (PSLS 1S). Only tags at liberty after the four quarter mixing period are included. Tag recoveries are aggregated for each release group. Base model '7\_update\_cpue\_LLq'.

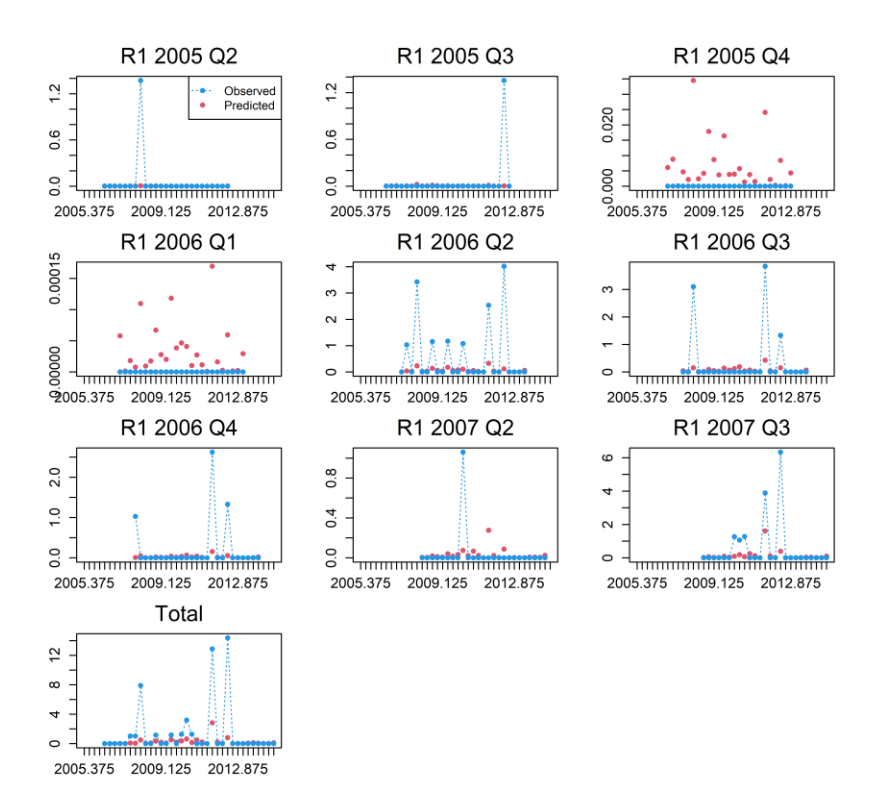


Figure 22a: Observed and predicted number of tags recovered by quarter for the PSLS fishery in region 1N (PSLS 1N). Only tags at liberty after the four quarter mixing period are included. Tag recoveries are aggregated for each release group. Base model '6\_update\_bias'.

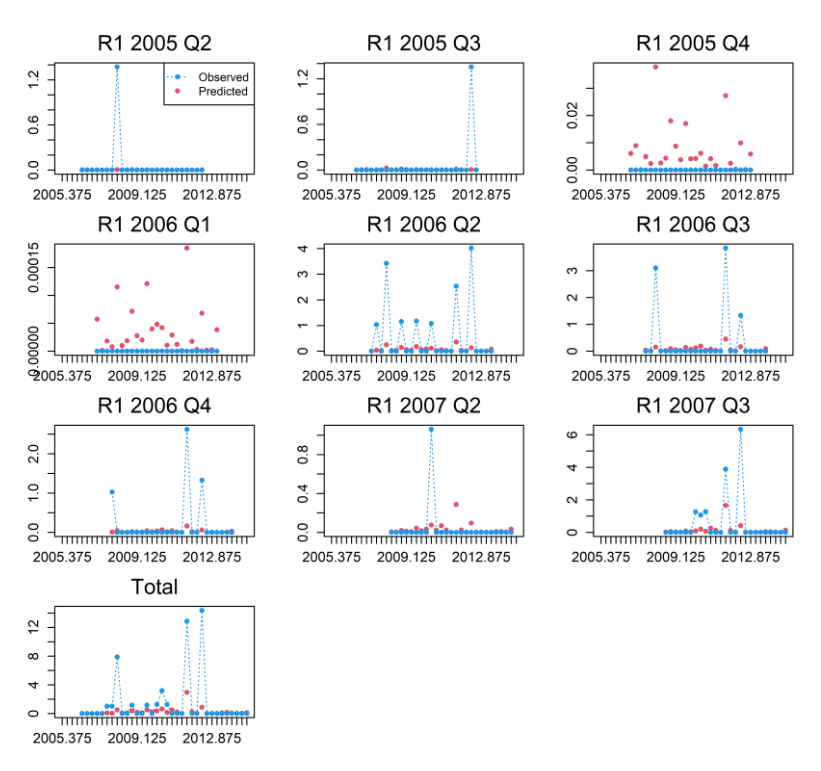


Figure 22b: Observed and predicted number of tags recovered by quarter for the PSLS fishery in region 1N (PSLS 1N). Only tags at liberty after the four quarter mixing period are included. Tag recoveries are aggregated for each release group. Base model '7 update cpue LLq'.

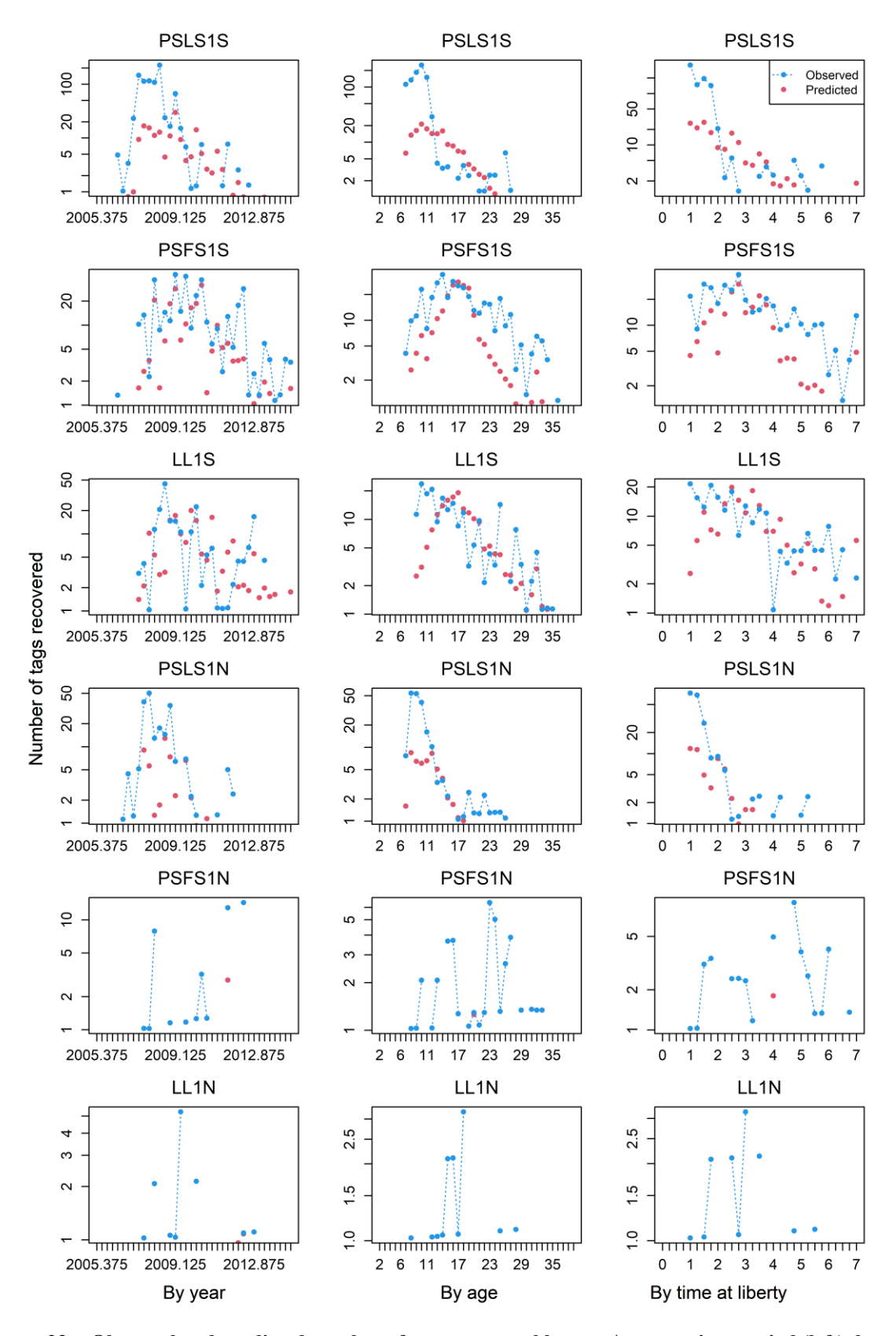


Figure 23a: Observed and predicted number of tags recovered by year/quarter time-period (left), by age (mid), and by time at liberty (in quarters, right) for main Purse seine and longline fisheries in region 1N and 1S (PSLS 1S, 1N, PSFS 1S, 1N, and LL 1S, 1N) from '6\_update\_bias'. Only tags at liberty after the four-quarter mixing period are included. Tag recoveries are aggregated for each of the regional fisheries.

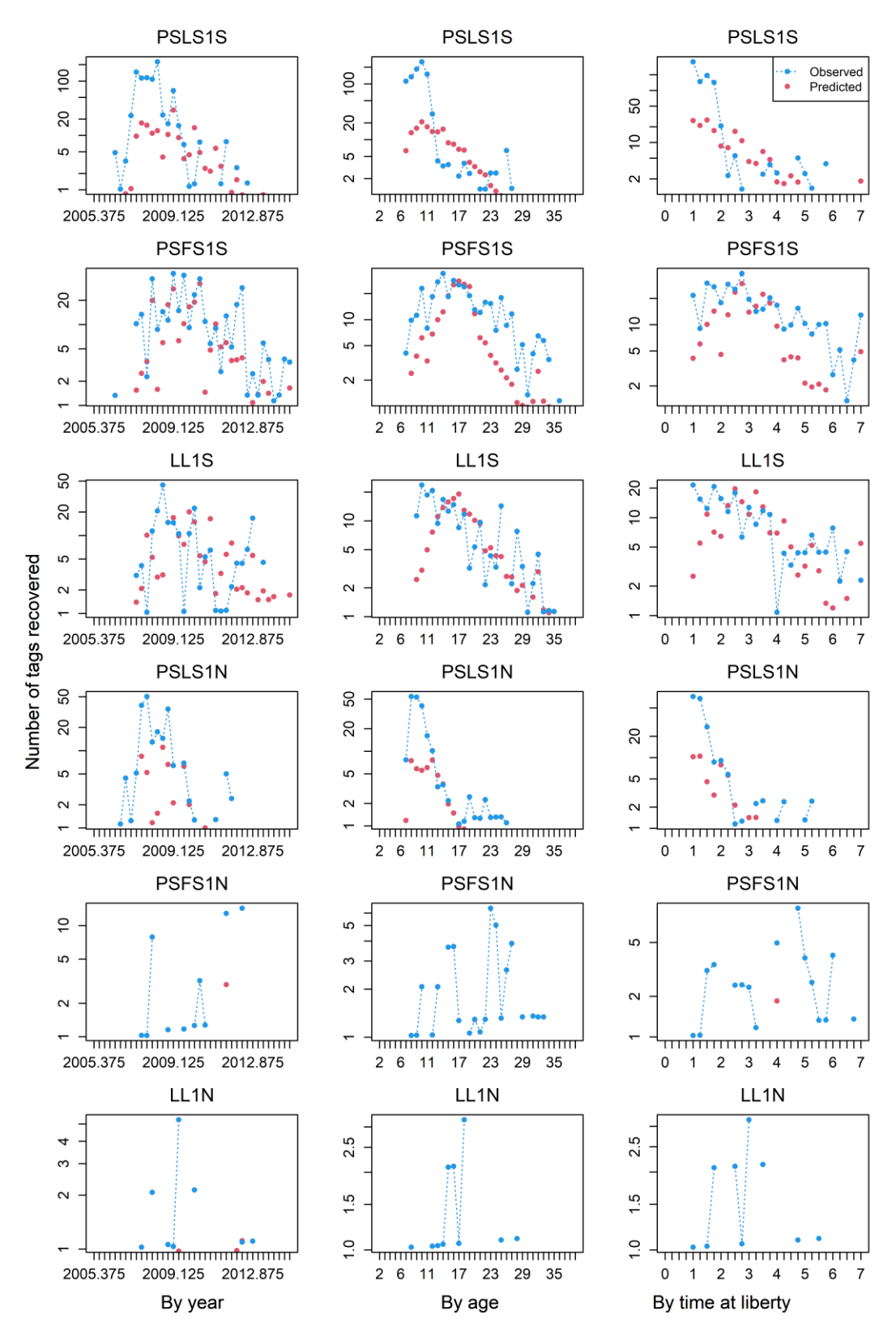


Figure 23b: Observed and predicted number of tags recovered by year/quarter time-period (left), by age (mid), and by time at liberty (in quarters, right) for main Purse seine and longline fisheries in region 1N and 1S (PSLS 1S, 1N, PSFS 1S, 1N, and LL 1S, 1N) from '7\_update\_cpue\_LLq. Only tags at liberty after the four-quarter mixing period are included. Tag recoveries are aggregated for each of the regional fisheries.

#### **6.3. Model estimates**

## 6.3.1. Selectivity

As in the 2022 model, the estimated parameters in the basic model include: the overall population scale parameter R0, the time series of recruitment deviates, the distribution of recruitment among regions, age specific movement parameters, the fishery selectivity parameters, fishery tag reporting rates and the catchability parameters for the CPUE indices.

The age-specific selectivity functions are presented in Figures 20 a,b Full selectivity is reached for the R1N and 1S longline fisheries at around age 22 (quarters), which is older than the 18 quarters in the 2022 model, presumably due to updates in the growth function in 2025.

Selectivity for the longline fishery in R2 was predicted to be asymptotic with a steep transition. The selectivity for the longline fishery in R3 was estimated to be dome-shaped, with a diminishing right limb from roughly 18 to 22, as in 2022. Peak selectivity for the PSLS1N and PSLS1N fisheries is estimated to be a much tighter peak, occurs at ages 5 quarters, compared to ages 5-8 in 2022. (Figures 20 a,b). For the PSFS fisheries, selectivity was estimated to be bimodal with lower levels of selectivity for younger fish compared to older fish. This represents a departure from 2022 when the modes showed similar levels of selectivity.

#### 6.3.2. Recruitment

As in 2022, recruitment deviates were estimated for the quarterly time steps from 1984–2023. Estimating the recruitment prior to 1984 was quite uncertain. There are longer-term trends visible in the recruitment deviates, with higher-than-average recruitment estimated from 2000 to 2005 (as opposed to 1990-2000 in the 2022 model), and reduced recruitment between 2010 and 2015 (Figure 24), similar to 2022. These trends correspond to periods of higher and lower catches from the PSLS fishery, after revised catches. Recruitment for 2020 to 2022 was estimated to be higher than the long term mean, presumably to account for the recent increase in CPUE in the longline indices.

Recruitment was assumed to occur in all regions equally as there were no significant differences in CPUE indices between the regions, unlike in the previous model.

#### 6.3.3. Movement rates

Movement rates were estimated amongst the model regions. The model estimates high movement rates of mature fish amongst regions 1N and 2 (reciprocal movement) (Figures 25 a,b). Very low mixing was estimated to occur between regions 1S and any other region (as supported by the tag-return data). Some reciprocal movement of younger fish between regions 1S and region 2 is estimated to occur. These higher rates of movement are a departure from the low rates estimated by the 2022 model, presumably to account for the lack of recruitment variability between regions. This represents an uncertainty in the model structure and / or biological information available for bigeye tuna in the Indian Ocean. Increased information on adult movement would improve the model, especially as the CPUE indices appear to influence the estimated movement rates (Figures 25 a,b).

### 6.3.4. Tag reporting rates

Tag reporting rates were estimated for the non-purse seine fisheries (Figure ). For some of these fisheries, the estimated reporting rates are unlikely to be influential in the overall assessment as the reported tags were predominately recovered during the tag mix period. However, a considerable proportion of the tag recoveries from the LL1S and LL3 fisheries occurred during the post mixing phase and, hence, the tag reporting rates will have some influence in the model likelihood. For these fisheries, tag reporting rates were estimated at 0.21 and 0.52, respectively. while the reporting rate for the LL1N fishery was estimated to be considerably lower (0.1). The estimates for the LL2 and LL3 fisheries are associated with high uncertainty and probably have reflected the large inter-annual variabilities in the tag recoveries (and reporting) from these fisheries.

## 6.3.5. Spawning stock biomass

In the first base model (6\_update\_bias), region 3 accounted for approximately 34% of the initial spawning stock biomass (hereafter biomass), and approximately 24 % in R1S (area 1) and Region 2 (area2), with the final 18 % in region 1N (area 4). In the second base model, the percentage distribution was similar, but there were differences between areas 1 and 2, presumably a reflection of the CPUE adjustment in this model (Figures 28 a,b). These estimates are very similar to the previous assessment. There is a double normal selectivity function for the longline fisheries in areas 2 and 3, and the additional biomass in region 3 is potentially a reflection of cryptic biomass in this area (biomass associated with large fish that are unavailable to the LL3 fishing fleet).

Spawning biomass decreases across all regions until the beginning of the 2000s (year quarter 300; Figures 28 a,b) and the beginning of the 2000s. Between 2009 and 2014, biomass somewhat increased before declining quickly to historical low levels in 2020. The spawning biomass increased in all regions over the last three years, particularly in area (Region 1S) (Figures 27 a,b), mirroring the increases in frozen longline CPUE indices.

## 6.3.6. Trends in fishing mortality

The estimates of fishing mortality for the fisheries in regions 2 and 3 were low (Figures 28 a,b), with the notable exception of the PSLS2 fleet in region 2. The relative mortality rates between fleets has changed since the last assessment, with rates for the longline fleets being much lower than that of the purse seine fleets, with a notable increase in the PSLS fleet in region 1 (PSLS1N).

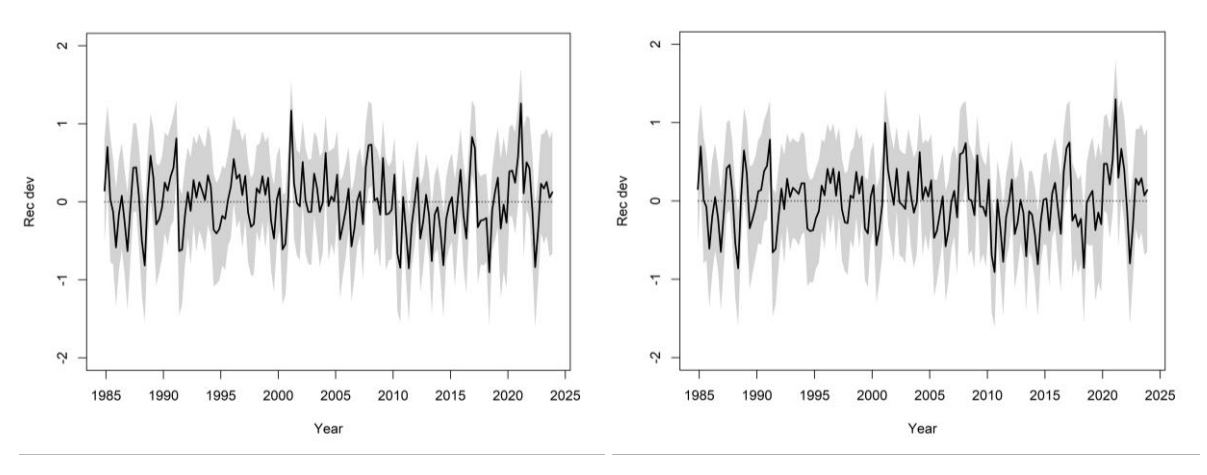


Figure 24: Recruitment deviates from the SRR with 95% confidence interval from (LHS) ' $6\_update\_bias$ ' and (RHS) ' $7\_update\_cpue\_LLq$ '.

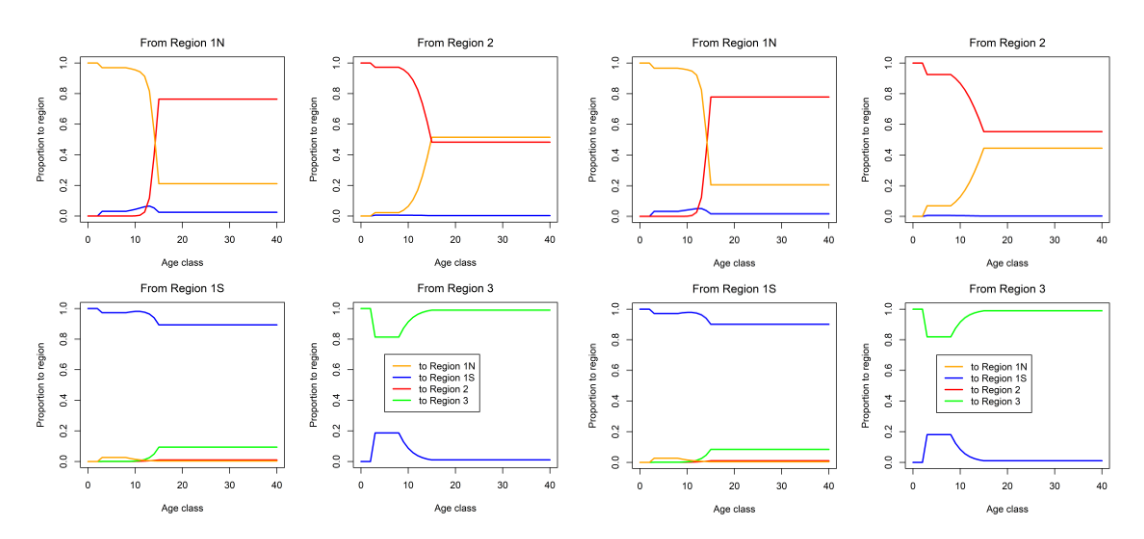


Figure 25: Estimated age specific movement parameters for the base models: (LHS)  $^{6}$ \_update\_bias' and (RHS)  $^{7}$ \_update\_cpue\_LLq'.

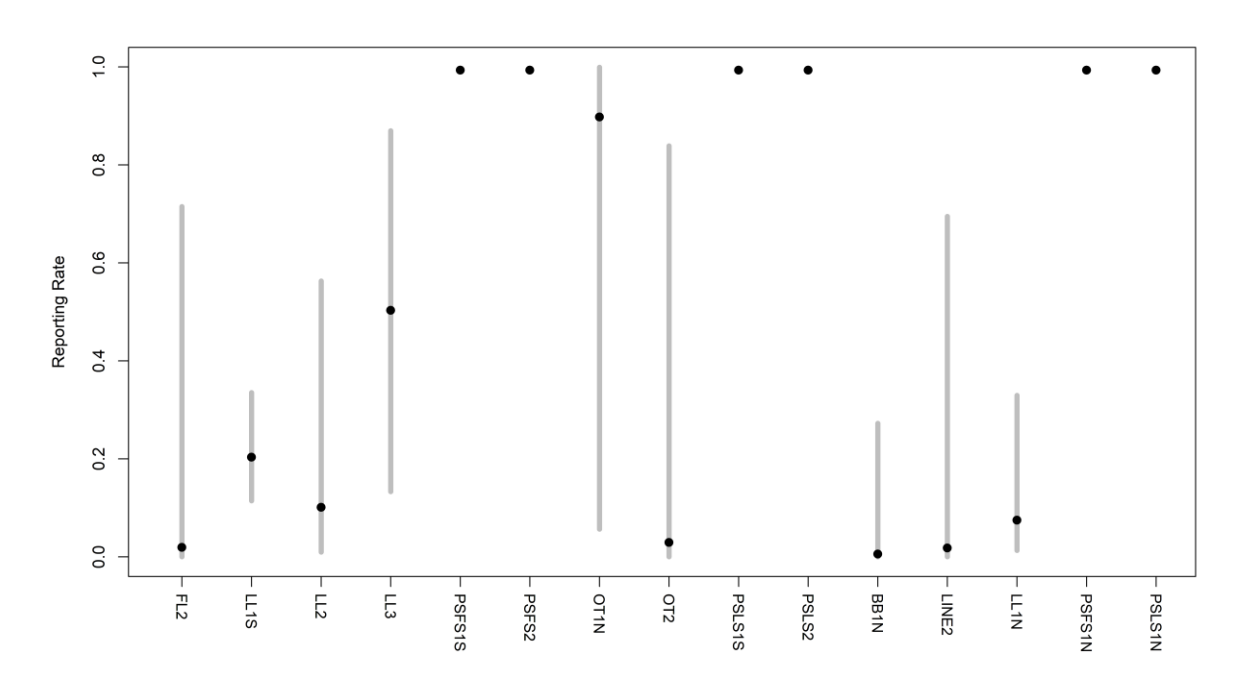


Figure 26a: Tag reporting rates for each fishery from the base model '6\_update\_bias'. Purse seine reporting rates were fixed at a value of 1.0. Reporting rates for the other fisheries were estimated. The grey lines represent the 95% confidence interval for the estimated values.

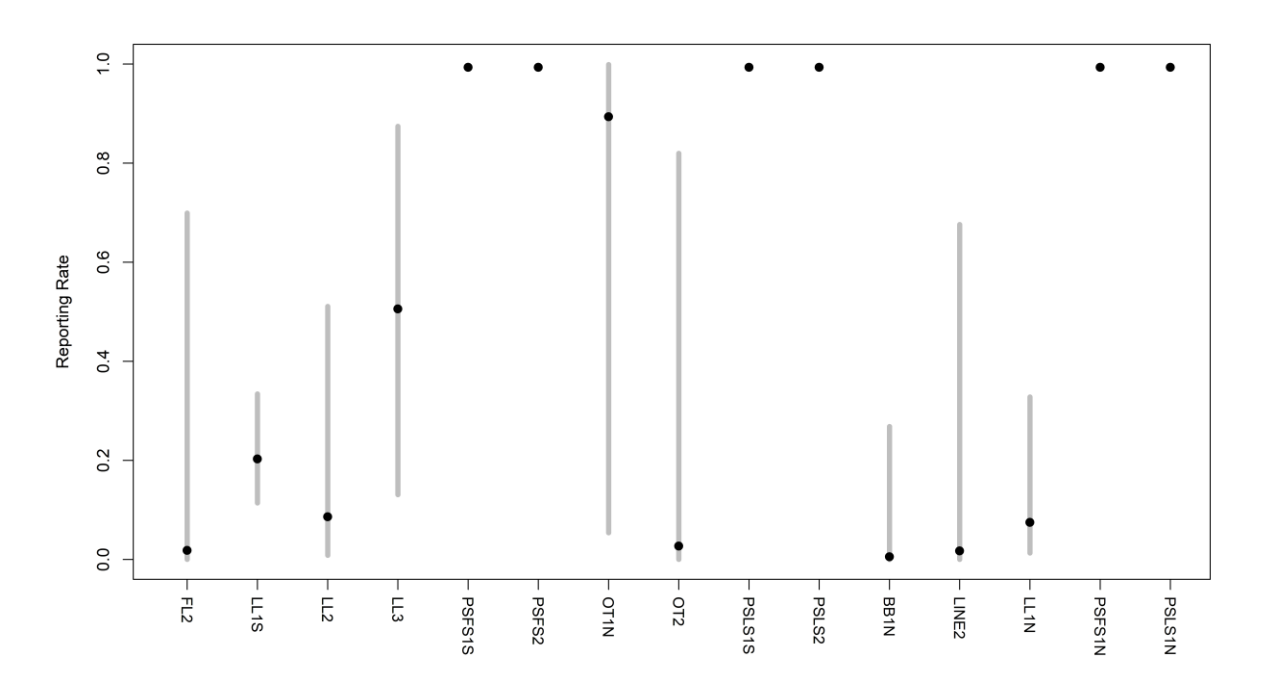


Figure 26b: Tag reporting rates for each fishery from the base model '7\_update\_cpue\_LLq'. Purse seine reporting rates were fixed at a value of 1.0. Reporting rates for the other fisheries were estimated. The grey lines represent the 95% confidence interval for the estimated values.

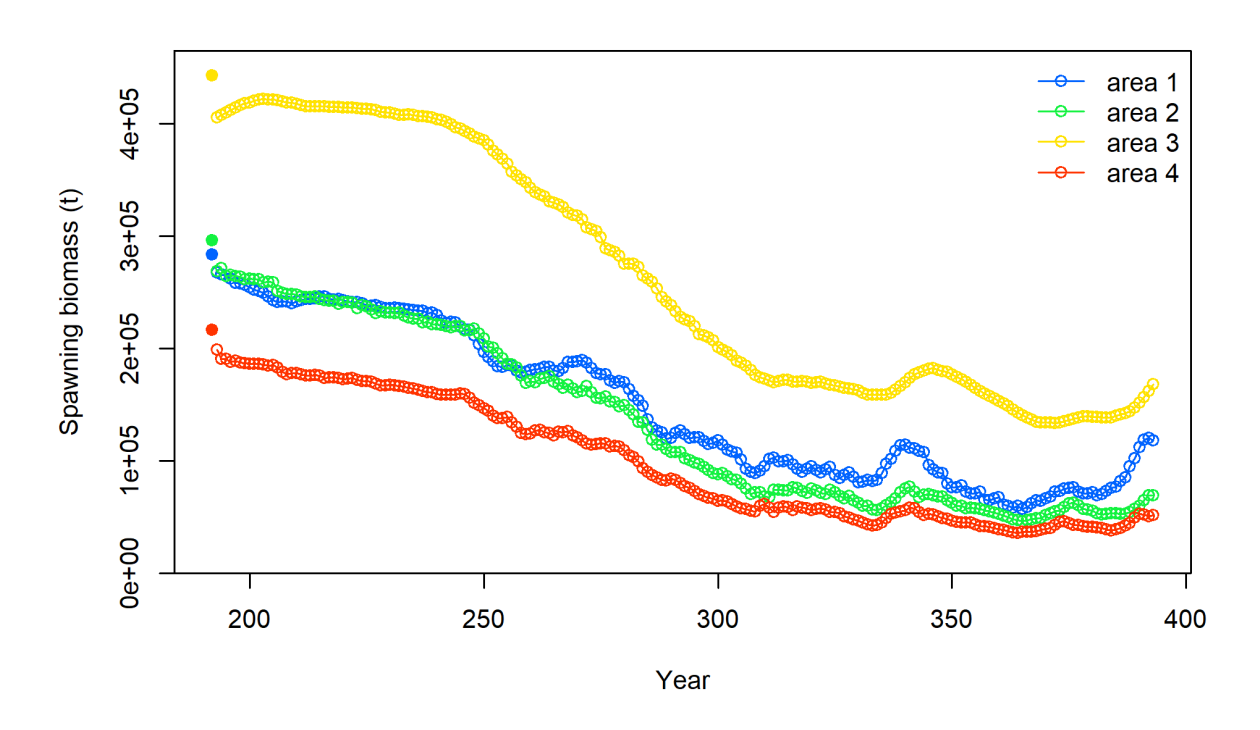
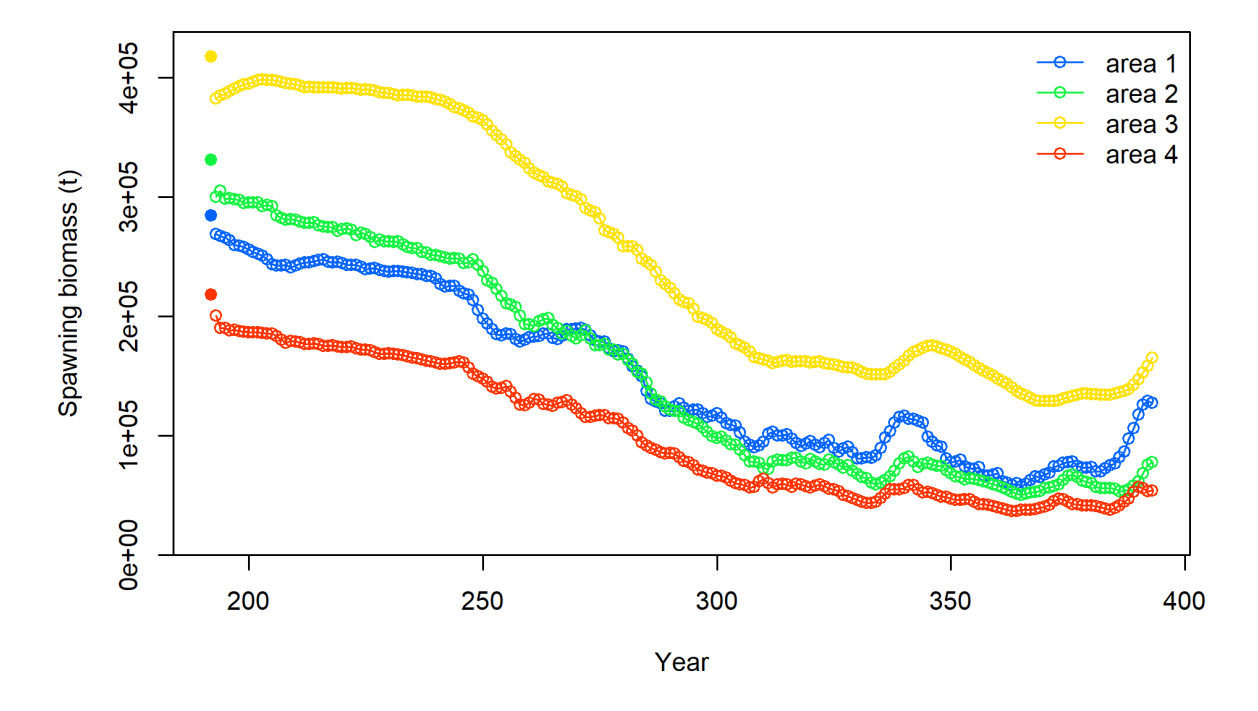


Figure 27a: Estimated spawning biomass trajectories for the individual model regions from the base model '6\_update\_bias'.



 $Figure\ 27b:\ Estimated\ spawning\ biomass\ trajectories\ for\ the\ individual\ model\ regions\ from\ the\ base\ model\ `7\_update\_cpue\_LLq'.$ 

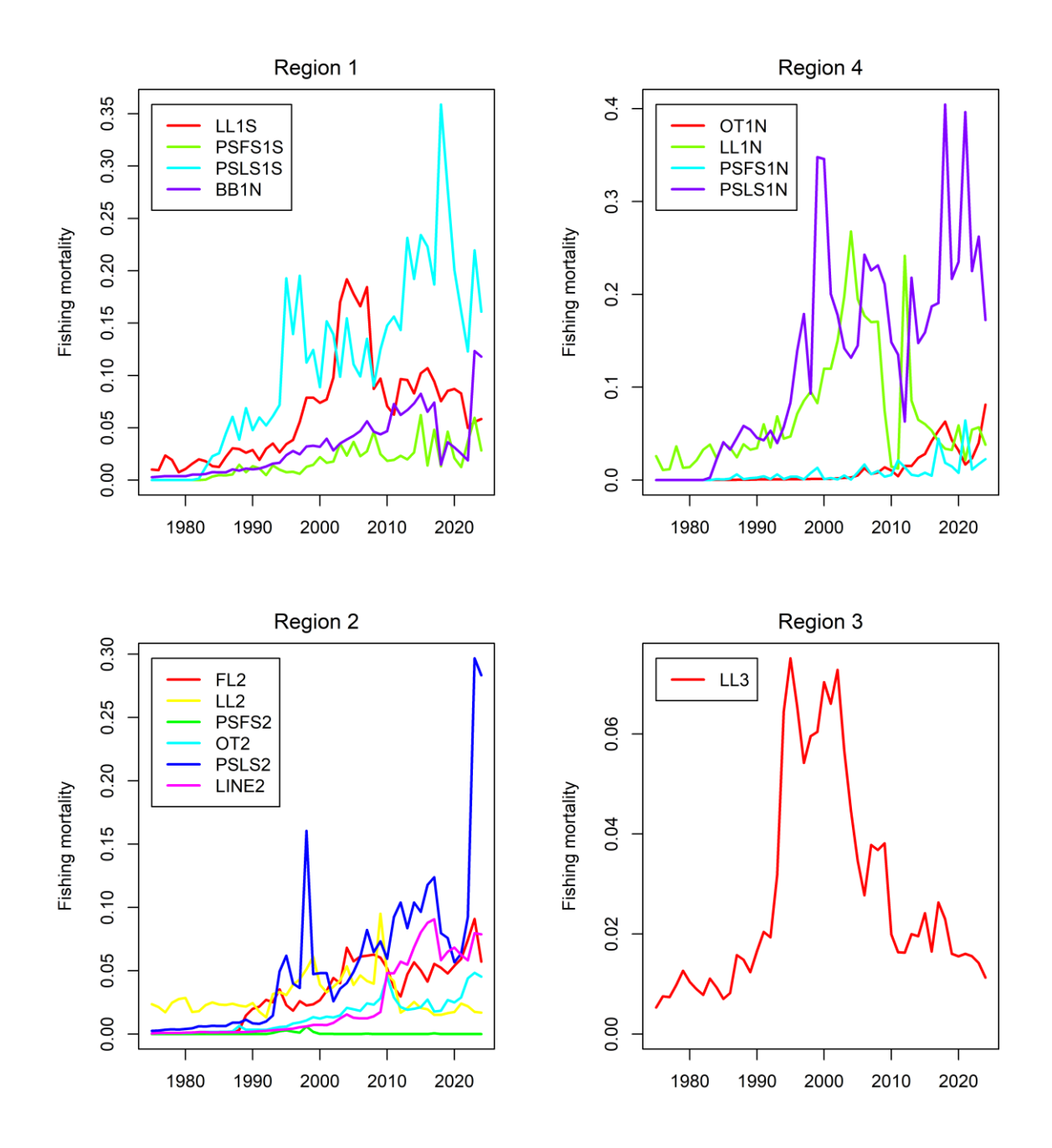


Figure 28a: Trends in fishing mortality (yearly) by fleet for the base model '6\_update\_bias'.

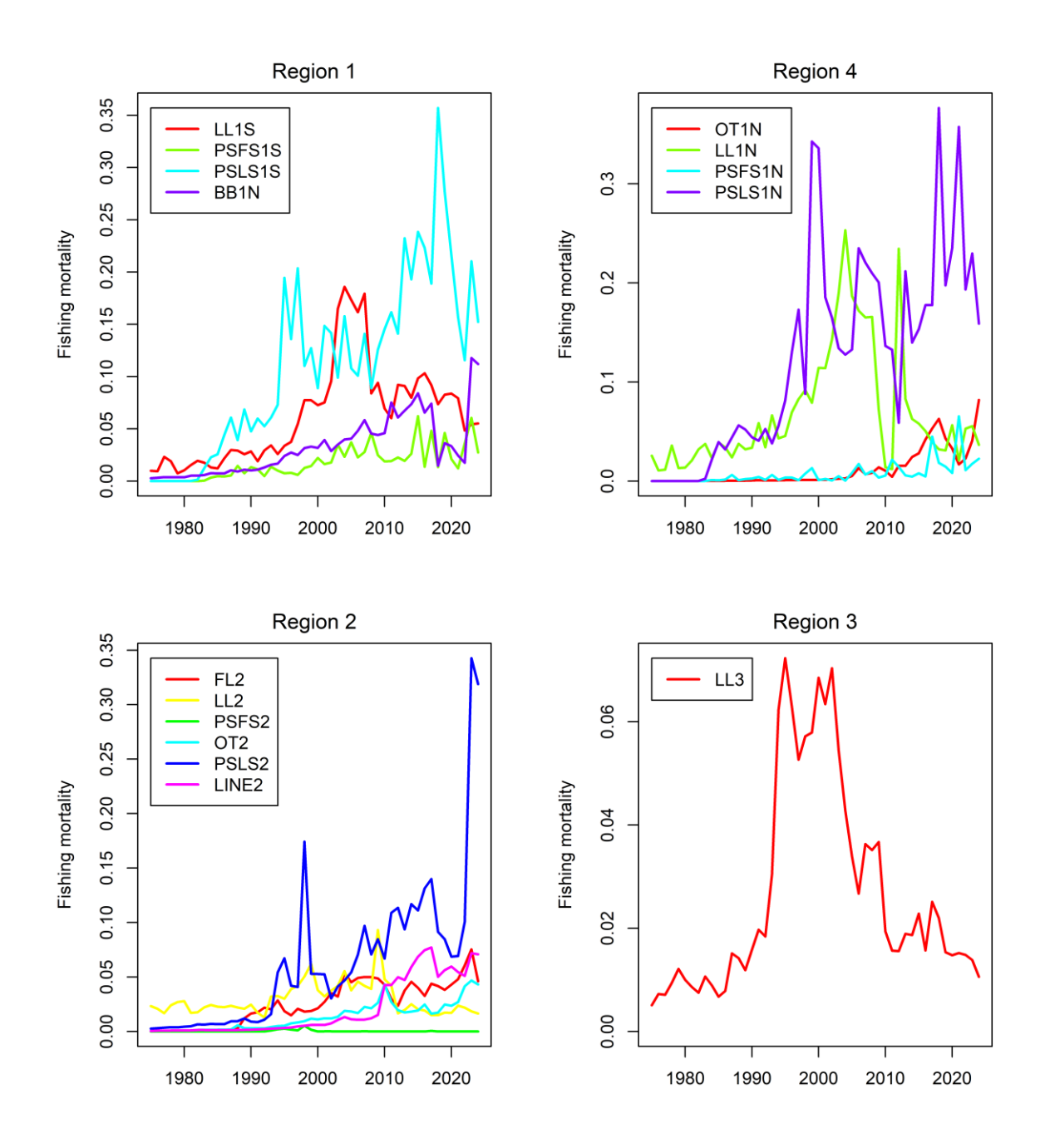


Figure 28b: Trends in fishing mortality (yearly) by fleet for the base model '7\_update\_cpue\_LLq'.

## 6.4. Diagnostics

Some diagnostic tools were run for both base models, including running an age structured production model for both base models a retrospective analysis, and a hindcasting analysis.

## 6.4.1. ASPM analysis

The Age Structured Production Model (ASPM) analysis (Maunder & Piner, 2015) was used to illustrate the main drivers of the population trend, and to understand whether the composition data has an undue influence on the estimates of abundance. The ASPM analysis involved running two variations of the reference models: *ASPMfixed* where length composition data were removed from the model (by fixing selectivity parameters) and recruitment deviates were fixed at zero; and *ASPMrec* where fixed recruitment deviates (estimates from the reference model) were added back into the model (and selectivity remained fixed).

The estimated spawning stock biomass from both ASPM model runs for both base models are shown in Figures 29a & b. The analyses indicated that the catches and abundance indices for the bigeye tuna stock generally agree, suggesting that the catch by itself may adequately explain the overall degree of stock depletion seen in the historical CPUE indices.

The stock would be expected to fall at a slower rate (but from a lower starting point) and then increase from around 2000 to present (quarter 300) with no variation in recruitment (ASPMFixed). All ASPM models provided similar estimates of relative abundance. To account for changes in the CPUE indices (abundance indices), the model requires variation in recruitment. For all other diagnostics the ASPM analysis provided similar results for the SS3 model, the ASPMFixed and ASPMrec, suggesting there is no undue influence of the length frequency data on the model outputs.

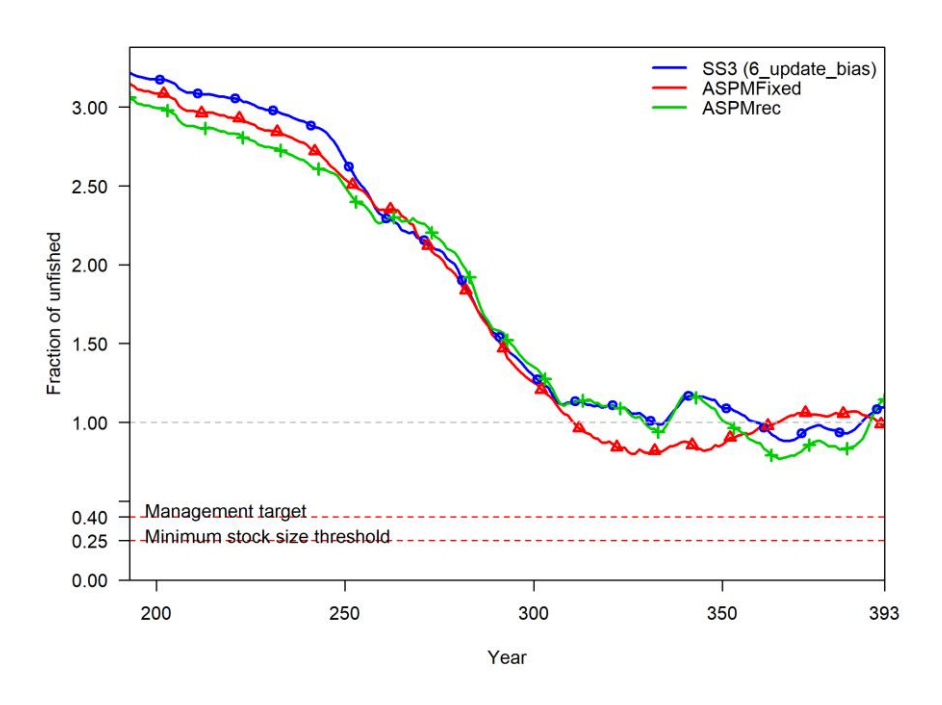


Figure 29a: ASPM analysis for the base model '6\_update\_bias': ASPMfixed (no recruitment deviations), and ASPMrec (recruitment deviates from the reference model added back). Both runs excluded the length composition data and fixed the selectivity parameters.

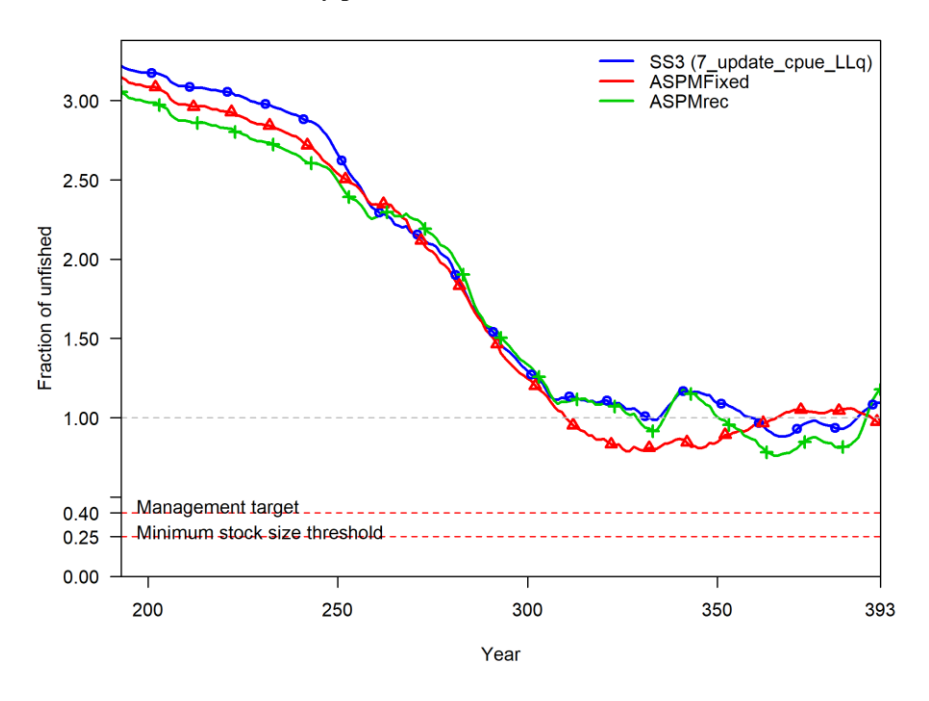


Figure 29b: ASPM analysis for the base model '7\_update\_cpue\_LLq': ASPMfixed (no recruitment deviations), and ASPMrec (recruitment deviates from the reference model added back). Both runs excluded the length composition data and fixed the selectivity parameters.

## 6.4.2. Retrospective analysis

Retrospective analysis is a diagnostic approach to evaluate the reliability of parameter and reference point estimates and will allow the revelation of systematic bias in the model estimation. It involves fitting a stock assessment model to the full dataset, and then sequentially removing data from the inputs from the most recent years. The analysis was conducted using the two base models, and the last 5 years (20 quarters) of data were removed in 4-quarter increments to evaluate whether there were any notable changes to the model results. The selected period mirrors that of previous assessments and was intended to avoid removing any tag recovery data. The analysis of the impact of data removal was conducted on the outputs of estimated spawning stock biomass (SSB) and the ratio of SSB<sub>current</sub> to SSB<sub>0</sub>..

There were no apparent retrospective patterns in the estimates for SSB or SSB<sub>2024</sub>/SSB<sub>0</sub> (Figure 30a,b), and this provides significant confidence in the robustness of the model with respect to inclusion of recent observational data.

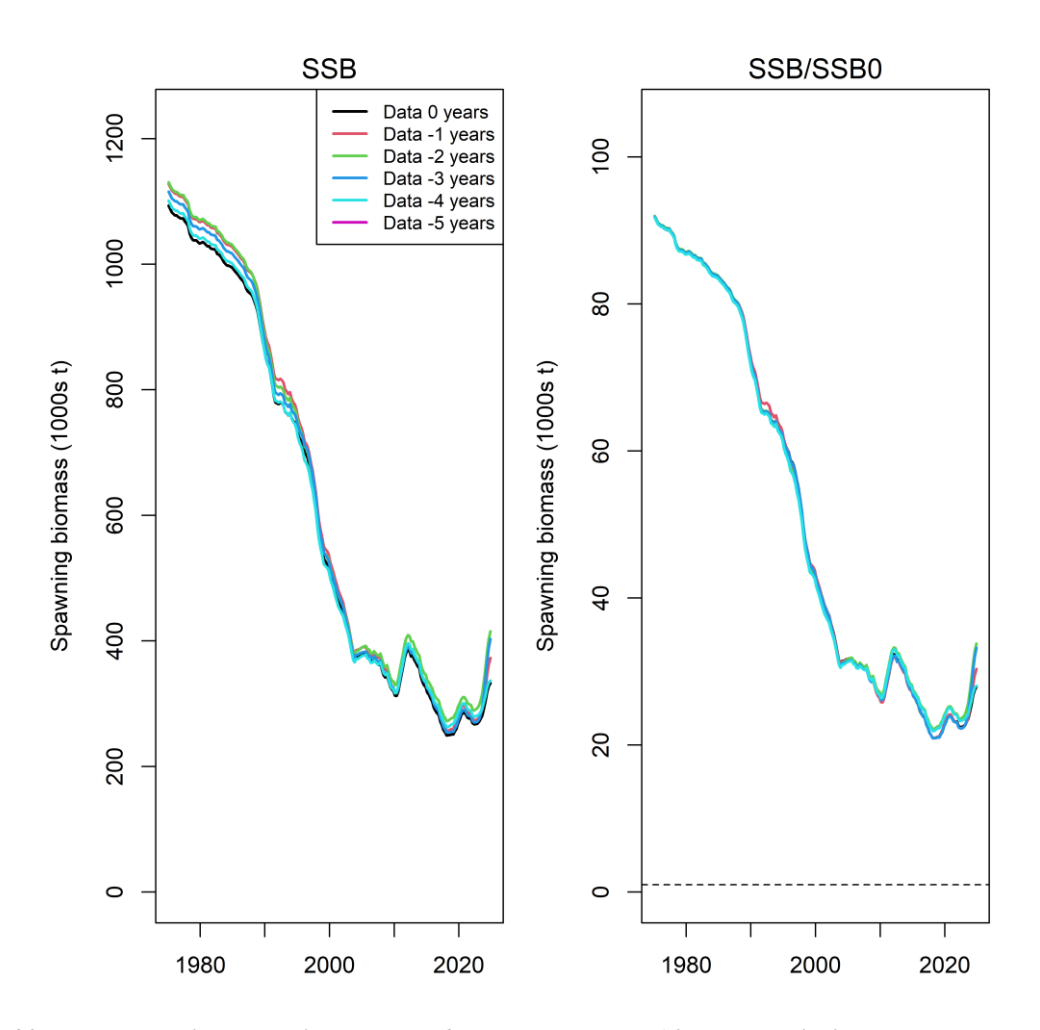


Figure 30a: Retrospective analysis summary for the base model '6\_update\_bias'.

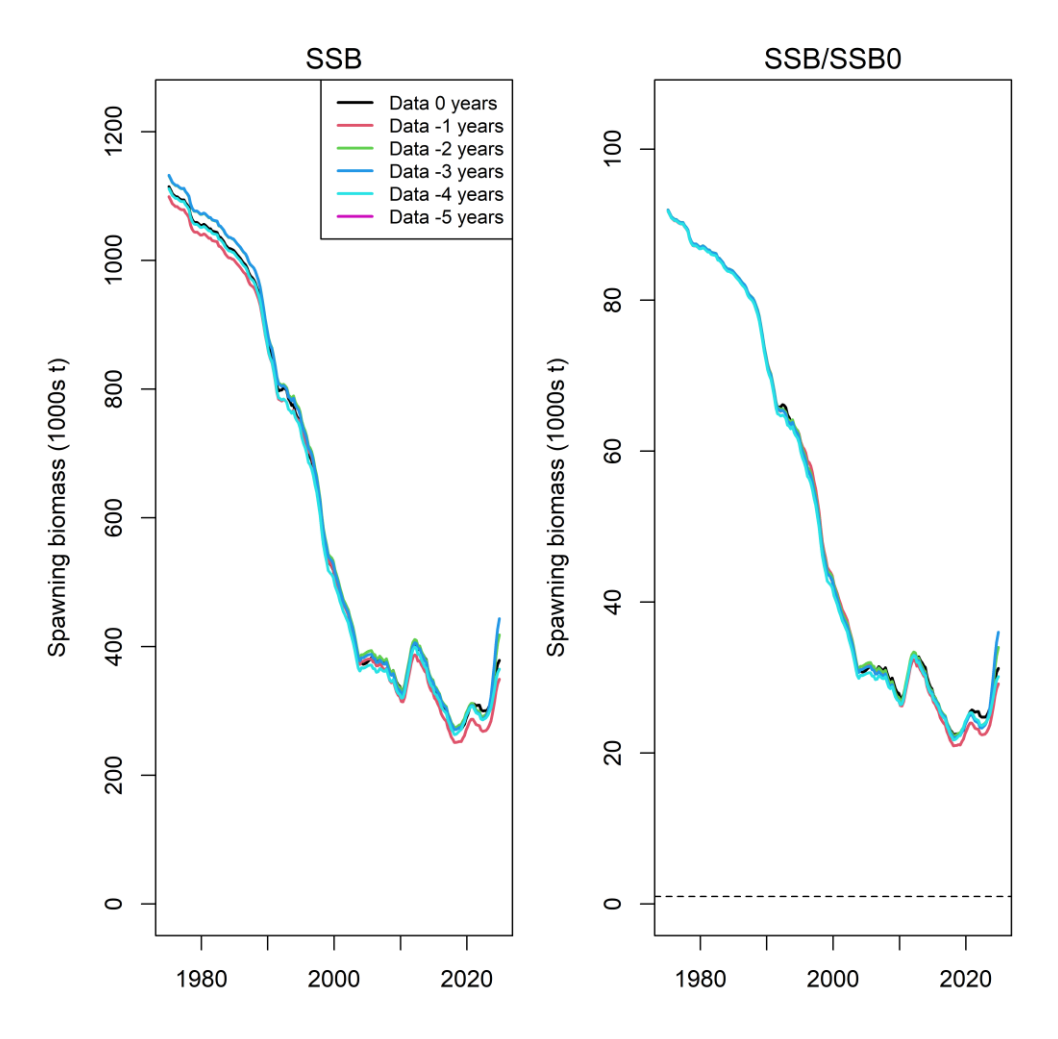


Figure 30b: Retrospective analysis summary for the base model '7 update cpue LLq'.

## 6.4.3. Hindcasting analyses

Hindcasting analyses follow methods from Kell et al., (2016) that further assess the model's predictive power by making forward projections of the CPUE indices using truncated models (e.g. the models that were fitted with sequentially removed data in the retrospective analyses in Section 6.4.2). The models have data sequentially removed, and then project forward with the reduced information, but with catches added back in. Hindcasting diagnostics followed methods used in the 2022 assessment, with tools provided by Carvalho et al., 2021.

The results of these analyses suggest that the predictive power of the base models is relatively stable with truncated data, as the estimated biomass from these models in all quarters are close to the predicted estimates from the full model (Figure 31 a,b).

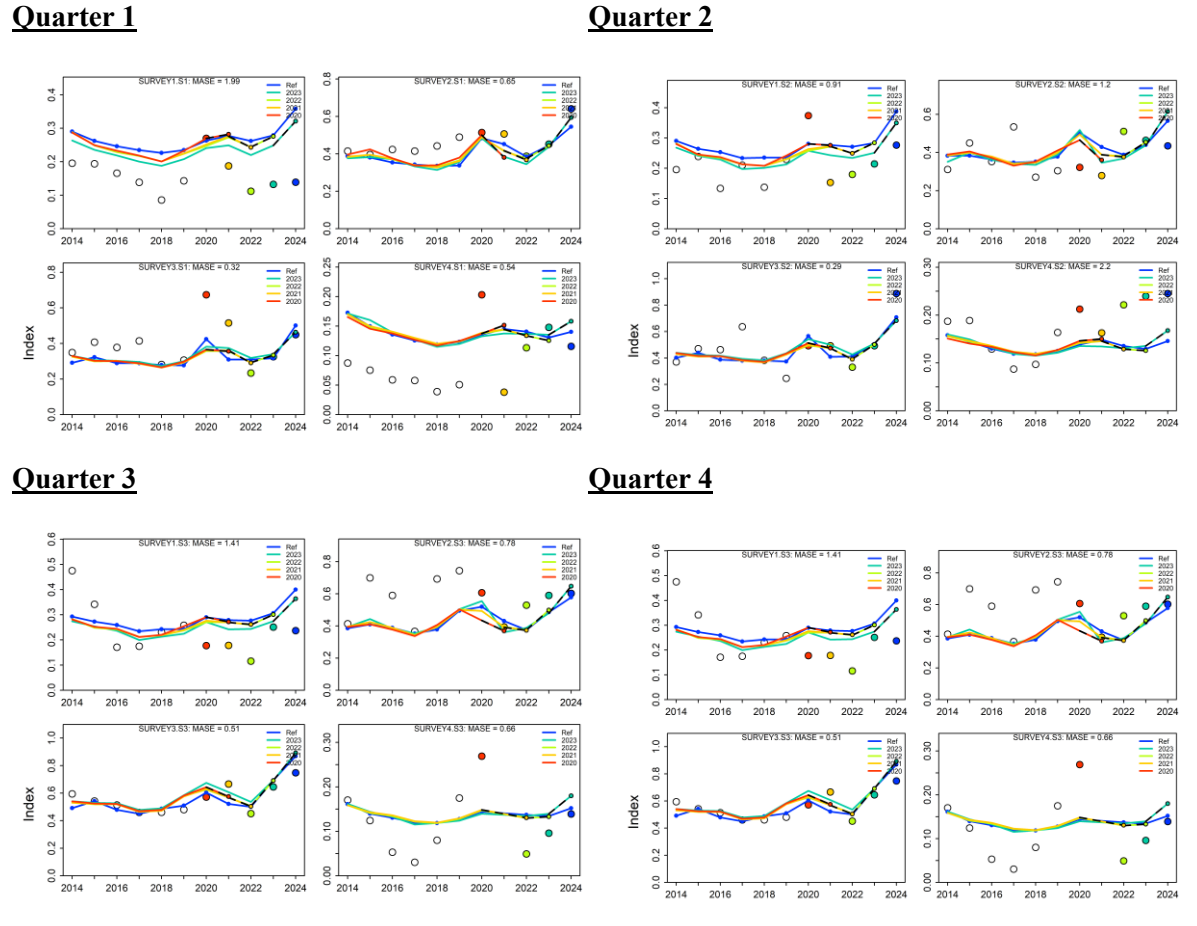


Figure 31a: The Hindcasting analysis summary for the base model '6\_update\_bias': each panel shows the predicted quarterly longline CPUE index from models with data sequentially removed for 1, 2, 3, 4, 5 years.

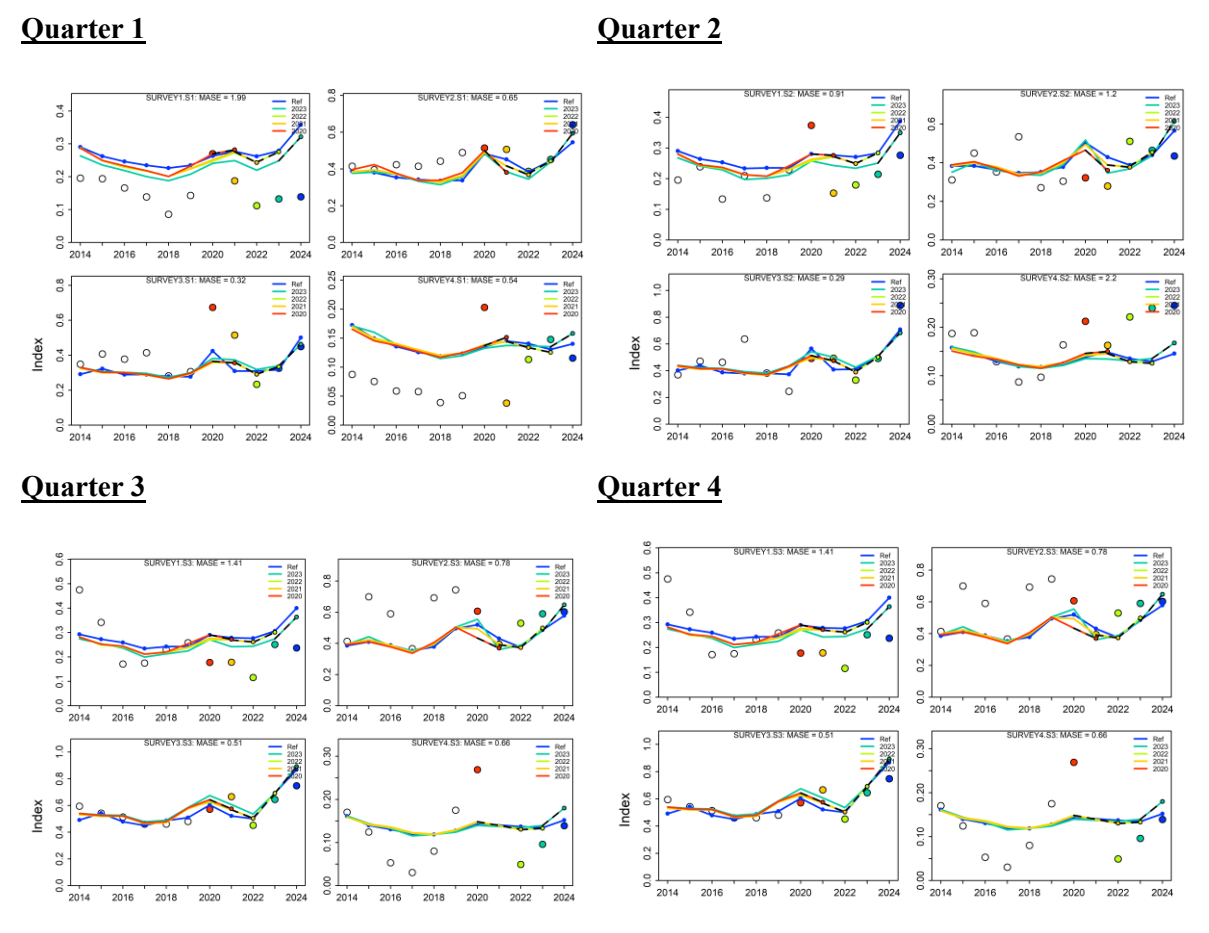


Figure 31b: The Hindcasting analysis summary for the base model '6\_update\_bias': each panel shows the predicted quarterly longline CPUE index from models with data sequentially removed for 1, 2, 3, 4, 5 years.

## 7. SENSITIVITY RUNS

The exploration of the model's sensitivity to input parameters aimed to identify potential revisions to the base models, and to guide the assessment group in choosing the most appropriate values for running the grid or ensemble of models that encapsulates the uncertainty within the model. Key results for the sensitivity runs are provided in Appendix A and summarised below. As the catch was received only a few days prior to the report finalisation, the sensitivity diagnostics are based solely on visual analyses of the fits to various aspects of the model (length composition data, indices of abundance), and comparisons of estimated parameters (selectivity, recruitment, and biomass).

## 7.1. Non-biological parameters

## 7.1.1. CPUE indices

The PSLS indices developed by the European Union (Spain) and presented to the 27<sup>th</sup> WPTT(DP) meeting in 2025 were added to one half of the models tested in sensitivity runs, as outlined in Table 6 (therefore there were a suite of models that had longline CPUE indices with gear creep/changing catchability (*LLq*); and another suite of models with the purse seine CPUE indices – either the 'long' (*PSlong*) version (1991-2024) or 'short' (*PSshort*) version (2010-2024). CPUE indices were attributed to the appropriate model regions, as suggested by the authors at the 27<sup>th</sup> WPTT (DP).

Prior to inclusion of the indices as a sensitivity run, an additional analysis was run to compare the trajectories of the PSLS and LL indices, and is included in Appendix B. In summary, the PSLS and LL indices follow similar trajectories and will not introduce conflict within the model.

Including the PSLS indices did not have significant impacts on the estimates of biomass (Table 9), or selectivity, and the models fit well to the PSLS indices (Figures A1a,b), and were able to estimate well the recent increase, and then decrease in CPUE in Survey 5 (region 1N). Fits to the length composition data were slightly improved for the PSLS fleets but were markedly worse for the line-based fleets, particularly the LINE2, and LL2 fleets.

In general, the models that used the shorter version of the PSLS index (*PSshort*) showed slightly better fits to the length composition data, while still fitting well to the abundance indices.

The addition of 0.5% 'discount' on the joint frozen longline CPUE indices had only a small impact on the estimates of biomass and other management parameters (Table 9), resulting in an estimation of stock depletion at SSB<sub>2024</sub>/SSB<sub>0</sub> = 0.312 for the base model '7\_update\_cpue\_LLq' compared to 0.308 for the base model with no change to the longline CPUE indices ('6\_update\_bias'). The addition of the gear creep marginally improved the fits to the length composition data, while the fits to the CPUE indices were very similar between models.

## 7.1.2. Selectivity for the LL2 and LL3 fleets

There was a discernible decline in the fits to the length composition data in the two regions for the longline fisheries in region 2 and region 3 when using an asymptotic, logistic selectivity. When all the years are combined, the estimated length composition is biased in region 2 (Figure A2) and fits to the PSLS fisheries also decline. The fits to the length composition in the LINE2 fishery is also worse with estimated lengths biased towards smaller fish, presumably to account for smaller fish not selected under logistic selectivity functions for the LL2+LL3 fisheries.

### 7.2. Biological parameters

### 7.2.1. Growth

The mean size of the new growth (Farley et al., 2025) is larger across all age groups. According to the mean size at age, the new growth significantly altered the age distribution of the tagging data towards younger fish. Overall, there was not much of a difference in the fits to the CPUE, size, and tagging data. The new growth predicted lower population numbers but greater annual biomass estimations (Figure A3). Fits to the length composition data were generally improved, with only minor differences compared to the base model.

This year, conditional-age-at-length was implemented in the SS3 model, where the growth curve is internally estimated, based on age-length data supplied to the model. Data were provided from 253 aged fish, including both annual ring counts (older fish), and daily ring counts for juvenile fish. These data are the same as used in Eveson et al. (2025), so the aim was to test whether the internally estimated growth curve was similar to that estimated outside of the model. In SS3, each aged fish is required to be allocated to a spatial region of the model, a specific fleet, and also a quarter (so year / month information is required, as well as where the fish was collected, when, and by what fishing vessel). For a significant portion of the dataset, this information was only partially available, so many assumptions were made to allocate data. Briefly, all purse seine data were allocated to PSLS fleets, and all line data were allocated to frozen longline fleets. Data were loosely partitioned to one of the four regions, based on any information on location that was available.

Given the very small sample size, and the data requirements of the model, it was unlikely that this would provide any more information than estimating the growth curve externally to the model, given then all data are aggregated. However, estimates of growth curves were very similar (Figure A4) to those estimated externally (it is the same dataset!), however the model failed to converge unless either the length at maximum age, or the length at minimum age were fixed, rather than estimated.

Estimates of SSB were slightly lower than the base models (Table 9, Figure A3), and current stock status was estimated to be slightly lower than for the base models (0.24–0.26 for 6c\_CAAL models compared to 0.308 for 6\_update\_bias; 0.24-0.27 for 7c\_CAAL models compared to 0.312 for 7\_update\_cpue\_LLq). When combined with the 0.5 % discount on the CPUE ('7\_' models), the estimates for SSB were substantially higher than for the models without the 0.5 % discount (Table 9), highlighting how internal estimation of growth interacts with other parameters such as the abundance indices.

In general, this is a promising feature to test whether there is misspecification of the growth parameters in the model, however significantly more data are required for it to be a method that is used going forward for the Indian Ocean BET. It would be a useful first step to simulate a suitable sample size for aged fish within the model, given the data requirements of the model (e.g. how many samples per year are required, and across how many regions, fleets, gear types etc.) before continuing with this method.

## 7.2.2. Natural mortality

Changing the instantaneous rate of natural mortality (M) in the model had significant impacts on the estimates of biomass, and the scale of the biomass estimates (Figure 14, Figure A5; Table 9). Three different methods of incorporating M were tested in the sensitivity analyses – MHamel15, MHamel17, and MLorHam6Q. For the estimates of MLorHam6Q, the same method as implemented in ICCAT was used: the maximum age was set to 14.7 yr (as agreed at the DP meeting), and adults were assumed to be fully matured between 4 – 10 yrs, based on the maturity curve from Shono et al. (2009), and the growth curve provided by Eveson et al., (2025). Three starting values of M were used in the internal estimation – a "low" (M=0.30), "medium" (M=0.37), and "high" (M=0.45) estimate, based on the 50<sup>th</sup> quantiles of the probability distribution of values of M. Estimates were weighted, the weightings were estimated from the density function assuming lognormal distribution of M with SD=0.31 (also in the code provided). This was the same method as employed in ICCAT this year.

When estimated internally in the model (MLorHam6Q), estimates of biomass changed significantly (Figure A5; Table 9). The high starting estimates of M caused significantly higher estimates of initial biomass, and very low rates of fishing mortality. When combined with different datasets, the estimates of management quantities changed considerably (Table 9), possibly signalling some model misspecification, or interactions between the different datasets.

Changing the maximum age of fish (MHamel15 (Age<sub>max</sub> = 14.7 yr); MHamel17 (Age<sub>max</sub> = 17 yr)), had less of an effect on the overall estimates of biomass, although the trend in biomass depletion changed (Figure A5). The model is most sensitive to changes in this parameter, and so it is recommended, in the absence of more biological data, that further research and/or focus is applied to this parameter in future assessments. For the current assessment, including two or three parameters for M is recommended in the grid, but not to include the high estimates of M used in the internal estimation process.

Table 9 (next page): Estimates of management quantities for the sensitivity testing from the base model options. Current catch (2024) is estimated at 101,722 t. Base models are highlighted green. Internal estimation of M (MLorHam6Q results in varying outcomes – very high estimates of SSB0, and SSB2024/SSB0 and lower than expected estimates of  $F_{2024}/F_{MSY}$  (yellow highlighted fields). Mbase also produced similarly high SSB0 but other values were similar to base models (blue highlighted fields). All models (except 6d PSlong MLorHam6Q hi) estimated  $C_{MSY}$  at values lower than current catch.

	SSB0	SSBMSY	SSBY	SSB2024SSB0	SSB2024SSBMSY	FMSY	FY	F2024FMSY	CMSY
6_update_bias	1238880	367060	381361.5	0.3078276	1.0389623	0.2445436	0.29493756	1.2060735	100594
6a_PSlong_2area	1205860	344838	313456.2	0.2599441	0.9089957	0.2643224	0.33899943	1.2825225	95339.2
6b_PSshort_2area	1176250	327350	309661	0.2632612	0.945963	0.26544	0.33158008	1.2491715	94829.2
6c_CAAL	1317390	350294	354483.5	0.2690802	1.01196	0.2145844	0.22609685	1.05365	94694
6c_CAAL_lmax	1277070	335200	361729	0.2832492	1.0791438	0.2209768	0.21514412	0.973605	96152.8
6c_CAAL_lmin	1249420	322280	366452	0.2932977	1.1370609	0.2637236	0.2390007	0.9062545	96828
6c_PSlong_CAAL	1133110	307558	290325	0.2562196	0.9439683	0.1969672	0.26565065	1.348705	89640.4
6c_PSlong_CAAL_lmax	1228690	354340	295074.2	0.2401535	0.8327433	0.2011604	0.28947585	1.43903	93075.6
6c_PSlong_CAAL_lmin	1184450	317053	297851.8	0.2514684	0.9394384	0.251198	0.33146016	1.3195175	89811.6
6d_MLorHam6Q_hi	<mark>2714100</mark>	849370	773768.2	0.285092	0.9109908	0.2312692	0.28204227	1.219541	93352
6d_MLorHam6Q_lo	<mark>2724380</mark>	852215	776039.5	0.2848499	0.9106147	0.2312568	0.2821596	1.2201137	93316
6d_MLorHam6Q_me	1944210	582549	522544	0.2687693	0.8969958	0.245152	0.30290405	1.2355765	95983.6
6d_PSlong_MLorHam6Q_hi	<mark>2317350</mark>	587507	1514425	<mark>0.6535159</mark>	2.577714	0.2935452	0.02788894	<mark>0.0950073</mark>	<mark>270687.2</mark>
6d_PSlong_MLorHam6Q_lo	1744980	518603	437988.5	0.2509992	0.8445545	0.2472704	0.34819258	1.408145	93089.6
6d_PSlong_MLorHam6Q_me	2028560	607370	507261.2	0.2500598	0.8351767	0.2460932	0.35233225	1.4317025	92528
6e_MHamel17	1585710	475405	433716.2	0.2735155	0.912309	0.2487372	0.30452336	1.2242775	97532.8
6e_PSlong_MHamel17	1505340	442926	381354.2	0.2533343	0.8609886	0.2505916	0.35961962	1.4350825	93915.2
6f_Mbase	<mark>2089640</mark>	643846	612262.8	0.2929992	0.950946	0.2536016	0.28932785	1.1408755	96482.8
6f_PSlong_Mbase	1990500	633834	552338.5	0.2774873	0.8714245	0.2425844	0.32613956	1.3444375	93650.8
6g_PSlong_sL	1088800	309465	293297.5	0.2693768	0.9477566	0.2535172	0.35983661	1.4193775	89730
6g_sL	1299770	337935	434617.8	<mark>0.3343805</mark>	1.2860987	0.3162396	0.25892149	<mark>0.818751</mark>	97314.4
7_update_cpue_LLq	1447500	417686	448149	0.3096021	1.0729328	0.3508032	0.32408129	0.9238265	92023.6
7a_PSlong_2area_LLq	1154990	319125	297807.5	0.2578442	0.9332002	0.2654616	0.34549429	1.301485	93754
7b_PSshort_2area_LLq	1234160	358171	328100	0.2658488	0.9160429	0.2650116	0.33289247	1.256143	96481.6
7c_CAAL_LLq	1317400	350295	354483.5	0.2690781	1.0119571	0.2145848	0.22609727	1.05365	94694
7c_CAAL_LLq_lmax	1270560	335949	373700	0.2941223	1.1123712	0.2140252	0.20369629	0.9517397	97337.6
7c_CAAL_LLq_lmin	1277060	333338	344650.2	0.2698779	1.0339363	0.2597584	0.27104211	1.0434393	94128
7c_PSlong_CAAL_LLq_lmin	1382730	402648	327138	0.2365885	0.8124665	0.2045416	0.29996332	1.466515	93424.4
7d_MLorHam6Q_LLq_hi	1452160	376891	414948.8	0.2857459	1.1009781	0.2993028	0.29174907	0.9747622	95192.8
7d_MLorHam6Q_LLq_lo	<mark>2724380</mark>	852215	776039.5	0.2848499	0.9106147	0.2312568	0.2821596	1.2201137	93316
7d_MLorHam6Q_LLq_me	<mark>2718550</mark>	850843	775109.2	0.2851186	0.9109897	0.2312112	0.28201188	1.2197155	93340
7d_PSlong_MLorHam6Q_LLq_hi	1961290	586105	485328	0.2474535	0.8280564	0.245652	0.3547829	1.44425	92711.6
7d_PSlong_MLorHam6Q_LLq_lo	1709550	505779	422012.2	0.2468558	0.8343807	0.2466408	0.35125226	1.424145	93166.4
7d_PSlong_MLorHam6Q_LLq_me	1173690	320357	287611.5	0.2450489	0.8977843	0.2575216	0.35225414	1.3678625	93967.2
7e_MHamel17_LLq	1574120	468063	423790.5	0.2692238	0.9054134	0.2487472	0.30538464	1.2276908	97553.6
7f_Mbase_LLq	<mark>2089640</mark>	643846	612262.8	0.2929992	0.950946	0.2536016	0.28932785	1.1408755	96482.8
7g_PSlong_sL_LLq	1062830	307566	288341.5	0.271296	0.9374947	0.2399048	0.33554465	1.3986575	89463.6
7g_sL_LLq	1299770	337935	434617.8	0.3343805	1.2860987	0.3162396	0.25892149	<mark>0.818751</mark>	97314.4

## 7.3. Proposed final model options for grid / ensemble

On basis of the sensitivity models, final options were configured to capture the uncertainty related to assumptions on biological parameters including growth and natural mortality, stock-recruitment steepness, and selectivity configurations, which are shown to have contributed to the main sources of uncertainty around the key model estimates. These are outlined in Table 8.

The proposed final models involved running a combination of options on, LL 2 and 3 selectivity configurations (2 scenarios), steepness (3 values), natural mortality (5 values/specifications) (Table 8). The final model grid is, therefore almost the same as the 2022 assessment, providing a degree of continuity. Final models did not include the purse seine CPUE indices but did include the 0.5 % discount on the longline CPUE indices (thus, the models in the grid are based on '7\_update\_cpue\_LLq'). The model io\_h80\_Gnew\_MHamel15\_sD can be considered as a reference model in the final model ensemble. These models encompass a wide range of stock trajectories, with low steepness values generally yielding lower estimates of biomass (Table 9).

These results presented below are preliminary and will be presented to the 28th WPTT for discussion and finalisation. After running the final assessment grid, the report will be finalised, including the discussion, which will summarise the WPTT(AS) discussions, and include future work proposed to improve the assessment for 2028.

## 8. STOCK STATUS

## 8.1. Current status and yields

MSY based estimates of stock status were determined for the final model options, including alternative assumptions on selectivity, alternative values of SRR steepness, growth, and natural mortality. Stock status was determined for individual models (Table 10), as well as for all (24) models combined incorporating uncertainty from individual models based on estimated variance-covariance matrix of parameters (Table 11).

For the selected model options, point estimates of Catch at MSY ranged from 85,547 t to 99,540 t (Table 10, blue and pink highlights respectively) which are all above the current estimates of catch in 2023 and 2024 (Table 2 & Table 11). Model options with higher steepness generally yielded comparatively higher estimates of MSY. On average fishing mortality rates have remained well below the  $F_{MSY}$  through to 1990s and 2000s, increased significantly after 2015 (Figure 34). Biomass was estimated to have declined considerably from the late 1990s before stabilizing through the 2000s and declined again following a small increase after 2011 – 12 (Figure 32). Since 2020, the biomass is estimated to have stabilised and is now increasing, despite increasing fishing mortality.

Interactions between the longline selectivity and internal estimation of M are apparent in the results (Table 10), with all models that had selectivity estimated as double normal on LL2 and LL3 fleets estimating much higher SSB<sub>0</sub> than all other models (yellow highlight), however the stock status is estimated to be at a similar level as other models ( $\sim 0.30$ ; Table 10).

Current fishing mortality ( $F_{2024}$ ) was estimated to be higher than  $F_{MSY}$  for all models except two (where h = 0.90), and current biomass ( $SSB_{2024}$ ) was estimated to be between 81.5% and 124 % of  $SSB_{MSY}$  (Figure 34; Table 10). In general, current stock status relative to the MSY based benchmarks are not fundamentally different for the range of model options, although the proximity to the MSY benchmarks is sensitive to the different of model assumptions. Current (2024) fishing mortality was estimated to be above the  $F_{MSY}$  level ( $F_{2024}/F_{MSY} > 1.0$ ) for all models except two; current spawning biomass was estimated to be below the  $SB_{MSY}$  level ( $SB_{2024}/SB_{MSY} < 1.0$ ) for 15 models, while 8 models estimated it to be above (they are associated with h = 0.80 or h = 0.90).

Estimates were combined across from the 24 models to generate the final KOBE stock status plot (Figure 33). For individual models, the uncertainty is characterised using the multivariate lognormal Monte-Carlo approach (Walter et al. 2019, Walter & Winker 2019, Winker et al. 2019), based on the maximum likelihood estimates and variance-covariance of the untransformed quantities  $F/F_{MSY}$  and  $SSB/SSB_{MSY}$ . Thus, estimates of stock status included both within and across model uncertainty. Combined across the model ensemble,  $SSB_{2024}$  was estimated to be of 0.99  $SSB_{MSY}$  (0.84–1.15), and  $F_{2024}$  was estimated 1.22  $F_{MSY}$  (1.03–1.42) (Table 11). Critically, the current catch (101,722 t) is above all estimates of  $C_{MSY}$ . Taking all the available information into account, the stock is considered to be **overfished**, and **is subject to overfishing** in 2024.

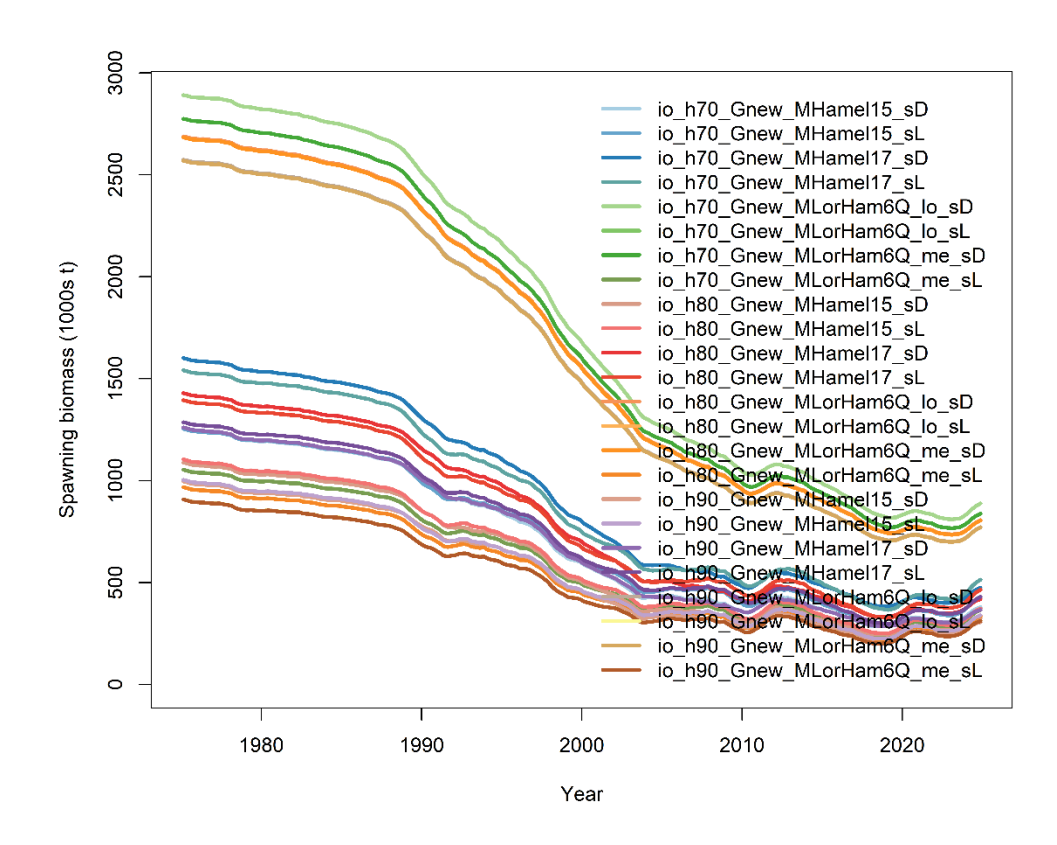


Figure 32: Spawning biomass trajectories from the proposed final model options in the grid

Table 10 Estimates of management quantities for the stock assessment model options. Current yield (mt) represents yield in 2024 corresponding to fishing mortality at the FMSY level.

	SSB <sub>0</sub>	SSB <sub>MSY</sub>	SSB <sub>2024</sub>	SSB <sub>2024</sub> SSB <sub>0</sub>	$SSB_{2024}SSB_{MSY} \\$	F <sub>MSY</sub>	F <sub>2024</sub>	$F_{2024}F_{MSY}$	C <sub>MSY</sub>
io_h70_Gnew_MHamel15_sD	1,355,430	432,782	363,943	0.26851	0.84094	0.21627	0.30985	1.43267	95,175
io_h70_Gnew_MHamel15_sL	1,349,550	420,322	408,969	0.30304	0.97299	0.23114	0.29104	1.25915	92,795
io_h70_Gnew_MHamel17_sD	1,722,250	561,224	457,592	0.26569	0.81535	0.21618	0.31846	1.47312	91,816
io_h70_Gnew_MHamel17_sL	1,652,420	523,834	490,225	0.29667	0.93584	0.22578	0.30730	1.36107	87,826
io_h70_Gnew_MLorHam6Qlo_sD	3,083,510	1,015,470	867,463	0.28132	0.85425	0.20260	0.29855	1.47356	88,652
io_h70_Gnew_MLorHam6Qlo_sL	1,142,420	347,367	346,915	0.30367	0.99870	0.22688	0.27889	1.22922	95,070
io_h70_Gnew_MLorHam6Qme_sD	<mark>2,961,920</mark>	978,284	819,354	0.27663	0.83754	0.21018	0.30567	1.45434	85,547
io_h70_Gnew_MLorHam6Qme_sL	1,141,590	347,080	346,720	0.30372	0.99896	0.22688	0.27879	1.22877	95,085
io_h80_Gnew_MHamel15_sD	1,186,820	339,446	314,391	0.26490	0.92619	0.25192	0.33956	1.34786	96,642
io_h80_Gnew_MHamel15_sL	1,199,470	338,622	354,100	0.29521	1.04571	0.27456	0.32029	1.16656	93,822
io_h80_Gnew_MHamel17_sD	1,549,140	461,838	402,983	0.26013	0.87256	0.25310	0.33653	1.32960	94,542
io_h80_Gnew_MHamel17_sL	1,505,830	432,775	442,336	0.29375	1.02209	0.26882	0.32297	1.20142	91,002
io_h80_Gnew_MLorHam6Qlo_sD	2,883,050	884,020	787,398	0.27311	0.89070	0.24475	0.31780	1.29846	88,632
io_h80_Gnew_MLorHam6Qlo_sL	1,058,700	288,309	316,688	0.29913	1.09843	0.27174	0.29621	1.09006	97,179
io_h80_Gnew_MLorHam6Qme_sD	<b>2</b> ,877,220	882,193	785,641	<mark>0.2730</mark> 6	0.89055	0.24481	0.31813	1.29951	88,649
io_h80_Gnew_MLorHam6Qme_sL	1,058,010	288,087	316,536	0.29918	1.09875	0.27175	0.29610	1.08962	97,194
io_h90_Gnew_MHamel15_sD	1,093,590	277,292	293,560	0.26844	1.05867	0.30176	0.34547	1.14483	99,398
io_h90_Gnew_MHamel15_sL	1,098,950	273,187	321,899	0.29292	1.17831	0.32871	0.33330	1.01398	96,506
io_h90_Gnew_MHamel17_sD	1,377,220	362,021	352,593	0.25601	0.9739	0.29306	0.35757	1.22013	96,870
io_h90_Gnew_MHamel17_sL	1,397,780	356,393	409,064	0.29265	1.14779	0.32182	0.33272	1.03384	94,353
io_h90_Gnew_MLorHam6Qlo_sD	2,773,530	779,280	752,124	0.27117	0.96515	0.27708	0.32326	1.16666	93,754
io_h90_Gnew_MLorHam6Qlo_sL	1,000,650	237,355	295,368	0.29517	1.24441	0.32916	0.31076	0.9441	99,523
io_h90_Gnew_MLorHam6Qme_sD	2,768,390	778,124	750,931	0.27125	0.96505	0.27702	0.32339	1.16738	93,770
io_h90_Gnew_MLorHam6Qme_sL	1,000,030	237,171	295,240	0.29523	1.24484	0.32919	0.31064	0.94365	99,540

Table 11: STOCK STATUS INDICATORS FROM MODEL ENSEMBLE

Catch in 2024:	101,722 t
Average catch 2016–2024:	88,965 t
MSY (1000 t) (plausible range):	94 (89 –99)
F <sub>MSY</sub>	0.26 (0.21–0.31)
SSB <sub>0</sub> (1000 t) (80% CI):	1677 (744-2609)
SSB <sub>2024</sub> (1000 t) (80% CI):	470 (222–719)
$SSB_{MSY}$	441 (194–689)
SSB <sub>2024</sub> /SSB <sub>0</sub> (80% CI):	0.28 (0.26–0.30)
SSB <sub>2024</sub> / SSB <sub>MSY</sub>	0.99 (0.84–1.15)
F <sub>2024</sub> / F <sub>MSY</sub>	1.22 (1.03-1.42)

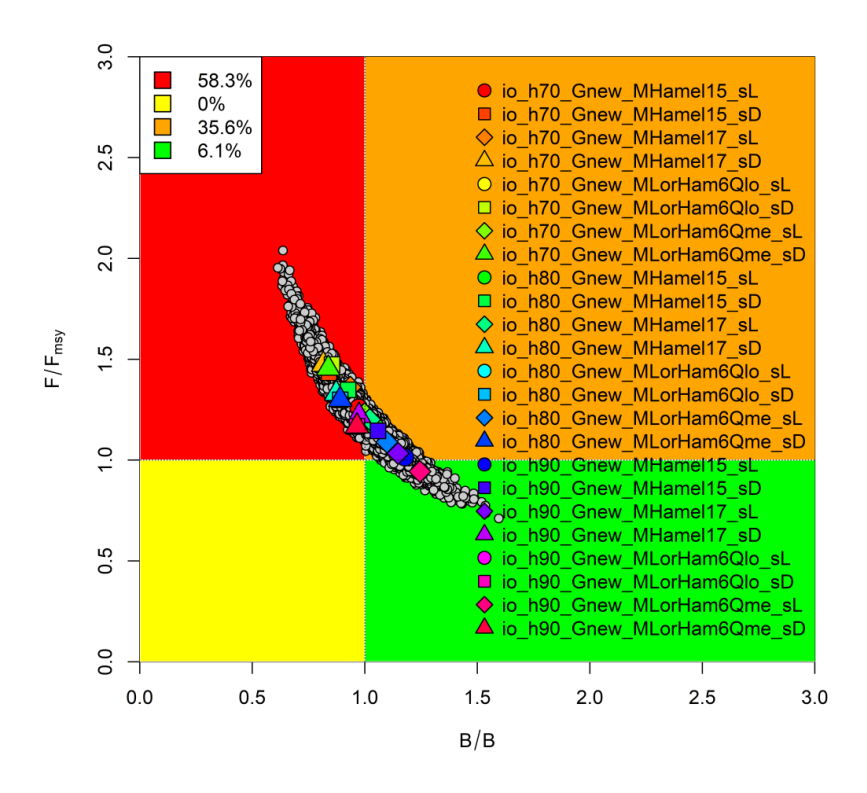


Figure 33: KOBE PLOT FROM GRID RUNS

In the 2022 assessment (using data up to 2021) the model ensemble estimated that the stock was **overfished** and **subject to overfishing** in 2021, this was a change from the 2019 assessment when the stock was estimated to be **not overfished** but subject to **overfishing**.

The estimated biomass trajectory shows a decline from exploited but equilibrium spawning stock biomass levels in 1975 to 2019 (Figure 37). Biomass levels appear to have stabilised and are increasing in the final years of the model, providing a more positive outlook for the stock, despite several years of increased catches that are estimated to be above MSY, and fishing mortality above that of F/F<sub>MSY</sub>. As there is a significant lack of representative biological data (length data, and representative ages), the model is forced to fit closely to the main abundance indices from the longline fleets. As there have been

increases in these indices in the three most recent years (2022-2024 inclusive), alongside increased catches, it is likely that the CPUE indices are driving the increase in estimated biomass in the model, rather than any biological parameters.

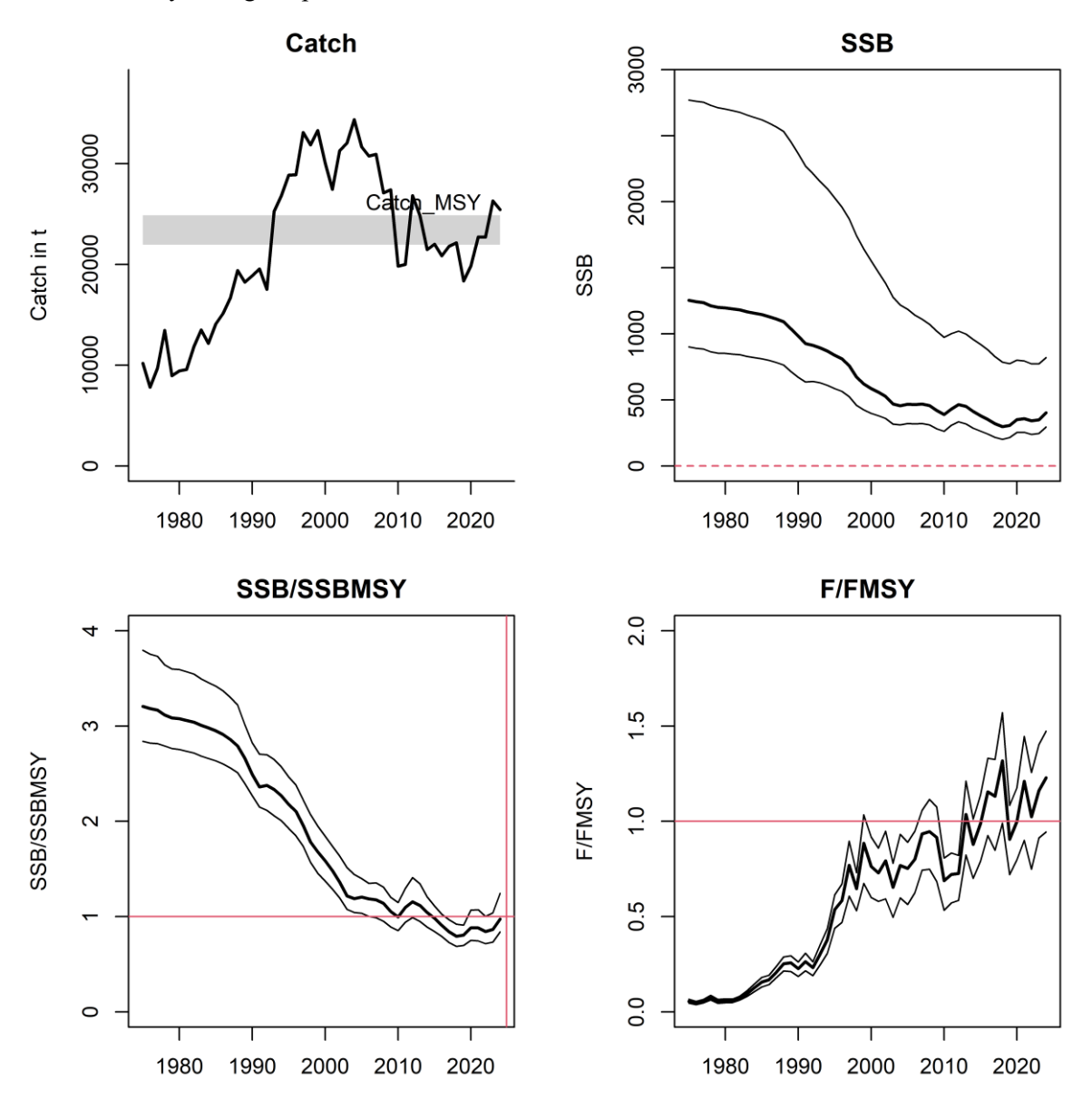


Figure 34: Management outputs from the ensemble of models (grid) used in 2024. Bounds around the main darker line represent the highest and lowest values from the grid of models. The grey band on the catch graph represents estimated optimal catch at MSY (80 % confidence interval). The horizontal red lines indicate limit or reference points for SSB/SSB $_{MSY}$  and F/F $_{MSY}$ .

## 9. DISCUSSION

This report presents a preliminary stock assessment for Indian Ocean bigeye tuna using a spatially explicit, age structured model. It represents an update and revision of the 2022 assessment model with newly available information. There are no fundamental changes in the structure of the current assessment models compared to the previous assessment, with most revisions concerning observational data, e.g., the inclusion of revised regional LL CPUE indices, and the incorporation newly available biological information including growth and natural mortality. A range of exploratory models are also presented to explore the impact of key data sets and model assumptions.

The overall stock status estimates obtained from a range of model options is similar to the previous assessment: current spawning biomass remained to be below  $SSB_{MSY}$  ( $SSB_{2024}/SSB_{MSY} = 0.90$ ), and fishing mortality is estimated to be above  $F_{MSY}$  ( $F_{2024}/F_{MSY} = 1.24$ ). (Current SSB was estimated to be above  $SSB_{MSY}$  in the 2019 assessment, but also at 0.90 in the 2022 assessment). This has been mostly caused by changes in CPUE indices for all regions, which have showed increases in the most recent years, that are supported by two years of very high catches (2023, 2024).

The scale of the abundance indices can be found in both CPUE and length composition. The two data sources frequently include contradictory information. The best practice is to place greater focus on the CPUE data because it is more direct, whereas length composition often suffers from sampling problems, and it is impossible to totally eliminate the influence of biased length samples. In this assessment, only length composition from major fisheries (i.e., longlines, purse seine, and longlines for fresh tuna) is incorporated into the model. Following Hoyle et al. (2021), the longline fishery excludes Taiwanese and Seychelles length data due to sampling bias, and size data from the bait boat, line, and other fisheries are not used because the samples are of poor quality and representativeness, even though these fisheries' selectivity is linked to fisheries with a similar pattern of selection. By doing so, the impact of these length samples on estimates of the abundance is lessened.

Growth is one major source of uncertainly. The otolith aging approach utilized in the growth study of Farley et al. (2025) is supported by age validation work. The new growth curve is quite different from the integrated VB-logK curves of Eveson et al. (2012) used in the 2022 and 2019 assessments. Estimates of growth curves using the conditional-age-at-length methods of internal estimation showed that these growth curves may be well-specified. However, there are only 253 aged fish used in the model, over a short time period (2017-2024), that is not spatially- or temporally-representative of the fish within the entire Indian Ocean stock.

The assessment model adopted a 4-region spatial structure. Movement rates between regions were estimated to be much higher than in 2022, presumably due to the removal of variable recruitment between regions. As in 2022, There is very little information on the movement dynamics of bigeye tuna but a higher level of mixing among subpopulations is likely to be more plausible than the low movement rates estimated in 2022.

More research and information on the movement rates of adult and sub-adult bigeye tuna in the Indian Ocean would go some way to improving our understanding of the likelihood of these estimates of movement.

### 9.1. Recommendations for future assessments

- Improved quality and quantity of length composition data: It is recommended that improvements in both quantity and quality of length frequency data are provided to the Secretariat prior to the next assessment of bigeye tuna in 2028, and that any length data omitted in this assessment are reassessed for suitability and inclusion in 2028. Results from a recent consultancy with Dr. Paul Medley may inform the next BET assessment, alongside other tropical tuna stock assessments.
- Further development of additional abundance indices: as with other tuna assessments in the IOTC, the abundance indices are not representative of the total extent of the tuna fishery and associated catch data used in the assessment. There is additional concern regarding the contracting spatial extent of Korean and Japanese frozen longline fleets. It is recommended that other CPCs develop CPUE series for consideration in stock assessment of bigeye tuna. Standardised CPUE indices can either be included in an integrated modelling platform or contribute to overall knowledge of various components of the stock. Development of appropriate CPUE standardisations can be supported by the Secretariat or completed by the Secretariat (if appropriate operational data are provided).
- Ageing data: Currently there are a total of 253 data points for BET within the assessment model. This represents a minute percentage of the fish being caught. The samples cover only a few years of fishing, all within the last 10 years. It is strongly recommended that more fish are aged, encompassing both male and female fish, from all length-bins across the spatial extent of the fishery, to build a reasonable timeseries of biologically informative data. Age data should be accompanied by detailed information on the source of the fish (e.g. time, date, location, sex, fishing gear, vessel flag etc.) if the data are to be used to either estimate age-at-length within the model (as data need to be allocated to appropriate timesteps, model areas, and model fleets) or to account for changes in age-at-length over time or space (due to population dynamics, environmental factors, such as climate change or high fishing effort).

### 10.REFERENCES

- Aires-da Silva, A. M., Maunder, M. N., Schaefer, K. M., and Fuller, D. W. (2015). Improved growth estimates from integrated analysis of direct aging and tag-recapture data: An illustration with bigeye tuna (Thunnus obesus) of the eastern Pacific Ocean with implications for management. Fisheries Research, 163:119–126.
- Akia, S., Guery, L., Grande, M., Kaplan, D., Baéz, J.C., Ramos, M. L., Uranga, J., Abascal, F., Santiago, J, Merino, G., Gaertner, D. 2022. European purse seiners CPUE standardization of Big Eye tuna caught under dFADs. IOTC-2022-WPTT24-12.
- Appleyard SA, RD Ward, PM Grewe. 2002. Genetic stock structure of bigeye tuna in the Indian Ocean using mitochondrial DNA and microsatellites. J. Fish Biol. 60: 767-770.
- Carvalho, F., Winker, H., Courtney, D., Kapur, M., Kell, L., Cardinale, M., Schirripa, M., Kitakado, T., Yemane, D., Piner, K.R., Maunder, M.N., Taylor, I., Wetzel, C.R., Doering, K., Johnson, K.F., Methot, R.D., 2021. A cookbook for using model diagnostics in integrated stock assessments. Fish. Res. 240, 105959. https://doi.org/https://doi.org/10.1016/j.fishres.2021.105959
- Chassot E, Assan C, Esparon J,, Tirant A, Delgado d, Molina A, Dewals P, Augustin E, Bodin N. 2016. Length-weight relationships for tropical tunas caught with purse seine in the Indian Ocean: Update and lessons learned. IOTC-2016-WPDCS12-INF05.
- Chow, S., Okamoto, H., Miyabe, N., Hiramatsu, K., and Barut, N. (2000). Genetic divergence between Atlantic and Indo-Pacific stocks of bigeye tuna (Thunnus obesus) and admixture around South Africa. Molecular Ecology, 9(2):221–227.
- Cope, J.M., Hamel, O.S. (2022). Upgrading from M version 0.2: An application-based method for practical estimation, evaluation, and uncertainty characterisation of natural mortality. *Fisheries Research* 256.
- Correa, G.M., Kaplan, D.M., Uranga, J., Grande, M., Imzilen, T., Merino, G., Ramos Alonso, M.L. 2025. Standardised catch per unit effort of bigeye tuna in the Indian Ocean for the European purse seine fleet operating on floating objects. IOTC-2025-WPTT27DP-14.
- Day, J., Magnusson, A., Teears, T., Hampton, J., Davies, N., Castilo Jordan, C., Peatman, T., Scott, R., Phillips, J.S., McKechnie, S., Scott, F., Yao, N., Natadra, R., Pilling, G., Williams, P., Hamer, P. 2023. Stock assessment of bigeye tuna in the western and central Pacific Ocean: 2023. WCPFC-SC19-2023/SA-WP-05.
- Díaz-Arce, N., Grewe, P., Krug, I Artetxe, I., Ruiz, J., et al. (2020). Evidence of connectivity of bigeye tuna (Thunnus obesus) throughout the Indian Ocean inferred from genome-wide genetic markers. IOTC-2020-WPTT22(AS)-16.
- Eveson, P., Million, J., Sardenne, F., Le Croizier, G. 2012. Updated growth estimates for skipjack, yellowfin and bigeye tuna in the Indian Ocean using the most recent tag-recapture and otolith data. IOTC-2012-WPTT14-23.
- Eveson, P., Million, J., Sardenne, F., Le Croizier, G. 2015. Estimating growth of tropical tunas in the Indian Ocean using tag-recapture data and otolith-based age estimates. Fisheries Research 163, 58–68,
- Eveson, P., Farley, J., 2021. Investigating growth information for yellowfin and bigeye tuna from the IOTTP tag-recapture data.
- Eveson, P., Luque, P.L, Farley, J., Krusic-Golub, K., Artetxe-Arrate, I., Clear, N., Fraile, I., Duparc, A., Faucheux, C., Juan-Jorda, M.J., Mattlet, A-F., Nunes Alves, A.M., Silva Sousa, R.J., Guerreiro, A.C.S.G., Diaha, C., Murua, H., Zudaire, I. (2025) Updating the estimation of age and growth of bigeye tuna (*Thunnus obesus*) in the Indian Ocean from counts of daily and annual increments in otoliths. IOTC-2025-WPTT27DP-08.
- Farley, J.H., Clear, N.P., Leroy, Bruno., Davis, T.L.O., McPherson, G. 2004. Age and growth of bigeye tuna (Thunnus obesus) in the eastern and western AFZ.

- Farley, J., Krusic-Golub, K., Eveson, P., Clear, N., Luque, P.L., Artetxe-Arrate, I., Fraile, I., Zudaire, I., Vidot, A., Govinden, R., Ebrahim, A., Romanov, E., Chassot, E., Bodin, N., Murua, H., Marsac, F., Merino, G. 2021. Estimating the age and growth of bigeye tuna (*Thunnus obesus*) in the Indian Ocean from counts of daily and annual increments in otoliths. IOTC-2021-WPTT23-BET growth.
- Fonteneau, A., Pallares, P. 2004. Tuna natural mortality as a function of their age: the bigeye tuna case. IOTC-2004-WPTT-INF02.
- Fonteneau, A., Ariz, R., Delgado, A., Pallares, P., Pianet, R. 2004. A comparison of bigeye stocks and fisheries in the Atlantic, Indian and pacific oceans. IOTC-2004-WPTT-INF03.
- Francis, R.C. and Hilborn, R. 2011. Data weighting in statistical fisheries stock assessment models. Canadian Journal of Fisheries and Aquatic Sciences 68(6): 1124–1138. doi:10.1139/f2011-025.
- Fu, D. 2017. Indian ocean skipjack tuna stock assessment 1950-2016 (stock synthesis). IOTC-2017–WPTT19-47 rev1.
- Fu, D. 2019. Preliminary Indian Ocean Bigeye Tuna Stock Assessment 1950-2021 (Stock Synthesis). IOTC-2019-WPTT21-61.
- Fu, D., Merino, G., Winker, H. 2022. Preliminary Indian Ocean Bigeye Tuna Stock Assessment 1950-2021 (stock synthesis). IOTC-2022-WPTT24-10.
- Fu, D., Langley, A. Merino, G., Ijurco, A.U. 2018. Preliminary Indian ocean yellowfin tuna stock assessment 1950-2017 (Stock Synthesis). IOTC-2018-WPTT20-33.
- Gaertner, D., Hallier, J.P. 2015. Tag shedding by tropical tunas in the Indian Ocean and other factors affecting the shedding rate. Fisheries Research. 2015/163.
- Grewe, P. M., Wudianto, C., Proctor, C. H., Adam, M. S., Jauhary, A. R., Schaefer, K., Itano, D. G., Evans, K., Killian, A., Foster, S. D., Gosselin, T., Feutry, P., Aulich, J., Gunasekera, R. M., Lansdell, M., and Davies, C. R. (2019). Population Structure and Connectivity of Tropical Tuna Species across the Indo Pacific Ocean Region. Technical Report WCPFC-SC15-2019/SA-IP-15. Hampton. J. 2000. Natural mortality rates in tropical tunas: size really does matter. Can. J. Fish. Aquat. Sci. 57: 1002–1010 (2000).
- Hamel, O.S. 2015. A method for calculating a meta-analytical prior for the natural mortality rate using multiple life history correlates. ICES J. Mar. Sci. 72, 62–69.
- Hamel, O.S., and Cope, J.M. (2022) Development and considerations for application of a longevity-based prior for the natural mortality rate. *Fisheries Research* 256: 106477.
- Hamel, O.S., Ianelli, J.N., Maunder, M.N, Punt, A.E. (2023) Natural mortality: Theory estimation, and application in fishery stock assessment models. *Fisheries Research* 261: 106638.
- Hamer, P., Potts, J., Macdonald, J., and Senina, I. (2023). Review and analyses to inform conceptual models of population structure and spatial stratification of bigeye and yellowfin tuna assessments in the Western and Central Pacific Ocean. Technical Report SC19-SA-WP-02, Palau.
- Harley, S.J. 2011. Preliminary examination of steepness in tunas based on stock assessment results. WCPFC SC7 SA IP-8, Pohnpei, Federated States of Micronesia, 9–17 August 2011.
- Hillary, R.M., Eveson, J.P., 2015. Length-based Brownie mark-recapture models: derivation and application to Indian Ocean skipjack tuna. Fish. Res. 163, 141–151.
- Hillary, R.M., Million, J., Anganuzzi, A., Areso, J.J. 2008a. Tag shedding and reporting rate estimates for Indian Ocean tuna using double-tagging and tag-seeding experiments. IOTC-2008-WPTDA-04.
- Hillary, R.M., Million, J., Anganuzzi, A., Areso, J.J. 2008b. Reporting rate analyses for recaptures from Seychelles port for yellowfin, bigeye and skipjack tuna. IOTC-2008-WPTT-18.
- Hoyle, S.D., Leroy, B.M., Nicol, S.J., Hampton, J. 2015. Covariates of release mortality and tag loss in large-scale tuna tagging experiments. Fisheries Research 163, 106-118.

- Hoyle, S.D., Kitakado, T., Matsumoto, T., Kim, D.N., Lee, S.I., Ku, J.E., Lee, M.K., Yeh,Y., Chang, S.T., Govinden, R., Lucas, J., Assan, C., Fu, D. 2017a. IOTC–CPUEWS–04 2017: Report of the Fourth IOTC CPUE Workshop on Longline Fisheries, July 3th–7th, 2017. IOTC–2017–CPUEWS04–R. 21 p.
- Hoyle, S., Satoh, K., Matsumoto, T. 2017b. Exploring possible causes of historical discontinuities in Japanese longline CPUE. IOTC–2017–WPTT19–33 Rev1.
- Hoyle, S.D., Okamoto, H. (2015). Descriptive analyses of the Japanese Indian Ocean longline fishery, focusing on tropical areas. IOTC-2015-WPTT17-INF08.
- Hoyle, S.D., Langley, A. 2018. Indian Ocean tropical tuna regional scaling factors that allow for seasonality and cell areas. IOTC-2018-WPM09-13.
- Hoyle, S., Chang, ST., Fu, D., Geehan, J., Itoh, T., Lee, S.I., Matsumoto, T., Yeh, Y.M., Wu, R.F. 2021. IOTC-2021-WPTT(DP)23-08: Review of size data from Indian Ocean longline fleets, and its utility for stock assessment.
- Hoyle 2022. Natural mortality ogives for the Indian Ocean bigeye tuna stock assessment. IOTC–2022-WPTT24(DP)-17.
- IOTC 2016. Report of the 18th Session of the IOTC Working Party on Tropical Tunas. Seychelles, 5–10 November 2016. IOTC–2016–WPTT18–R. 126 pp.
- IOTC 2018a. Report of the 20th Session of the IOTC Working Party on Tropical Tunas. Seychelles, 29 October 3 November 2018. IOTC–2018–WPTT20–R. 127 pp.
- IOTC 2018b. Review of the statistical data and fishery trends for tropical tunas. IOTC-2018-WPTT20-07 Rev 1. IOTC-2004-WPTT-INF04.
- IOTC 2019a. Report of the 21st Session of the IOTC Working Party on Tropical Tunas. Seychelles, 21 26 October 2019. IOTC-2019-WPTT21-R: 146 pp.
- IOTC 2019b Report of the 15th Session of the IOTC Working Party on Data Collection and Statistics. IOTC, Karachi, Pakistan, 27-30 November 2019.
- IOTC 2021. Report of the 23nd Session of the IOTC Working Party on Tropical Tunas. Online, 22 24 June 2020. IOTC-2021-WPTT23(DP)-R[E]: 35 pp.
- IOTC 2022. Report of the 24th Session of the IOTC Working Party on Tropical Tunas, Data Preparatory Meeting. Online, 30-May 03 June 2022. IOTC–2022–WPTT24(DP)–R. 37 pp.
- ISSF (2011). Report of the 2011 ISSF stock assessment workshop. Technical Report ISSF TechnicalReport 2011-02, Rome, Italy, March 14-17, 2011.
- Kell, L.T., Kimoto, A., Kitakado, T., 2016. Evaluation of the prediction skill of stock assessment using hindcasting. Fisheries research, 183, pp.119-127.
- Kitakado, T., Wang, S.P., Matsumoto, T., Lee, S.I., Satoh, K., Yokoi, H., Okamoto, K., Lee, M.K., Lim, J.H., Kwon, Y., Tsai, W.P., Su, N.J., Chang, S.J., Chang, F.C. 2022. Joint CPUE indices for the bigeye tuna in the Indian Ocean based on Japanese, Korean and Taiwanese longline fisheries data up to 2020. IOTC–2022-WPTT24(DP)-15
- Kitakado, T., Wang, S-P., Lee, S.I., Tsuda, Y., Park, H., Lim, J-H., Nirazuka, S., Tsai, W-P. 2025. Update of joint CPUE indices for bigeye tunas in the Indian Ocean based on Japanese, Korean and Taiwanese longline fisheries data (up to 2024). IOTC-2025-WPTT27DP-09.
- Kolody, D., Herrera, M., Million, J., (2010). Exploration of Indian Ocean Bigeye Tuna Stock Assessment Sensitivities 1952-2008 using Stock Synthesis (updated to include 2009). IOTC-2012-WPTT10-4.
- Kolody, D. 2011. Can length-based selectivity explain the two stage growth curve observed in Indian Ocean YFT and BET. IOTC-2011-WPTT13-33.
- Langley, A.; Herrera, M.; Sharma, R. 2013a. Stock assessment of bigeye tuna in the Indian Ocean for 2012. IOTC-2013-WPTT15-30.

- Langley, A.; Herrera, M.; Sharma, R. 2013b. Stock assessment of bigeye tuna in the Indian Ocean for 2012. IOTC-2013-WPTT15-30-Rev 1.
- Langley, A. 2016. Stock assessment of bigeye tuna in the Indian Ocean for 2016 model development and evaluation.
- Matsumoto, T. 2016. Consideration on the difference of average weight by estimation method for tunas caught by Japanese longline in the Indian Ocean. IOTC-2016-WPDCS12-16.
- Maunder, M.N., Piner, K.R., 2015. Contemporary fisheries stock assessment: many issues still remain. ICES J. Mar. Sci. 72, 7–18.
- Maunder. A concise guide to developing fishery stock assessment models.
- Methot, R.D., Taylor, I.G. 2011. Adjusting for bias due to variability of estimated recruitments in fishery assessment models. Can. J. Fish. Aquat. Sci. 68: 1744–1760.
- Methot, R.D. 2013. User manual for Stock Synthesis, model version 3.24f.
- Methot, R.D., Wetzel, C.R. 2013. Stock synthesis: A biological and statistical framework for fish stock assessment and fishery management. Fisheries Research 142 (2013) 86–99.
- Merino, G., Urtizberea, A., Fu, D., Winker, H., Cardinale, M., Lauretta, M. V., Murua, H., Kitakado, T., Arrizabalaga, H., Scott, R., Pilling, G., Minte-Vera, C., Xu, H., Laborda, A., Erauskin-Extraminiana, M., Santiago, J., 2022. Investigating trends in process error as a diagnostic for integrated fisheries stock assessments. Fish. Res. 256, 106478.
- Moore, B. R., Lestari, P., Cutmore, S. C., Proctor, C., and Lester, R. J. G. (2019). Movement of juvenile tuna deduced from parasite data. ICES Journal of Marine Science, 76(6):1678–1689.
- Nishida, T., Rademeyer, R. (2011). Stock and risk assessments on bigeye tuna (*Thunnus obesus*) in the Indian Ocean based on AD Model Builder implemented Age-Structured Production Model (ASPM). IOTC-2011-WPTT-42.
- Okamoto, H. 2005. Recent trend of Japanese longline fishery in the Indian Ocean with special reference to the targeting. Is the target shifting from bigeye to yellowfin? IOTC-2005-WPTT-11.
- Preece, A., Williams, A. 2025. An update on Consideration of Exceptional Circumstances for the Bigeye Tuna MP 2025. IOTC-2025-WPM16-MSE-04.
- Punt A.E., Castillo-Jordan, C., Hamel, O.S., Cope, J.M., Maunder, M.N., Ianelli, J.N. (2021) Consequences of error in natural mortality and its estimation in stock assessment models. *Fisheries Research* 233 (105759).
- Schaefer, K., Fuller, D., Hampton, J., Caillot, S., Leroy, B., and Itano, D. (2015). Movements, dispersion, and mixing of bigeye tuna (1t Thunnus obesus) tagged and released in the equatorial Central Pacific Ocean, with conventional and archival tags. *Fisheries Research*, 161:336–355
- Shono, H., K. Satoh, H. Okamoto, and T. Nishida. (2009). Updated stock assessment for bigeye tuna in the Indian Ocean up to 2008 using Stock Synthesis III (SS3). IOTC-2009-WPTT-20.
- Then, A.Y.; Hoenig, J.M.; Hall, N.G.; Hewitt, D.A. Evaluating the predictive performance of empirical estimators of natural mortality rate using information on over 200 fish species. ICES Journal of Marine Science. 72:82-92; 2015
- Thorson, J.T., Johnson, K.F., Methot, R.D., and Taylor, I.G. 2017. Model-based estimates of effective sample size in stock assessment models using the Dirichlet-multinomial distribution. Fisheries Research 192: 84–93. doi:10.1016/j.fishres.2016.06.005.
- Vincent, M. T., Pilling, G.M., Hampton, J. 2018. Incorporation of updated growth information within the 2017 WCPO bigeye stock assessment grid, and examination of the sensitivity of estimates to alternative model spatial structures. WCPFC-SC14-2018/ SA-WP-03.

- Waterhouse, L, Sampson DB, Maunder M, Semmens BX. 2014. Using areas-as-fleets selectivity to model spatial fishing: Asymptotic curves are unlikely under equilibrium conditions. Fisheries Research. 158:15-25.
- Walter, J., Hiroki, Y., Satoh, K., Matsumoto, T., Winker, H., Ijurco, A.U., Schirripa, M., 2019. Atlantic bigeye tuna stock synthesis projections and kobe 2 matrices. Col. Vol. Sci. Pap. ICCAT 75, 2283–2300.
- Walter, J., Winker, H., 2019. Projections to create Kobe 2 Strategy Matrices using the multivariate log-normal approximation for Atlantic yellowfin tuna. ICCAT-SCRS/2019/145 1–12.
- Winker, H., Walter, J., Cardinale, M., Fu, D. 2019. A multivariate lognormal Monte-Carlo approach for estimating structural uncertainty about the stock status and future projections for Indian Ocean Yellowfin tuna. IOTC–2019–WPTT21–xx.
- Waterhouse, L, David B. Sampson, D., Maunder, M., Semmens, B. 2014. Using areas-as-fleets selectivity to model spatial fishing: Asymptotic curves are unlikely under equilibrium conditions. Fisheries Research 158 (2014) 15–25.
- Williams, A., Jumppanen, P., Preece, A., Hillary, R. 2022. Running the IOTC Bigeye Tuna Management Procedure for 2022. IOTC-2022-WPM13-10.
- Williams, A., Preece, A., Hillary, R. 2022 Specifications of the IOTC Bigeye Tuna Management Procedure. IOTC-2022-WPM13-11.
- Williams, A., Preece, A. 2025. Update on running the IOTC Bigeye Tuna Management Procedure for 2024. IOTC-2025-WPM16MSE-02.
- Iker Zudaire, Iraide Artetxe-Arrate, Jessica Farley, Hilario Murua, Deniz Kukul, Annie Vidot, Shoaib Abdul Razzaque, Mohamed Ahusan, Evgeny Romanov, Paige Eveson, Naomi Clear, Patricia L. Luque, Igaratza Fraile, Nathalie Bodin, Emmanuel Chassot, Rodney Govinden, Ameer Ebrahim, Umair Shahid, Theotime Fily, Francis Marsac, Gorka Merino. Preliminary estimates of sex ratio, spawning season, batch fecundity and length at maturity for Indian Ocean bigeye tuna. IOTC-2022-WPTT24(DP)-18.

# 11.APPENDIX A:

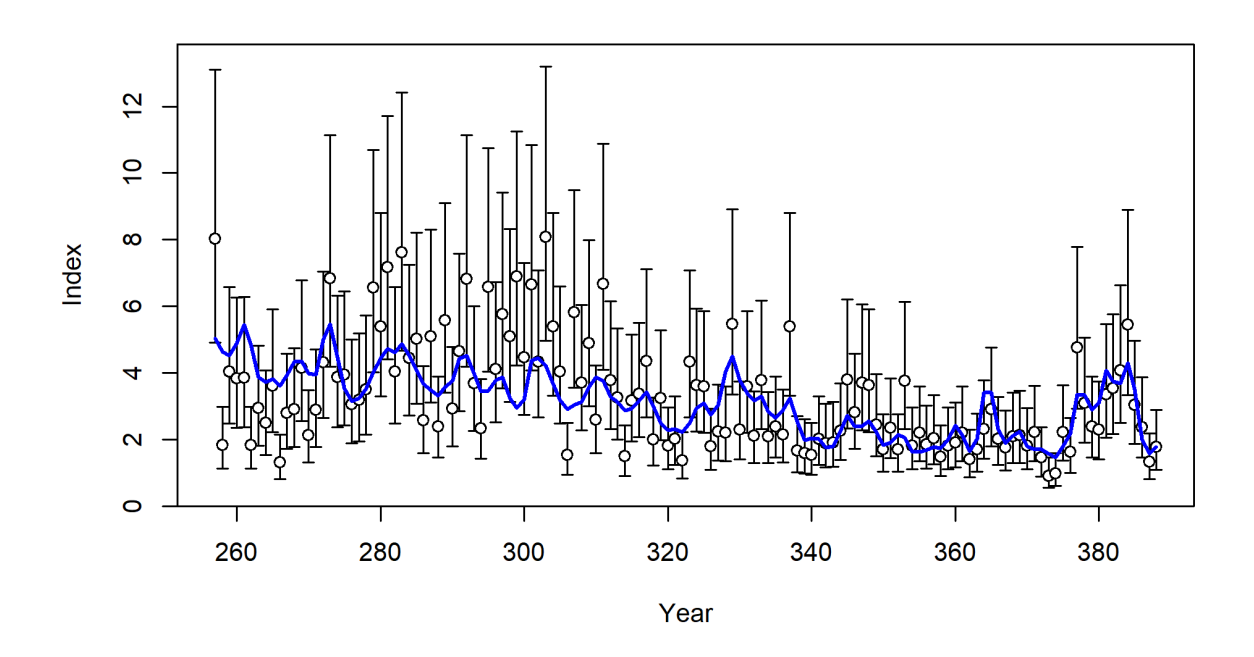


Figure A1: Fits to the PSLS CPUE index from one of the sensitivity runs ('6a\_PSlong\_2area') – SURVEY 5 (PSLS long index 1N, region 1N)

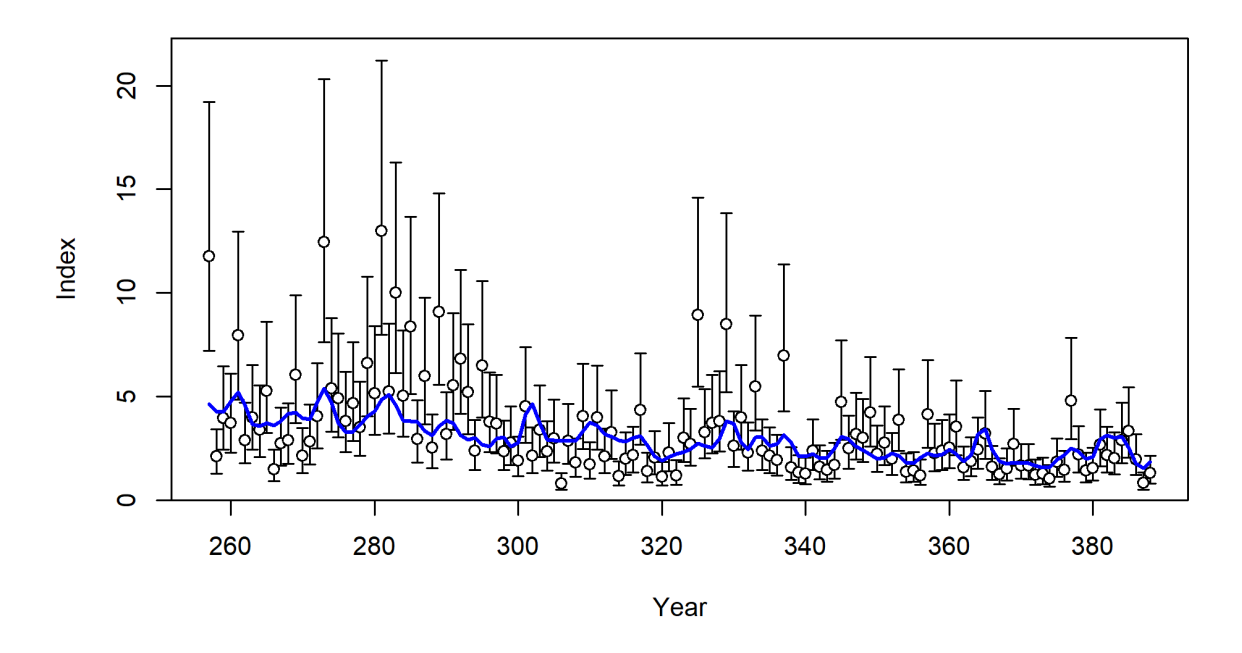


Figure A2: Fits to the PSLS CPUE index from one of the sensitivity runs ('6a\_PSlong\_2area') – SURVEY 6 (PSLS long index 1S, region 1S)

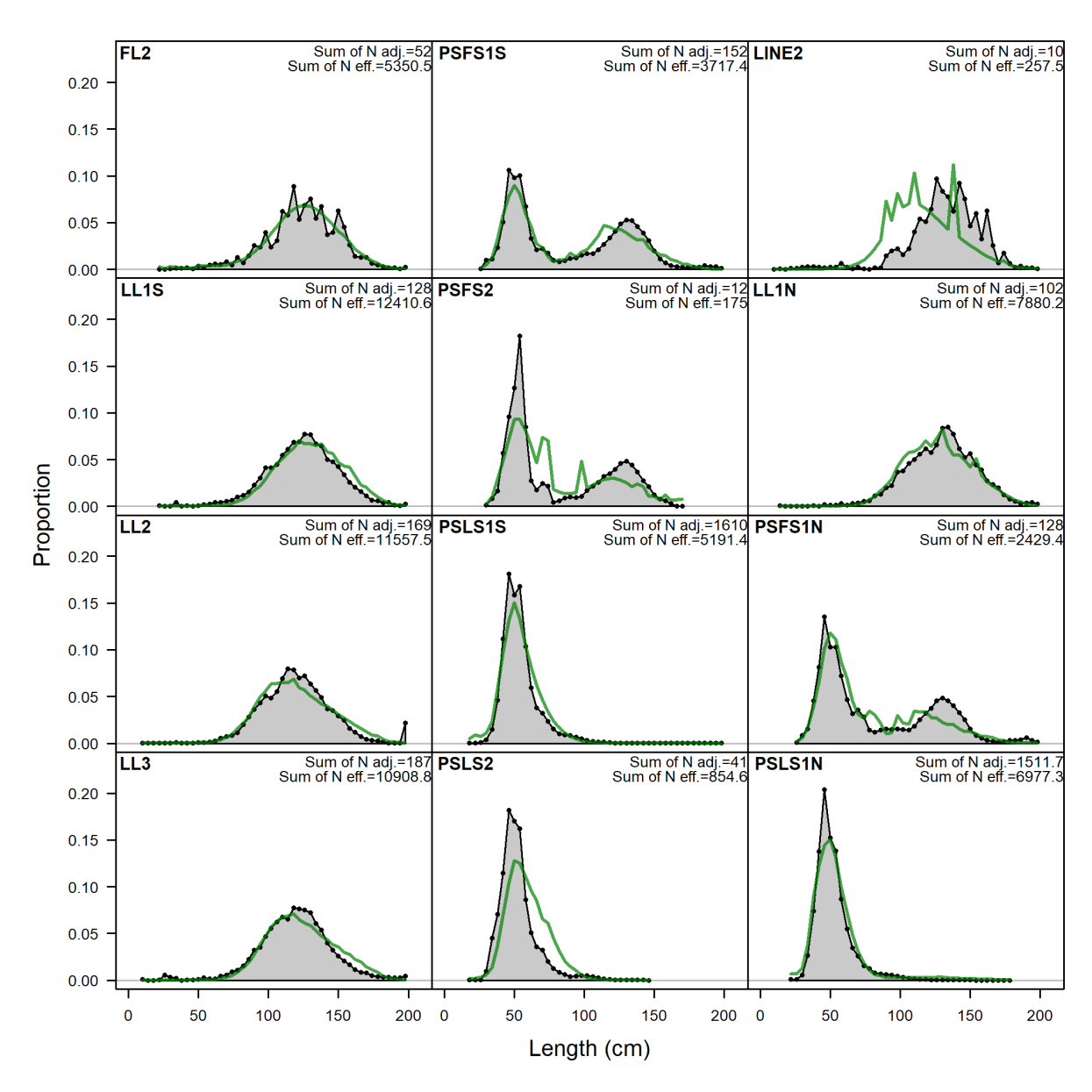


Figure A2: Fits to the length composition data when LL2 & LL3 fleets' selectivity is estimated to be logistic. For model ' $6\_sL$ '.

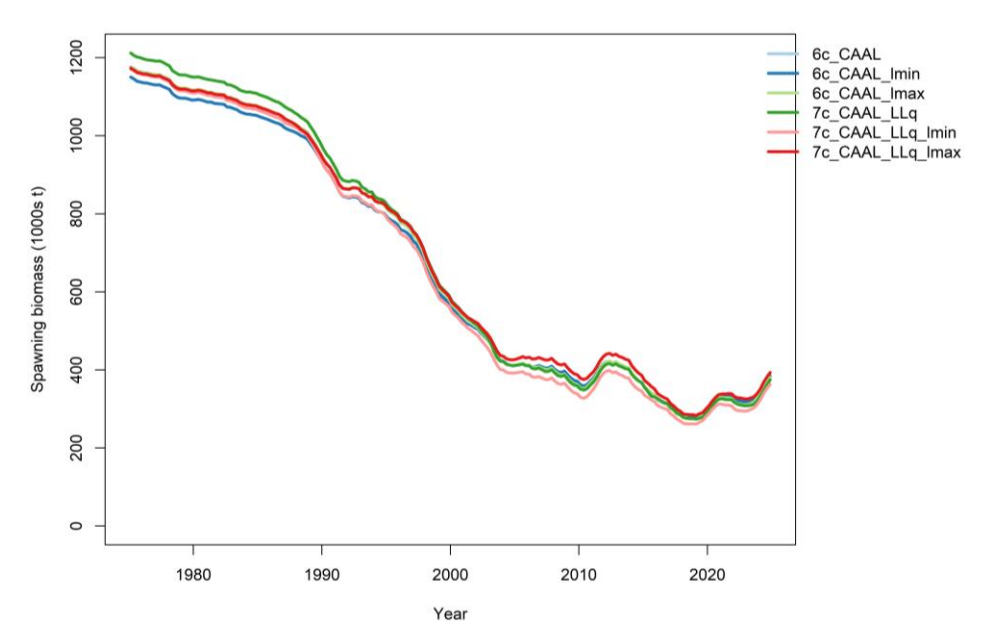


Figure A3: Estimates of biomass for different growth curves used in sensitivity runs. CAAL = 'conditional-age-at-length' – growth is internally estimated in the model. . Lmin = age at length min is fixed; Lmax = age at length max is fixed, otherwise von Bertalanffy parameters are estimated.

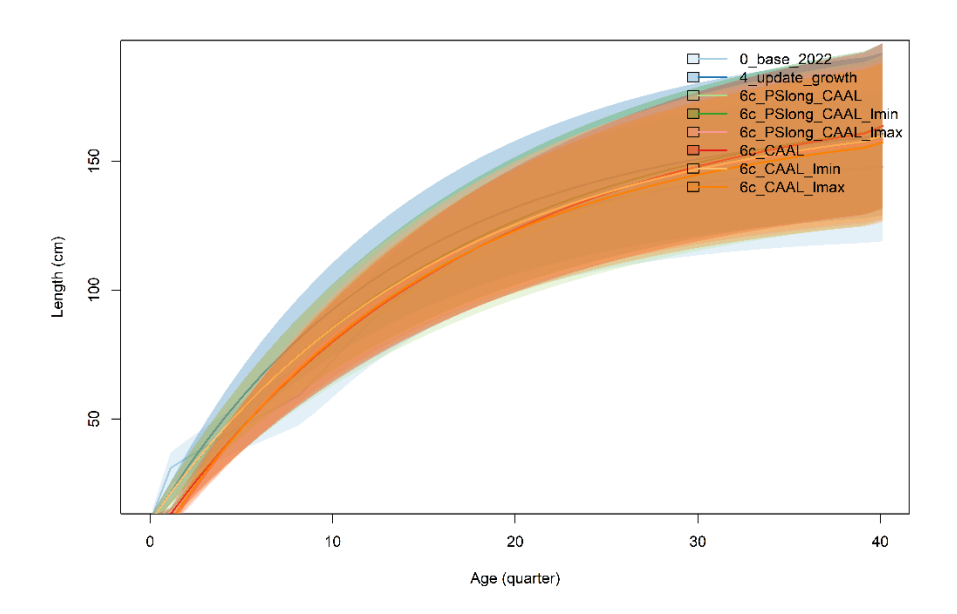


Figure A4: Estimates of growth curves for different growth curves used in sensitivity runs. CAAL = 'conditional-age-at-length' – growth is internally estimated in the model. Lmin = age at length min is fixed; Lmax = age at length max is fixed, otherwise von Bertalanffy parameters are estimated.

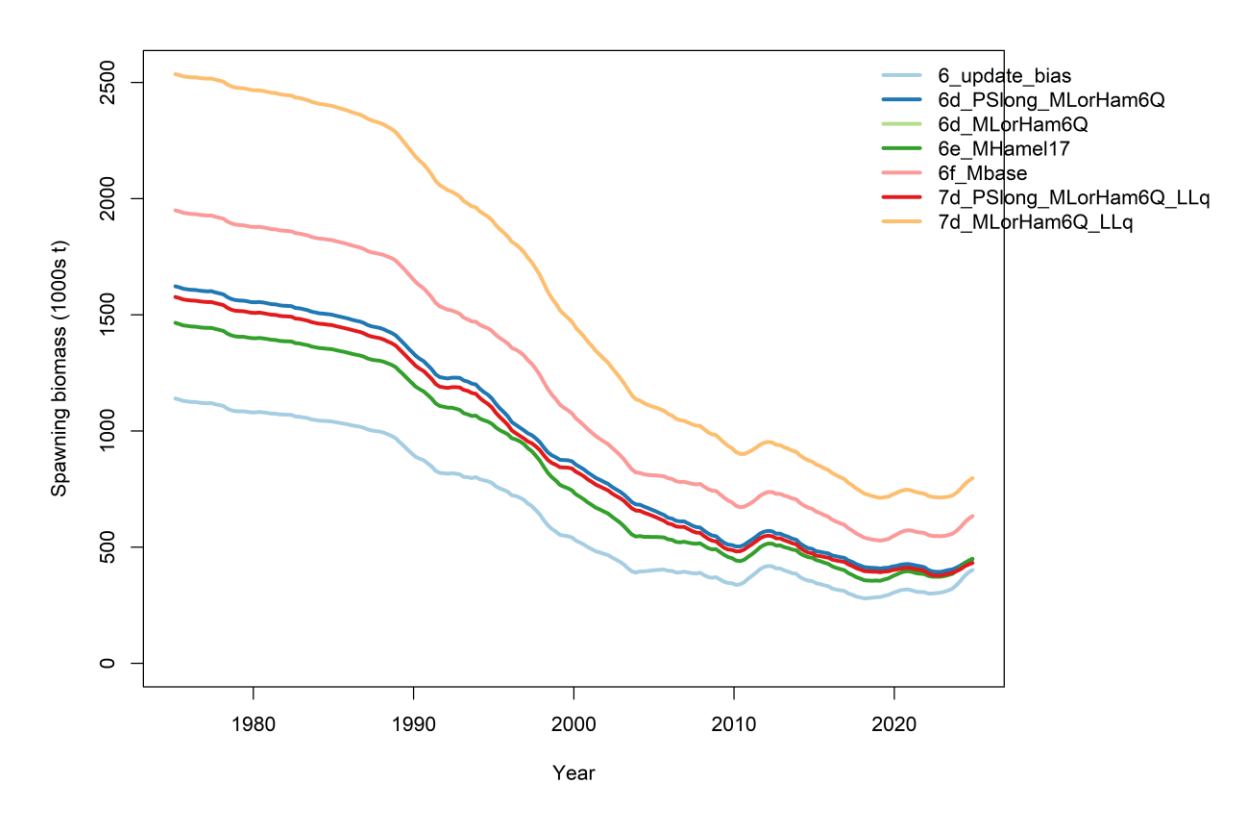


Figure A5: Biomass estimates when the instantaneous rate of natural moratliy (M) is changed in the model, highlighting the sensitivity of the model to these parameters. When estimated internally in the model (MLorHam6Q), estimates of biomass changed significantly. Changing the maximum age of fish (MHamel15 (Age  $_{max} = 14.7 \text{ yr}$ ); MHamel17 (Age $_{max} = 17 \text{ yr}$ )), had less of an effect on the overall estimates of biomass, although the trend in biomass depletion changed.

## 12.APPENDIX B: CPUE COMPARISON

Analysis of Indian Ocean CPUE - 2025 Bigeye Tuna Assessment

Genevieve Phillips (genevieve.phillips@fao.org), Joel Rice (ricemarineanalytics@gmail.com)

2025-06-26

### 12.1. Introduction

This document presents a comparison of the six catch per unit of effort (CPUE) series submitted for consideration in the 2025 IOTC bigeye tuna (*Thunnus obesus*) assessment in the Indian Ocean using methods developed for CPUE comparisons for a stock assessment model within ICCAT (Rice et al., 2025). The goals of this analysis are 1) to investigate any relative differences between model inputs so that data conflict is not introduced into the model via indices of abundance (CPUE series) that imply different, conflicting states of nature (i.e. do alternative indices of abundance indicate that the stock is increasing or the stock is decreasing); and 2) to understand whether it is reasonable to include the purse seine indices of abundance in the stock assessment (pending sensitivity runs on the assessment model).

### 12.2. Data and methods

#### 12.3. Catch and effort data

Within the fisheries landing bigeye tuna in the Indian Ocean, data are aggregated into four regional longline fleets (which in turn are comprised of several fisheries, aggregated by gear type and fishing behaviour), and two regional purse seine fleets. In total, there are six abundance indices (catch per unit effort (CPUE) series) which together span the Indian Ocean, however each index is related to a different region of the ocean. Four of the CPUE series are based on catch and effort data from three nations (JAP, TWN,China, and KOR), forming four joint CPUE indices. For more detail on the methods, please see Kitikado et al. (2025) and the paper presented to the data preparation meeting for Tropical Tuna in June 2025.

The purse seine CPUE series considered have been submitted by EU,Spain and in this analysis the regional (R1N and R1S split) 'long' indices have been used (time period 1991-2023). During WPTT09-DP there were discussions around whether these indices should be included within the stock assessment, as they are based on indices that are not considered to be highly accurate representations of fish biomass. The reasons behind this are that these indices are based on purse seine fisheries that use drifting fish aggregating devices (DFADs) to aggregate fish, and therefore increase the effectiveness of fishing operations. When using such CPUE indices, if there is little difference between the nominal and standardised CPUE indices (as in the case of the supplied indices) there are likely to be other variables impacting the CPUE that are not included within the model (for example fish behaviour, fish habitat availability, whether the fleet is targeting bigeye tuna or not). See Correa et al (2025) for further information regarding the purse seine CPUE indices.

For all the CPUE indices in the 2025 bigeye tuna stock assessment, there is uncertainty around the CPUE indices as accurate reflections of the population biomass. This is because bigeye tuna are not a primary target species throughout the Indian Ocean. They are often caught as bycatch when fishers are targeting yellowfin or skipjack tuna, as the three species often school together when individuals are smaller. This also causes identification issues as juvenile or sub-adult yellowfin tuna closely resemble

bigeye tuna. These issues are somewhat accounted for in both the purse seine and joint longline CPUE indices, by the use of clustering analyses and / or 'hooks between floats' in the longline (prior to 2025) to attempt to identify data that relates to targeted fishing of bigeye tuna as opposed to opportunistic fishing or bycatch data.

### 12.4. Methods

The CPUE time series for bigeye tuna (*Thunnus obesus*) in the Indian Ocean are plotted (**Figure 1**) along with a lowess smoother fitted to the CPUE each year using a general additive model (GAM) to compare trends for the submitted CPUEs. Residuals from the smoother fits to CPUE are compared to identify deviations from the overall trends. This allows conflicts between indices (e.g. highlighted by patterns in the residuals) to be identified.

Correlations between indices are evaluated in **Figure 3** via pairwise scatter plots for CPUE indices where they overlap. The lower triangle shows the pairwise scatter plots between indices with a regression line, the upper triangle provides the correlation coefficients, and the diagonal provides the range of observations along with a linear model fit between them.

A hierarchical cluster analysis was used to evaluate the indices using a set of dissimilarities and the results are plotted in **Figure 4**. This analysis can identify similar and dissimilar trends. If indices represent the same stock components, then it is reasonable to expect them to be correlated. If indices are not correlated or are negatively correlated, i.e. they show conflicting trends, then this may result in poor fits to the data and bias in the parameter estimates obtained within a stock assessment model. Therefore, the correlations can be used to select groups of indices that represent a common hypothesis about the evolution of the stock (Rice 2022, ICCAT 2017).

Cross-correlations for the region are plotted with a lag from -10 to 10 in **Figure 5** (i.e., the correlations between series when they are lagged by -10 to 10 years) which can help determine whether there is relationship between two time-dependent variables at different time lags. This approach can be particularly useful when comparing indices of abundance for bycatch species derived from fleets targeting diff species (i.e. tropical vs temperate tunas), or aggregated at different levels (trips vs sets).

If all CPUE series are thought to represent the overall dynamics of the stock, careful examination of how one index may lead or lag another, temporal shifts or delays in population dynamics may become apparent (e.g. migration patterns, or the effects of environmental drivers). For example, a strong correlation at a positive lag might indicate that changes in one index precedes changes in another, possibly suggesting sampling of separate part of the stock (e.g. juvenile vs adult).

Conversely, correlations at negative lags may reflect delayed responses in one component of the population to changes in another. Overall, lagged cross-correlation helps clarify potential lead-lag relationships between datasets, offering insights into the relative similarity of the CPUE series. Careful interpretation of the results is suggested given the potential bycatch nature of this stock and the changes fleet dynamics and potential gear or technological creep within the purse seine fisheries.

The diagonals in **Figure 5** show the auto-correlations of an index lagged against itself. This can help identify whether a relationship exists between the CPUE series and earlier years, which would be identified by a large correlation, with the correlations on both sides that quickly become small.

All analyses were conducted using R and FLR, including the *diags* package which provides a set of common methods for reading these data into R, plotting and summarising them (e.g., see: http://www.flr-project.org/).

#### 13. 3. Results and conclusions

The overall trend for the indices is an overall decreasing trend from the 1980s to the present day. The variation in the CPUE indices has reduced slightly over time, more so in the purse seine fisheries, possibly indicating improved efficiency relating to DFAD use, or overall improved knowledge of fish behaviour over time. Over the last 15-20 years, there has been little overall change in the CPUE indices, with the exception of a marked increase in the longline region 2 index in the last year (4 quarters of data; **Figure B1**).

Overall **Figures B1 and B2** indicate that the series follow the overall trend, and may provide some evidence of a potential recruitment pulse in 2004 (as seen by an increase in CPUE in the purse seine fisheries), followed by a subsequent increase in CPUE in the longline fisheries (particularly in region 1 south) in 2008-2009 approximately four years later.

Differences in the size, sign and trend in the residuals be evidence of a more rapidly decreasing trend in the stock trajectory in recent years in region 1 south, potentially lead by increases in efficiency in purse seine fisheries that capture juvenile fish, leading to fewer adult fish reaching maturity, and reproducing, and fewer adult fish available for the longline fishery in this key region. However, it is important to consider the potential that bigeye tuna are often considered a bycatch species, and decreases in CPUE may indicate a shift in targeting preferences to the main tropical tuna species. This requires further species identification data, and observer data for verification.

Correlations between indices are evaluated in **Figure B3**. The lower triangle shows the pairwise scatter plots between indices with a regression line, the upper triangle provides the correlation coefficients, and the diagonal provides the range of observations. The strongest correlation is between LL\_R1S and LL\_R1N (Corr: 0.782), suggesting a strong positive relationship. This indicates that these two fleets are sampling the same components of the stock, which is reassuring as they are both longline indices from the joint CPUE from TWN,China, KOR, and JAP. A strong positive correlation is also evident between PS\_R1S and PS\_R1N (Corr: 0.719), indicating similar spatiotemporal dynamics and/or operational practices, and likely sampling the same population. Only one pairing (PS\_R1N vs. LL\_R3) shows a near-zero correlation (Corr: 0.037), suggesting these indices may be relatively independent or reflect uncorrelated processes. This could be due to the inherent differences in gear type (PS vs LL), target species (if other tropical tuna are targeted), region (R3 vs R1), aggregation scale, or the different size classes caught by the gear (sub-adult vs adult).

All indices showed positive correlations, with only the LL\_R3 index having non-significant correlations (although positive trends) with the purse seine indices. This is likely due to the different regions being sampled by these fisheries.

The hierarchical cluster analysis (**Figure 4**) identified two groupings of time-series. The first group includes the purse seine CPUE indices. The second group includes the longline CPUE indices, showing strong correlations between the LL CPUE indices in all regions.

Lagged cross-correlations are plotted in **Figure 5** and the analysis revealed that the longline CPUE indices are likely targeting the same portion of the population, with little lag observed between the

datasets. The longline CPUE index from R2 (region 2) shows some lag between that index and the purse seine indices, suggesting that these two indices are sampling distinct components of the population (highly likely as the purse seine fisheries are targetting smaller individuals than the longline fleets), and also that these regions *may* have asynchronous abundance signals (driven by the differential portions of the population). Along with the positive correlations between these indices, this provides some evidence that the purse seine indices may reflect ontogenetic behaviour within the population dynamics of bigeye tuna (e.g. smaller subadults targeted by the purse seine fisheries potentially moving into region 2 as they get larger, where they are caught by the longline fleets.)

### 13.1. References

Indian Ocean Tuna Commission (IOTC) (2025). IOTC-2025-WPTT27(DP): Report of the 27th Meeting of the Working Party for Tropical Tunas - Data Preparatory Meeting. (Online, June 11-13 2025).

Correa, G.M., Kaplan, D.M., Uranga, J., Grande, M., Imzilen, T., Merino, G., Alonso, M.L.R. (2025). Standardised catch per unit effort of bigeye tuna in the Indian Ocean for the European purse seine fleet operating on floating objects. 27th Working Party for Tropical Tunas - Data Preparatory Meeting. (Online, June 11-13 2025).

Kitakado, T., Wang, S-P., Lee, S.I., Tsuda, Y., Park, H., Lim, J-H., Nirazuka, S., Tsai, W-P. (2025). IOTC-2025-WPTT27(DP)-09: Update of joint CPUE indices for bigeye tunas in the Indian Ocean based on Japanese, Korean and Taiwanese longline fisheries data (up to 2024). 27th Working Party for Tropical Tunas - Data Preparatory Meeting. (Online, June 11-13 2025).

Rice, J., Sant'Ana, R., Kikuchi, E., Gustavo Cardoso, L. (2025). Analysis and comparison and of Catch Per Unit Effort Series submitted for the 2025 South Atlantic shortfin make shark assessment in the ICCAT region.

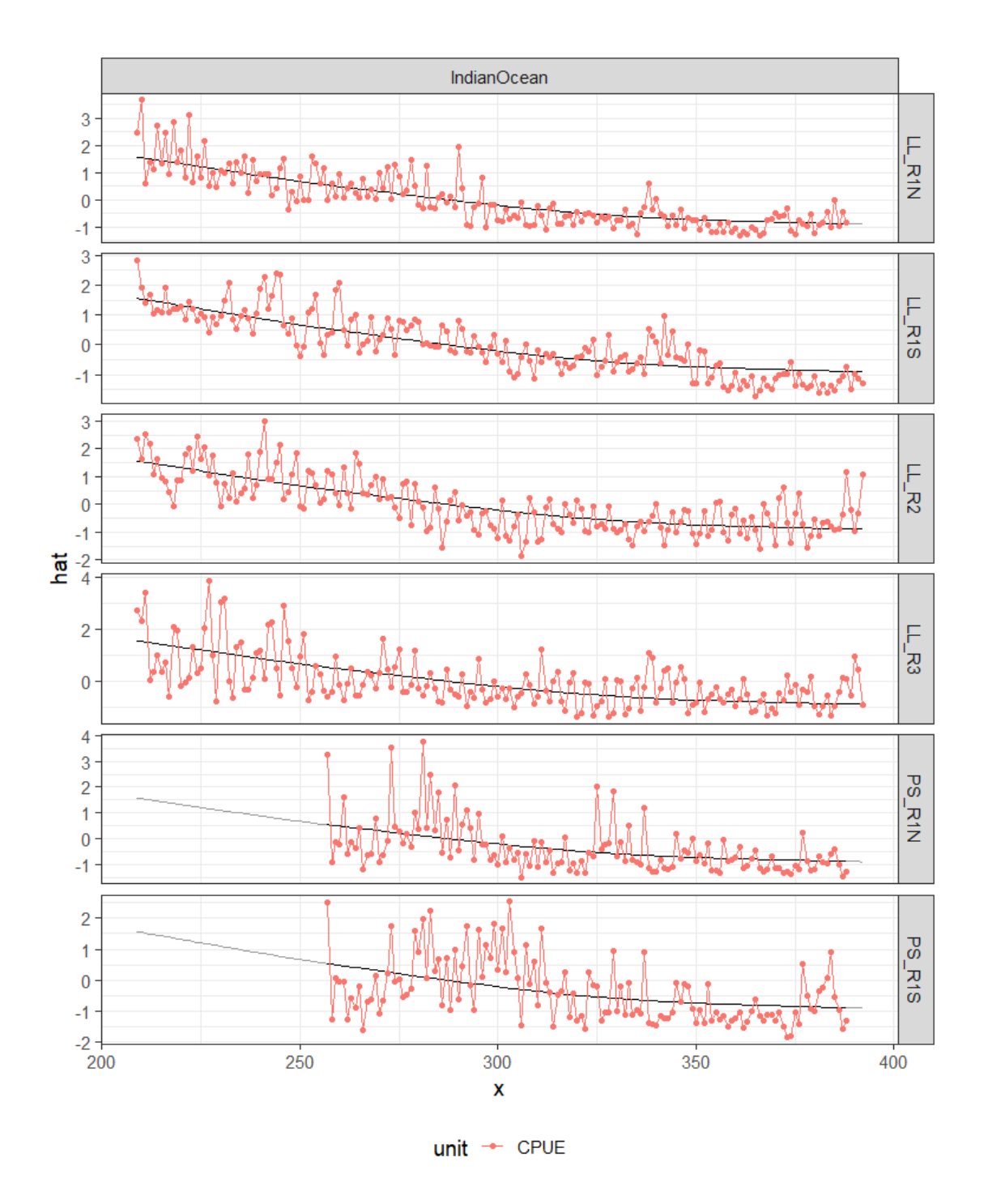


**Figure B1.** Indian Ocean time series of CPUE indices; Points are the standardized values, continuous black lines are a lowess smoother showing the average trend by area (i.e. fitted to year for each area with series as a factor). X-axis is time, Y-axis are the scaled indices.

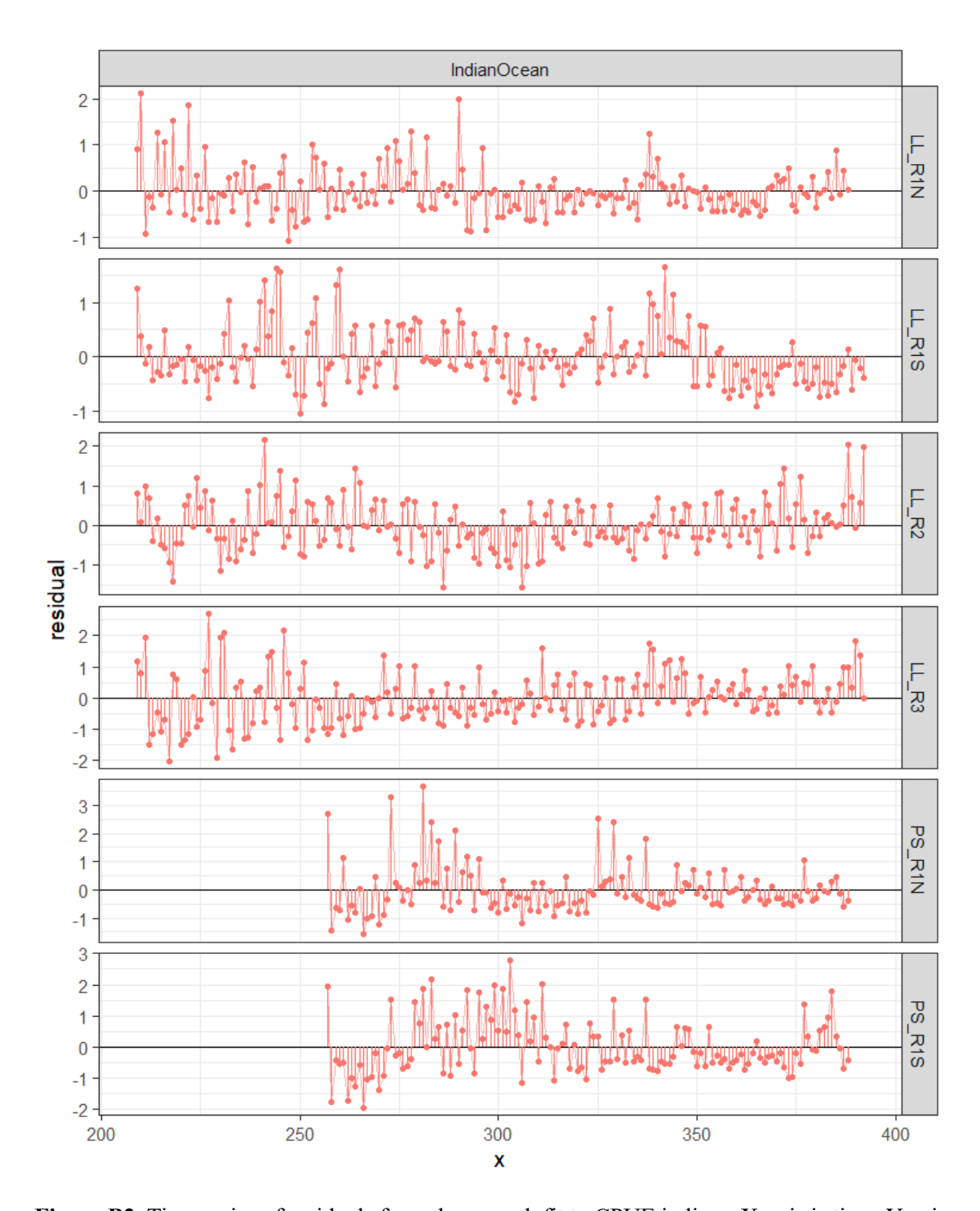


**Figure B2.** Time series of residuals from the smooth fit to CPUE indices. X-axis is time, Y-axis are the scaled indices.

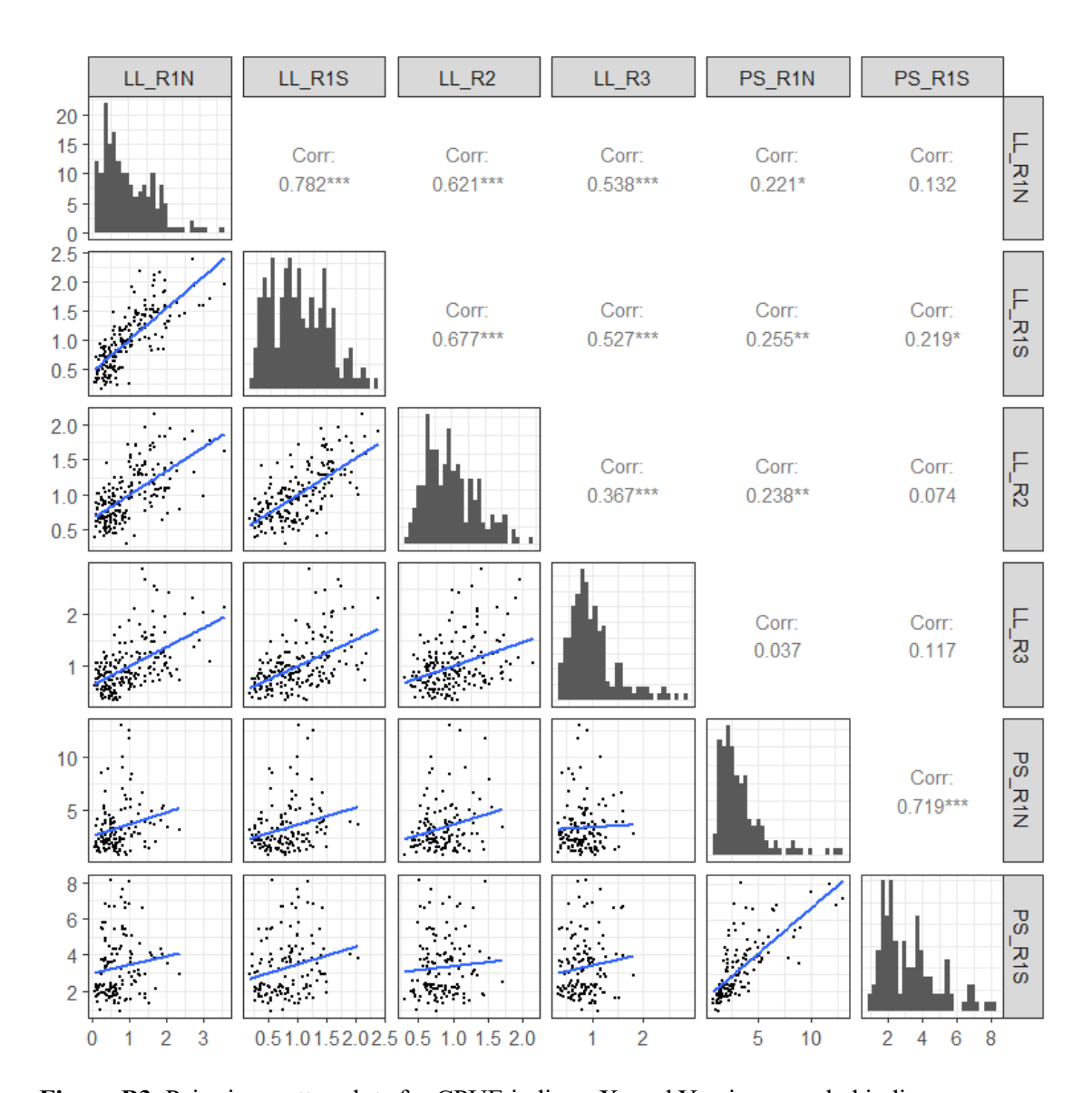
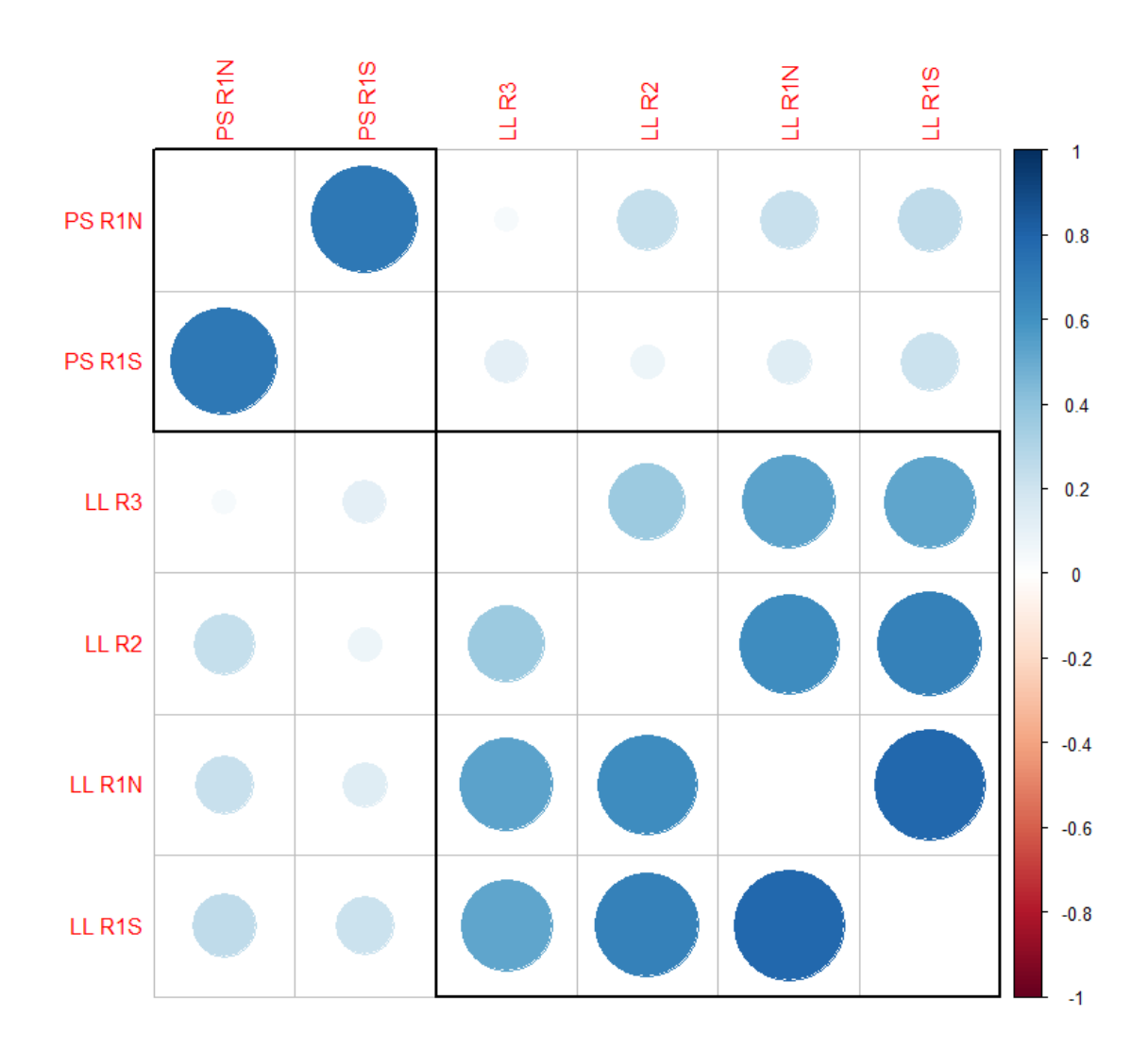
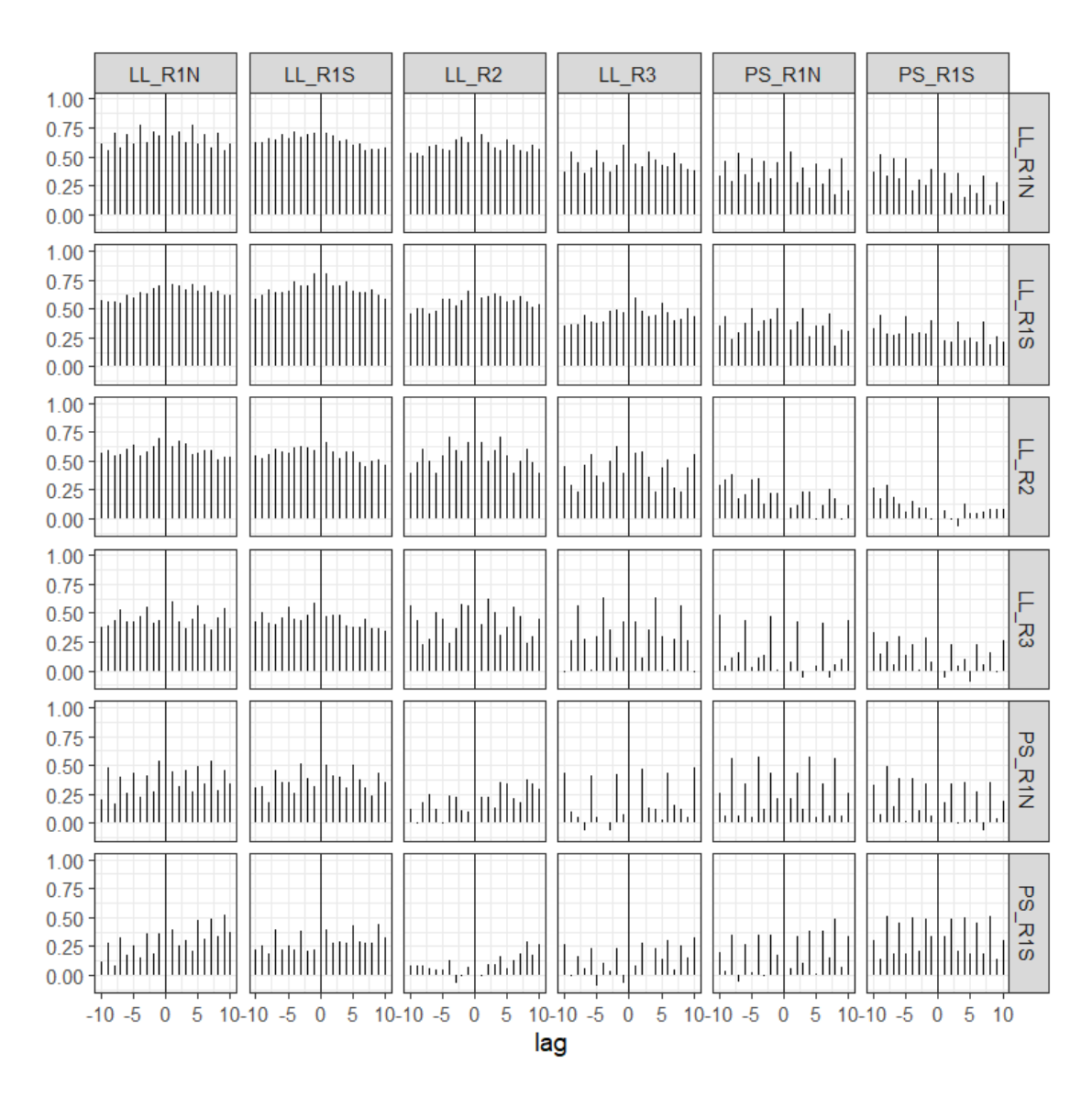


Figure B3. Pairwise scatter plots for CPUE indices. X- and Y-axis are scaled indices.



**Figure B4.** Correlation matrix for CPUE indices; blue indicates positive and red negative correlations, the order of the indices and the rectangular boxes are chosen based on a hierarchical cluster analysis using a set of dissimilarities.



**Figure B5** Cross-correlations between CPUE indices to identify lagged correlations (e.g., due to year-class effects). X-axis is lag number, and y-axis is cross-correlation.

S